

A flexible plant based irrigation control for greenhouse crops

Farai Malvern Simba

A thesis submitted in partial fulfillment for the requirements of the Master of Science Degree in Agricultural Meteorology

> Physics Department Faculty of Science University Of Zimbabwe

Abstract

The project sought to minimize water use, improve water use efficiency and improve crop productivity for greenhouse crops. A flexible plant based automated irrigation system was designed and implemented for a tomato crop in a greenhouse at the Biological Science Department, University of Zimbabwe. The system used stem heat balance sap flow gauges to measure the transpiration rate and the information was sent to a computer program via a K8000 Velleman interface card. The computer program used this information to calculate the daily crop water requirements and time to replace the lost water for the greenhouse crops. The performance of the automated system was evaluated by comparison of the leaf temperatures and amount of water used against an existing scheduling technique in which the crop water requirements were calculated using the Penman-Monteith equation. In order to find typical values for water lost during the day under different conditions, a ten-day monitoring of sap flow rates on the tomato crop was done and typical daily sap flow rates were varying from 0.11 to 0.98 L m⁻² d⁻¹ with an average sap flow rate of 0.53 L m⁻² d⁻¹. Corresponding external daily total solar radiation ranged from 9.19MJm⁻²d⁻¹ to 26.56 MJm⁻²d⁻¹, with an average of 20.05 MJ m⁻²d⁻¹, while air temperatures ranged from 27.25 °C to 14.73 °C, with an average of 20.99 °C. In addition, a control treatment was established, in which the plants were subjected to drought stress by withholding water for a number of days and the transpiration rates again measured using sap flow gauges as before in order to find typical values for water lost during the day under different drought stress conditions. Typical values were ranging from 0.1 L m⁻² d⁻¹ to 0.45 L m⁻² d⁻¹. In a separate six-day monitoring period, the average ET₀ values were 2.16 mm d⁻¹ and 2.15 mm d⁻¹ for the Penman-Monteith based treatment and the automated treatment, respectively. Total water replaced over the six days by the automated system was 88.03 L and by the Penman Monteith based method was 171.84 L and the total irrigation time used was 73.5 minutes and 180 minutes, respectively. For the six consecutive days, the automated irrigation system supplied the least amount of water daily and thus avoided under irrigating or over irrigating, cut on total working hours of the irrigation system, labour and energy costs and had good response time and was flexible. Leaf temperature ranged from 12.55 °C to 31.94 °C with an averaged value of 22.28 °C. We can conclude, therefore that the physiological response of the crop was not negatively affected by this reduction in water through the use of the automated scheduling.

Acknowledgements

Firstly I should thank the Almighty God for making me resolute and focused when circumstances were undesirable to the success of the project. I want to extend my heartfelt gratitude to my supervisor Mr. E. Mashonjowa who guided me and sacrificed his resources from the initial stages of the project to the end of it. I wish to pass my thanks to the Computer Science Department crew i.e. Mr. B. Nyambo, Mr. M. Munyaradzi, Mr. C Mukwandara, Mr. R. Sidimeli and Mr. Fariraishe Shumba for helping me with hardware and software materials. My thanks also go to the Physics department staff members in particular Mr. B.Chipindu, Dr L. Olumekor Dr. T. Mhizha and Mr. K. Gwara for the advice they gave in electronics and interest in my work. I wish to convey my appreciation to my MAGM colleagues who supported and motivated me throughout the two year period. Lastly I want to thank my friends and family in particular Fungai, Tendai, Lorraine, Charlotte, Stanley, Eric, Deborah, all GCF members and my mother Ms L. Simba for the moral support they gave me throughout the studies.

Table of contents	Pages
Abstract	i
Acknowledgements	
Table of contents	
List of Figures	
List of tables	ix
List of annexes	X
CHAPTER 1	1
1.1 Introduction	1
1.2 Problem statement	2
1.2.1 Aim	3
1.3 Objectives	3
1.4 Expected benefits	3
1.5 Thesis layout	4
CHAPTER 2	5
2.0 Introduction	5
2.1 Water requirements of greenhouse crops	6
2.1.1 The greenhouse water cycle	
2.1.2. Variation in water status in relation to greenhouse climatic factors	9
2.1.2.1Dynamic behavior of leaf water potential	
2.2 The microclimate of crops under a greenhouse	
2.2.1 Radiation balance	9
2.2.2 Air temperature and humidity	10
2.2.3 Gradients and profiles	11
2.3 Plant Physiology responses to shelter	12
2.4 Evapotranspiration	
2.5.1 Weather parameters	13
2.5.2 Crop factors	13
2.5.3 Management and environmental conditions	13
2.5.4 Reference crop evapotranspiration (ET _o)	14
2.6 Irrigation scheduling techniques in greenhouses	15
2.6.1 Meteorological based	15
2.6.1.2. Determination of ET _o using FAO Penman-Monteith method	15
2.6.1.3 Solar radiation based methods	17
2.6.1.4 ET computed from pan evaporation	18
2.6.1.5 Problems related to ET estimation of greenhouse crops	20
2.6.2 Soil Moisture Based Methods	21
2.6.2.1 Available water capacity and plant available water	21
2.6.2.1 .1 Lysimetry	21
2.6.2.1.2 Gravimetry	22
2.6.3 Plant based methods	23
2.6.3.1.2 Sap thermodynamics	
2.6.3.2 The trunk sector heat balance method	
2.6.3.2.1 Theory of operation	27
2.6.3.3 Heat-pulse method	

2.6.3.3.1 Theory of operation	30
2.6.3.4 Leaf thickness	
2.6.3.5 Stem and fruit diameter	
$2.6.3.6 \gamma$ -ray attenuation.	32
2.7 Different irrigation methods	
2.7 .1 Drip irrigation	
2.7 .4 Spray irrigation	
2.8 Automation of irrigation controls	
2.8.1 Irrigation control systems	
2.8.4 A computer based systems	
2.8 .1 Wireless technology in Greenhouse monitoring	
2.9 Analogue to digital signal conversion.	
2.9.1 Resolution	
2.9.2 Response type	
2.9 2.1 Linear Analogue to digital conversions (ADCs)	
2.9.2.2 Non-linear ADCs	
3.1 Introduction	
3.2.1 The greenhouse	46
3.3 Plant material and agronomic operations	
3.4 Instruments used	
3.4 .1 Meteorological instruments	
3.4.2 Radiation Energy Balance (REBS) net radiometer	49
3.4.3 Tube solarimeter	
3.4.5 HMP45C temperature and relative humidity probe	51
3.4.6 Wind, heated bead testo 425 anemometer	
3.4.7 PAR (Photosynthetically active radiation) sensor	53
3.4.8 A matrix sensor	
3.5 Physiological instruments	54
3.5.1 Copper constantan (T type) thermocouples	
3.5.2 Sap flow gauge	
3.6 Electronic instruments	56
3.6.1 A Zener diode	56
3.6.2 The Velleman K8000 interface card	56
3.6.3 A universal K6714 relay card	60
3.6.4 Electric pump	61
3.7 Computer software used	62
3.7.1 Power WinPLC	62
3.8 Calibration of sensors	62
3.8.1 Experiment 1: Calibration of temperature humidity sensors (Vaisala type)	63
3.8.2 Experiment 2: Calibration of radiation sensors	
3.9 Preliminary measurements and tests	64
3.9.1 The integrity test	64
3.9.2 Analogue voltage signal conversion to digital signal resolution test	65
3.9.4 Designing of a computer program	66
3.9.4.1 A flow chart for the control program (algorithm)	67
3.10 Field measurements	

3.10.2 Setting up of an automatic weather station outside the greenhouse	70
3.10. 3 Data collected from the sensors	
3.10.3.1 Installation of sap flow gauge sensors	
3.10.3.2 Determination of Ksh.	
3.10.3.3 Determination of stem diameters and cross sectional areas	73
3.11 Monitoring of transpiration rates from sap flow rates	74
3.11.1 The scaling up of the estimated evapotranspiration	74
3.12 Monitoring of transpiration rates using the FAO Penman –Monteith ed	quation
	75
3.12.1 Determination of the wind speed using the hot wire anemometer	75
3.13 Monitoring of the system signals with the data logger signals	75
3.14 Measurement of the drip emitter rate	76
3.15 Integration and implementation of control system	77
3.15.1 The flow chart of the control system (algorithm)	78
3.15.2 The irrigation control system	79
3.15.2.1	80
3.15.3 A computer display of the running system	80
3.15.4 Investigative crop treatments	81
CHAPTER 4	84
4.1 Introduction	84
4.2 Calibrations	84
4.3 Monitoring of sap flow rates	87
4.3.1 Temporal variation of weather parameters on different days inside the	
greenhouse	
4.3.2 Temporal variation of sap flow rate on different days	
4.3.6 Correlation between sap flow rate and weather parameters	
4.4 The automatic irrigation control system	107
CHAPTER 5	
Conclusions and Recommendations	116
Anneyes	128

List of Figures	Pages
Figure 2.1: The water balance of a cropped soil	8
Figure 2.2: A simplified representation of the (bulk) surface and aerody	namic
resistances. for water vapour	18
Figure 2.3 : Showing surfaces used to compute evapotranspiration	. 22
Figure 2.4: A Class A evaporation pan	. 23
Figure 2.5: Stem Gauge Schematic	25
Figure 2.6: A schematic dynagage diagram	26
Figure 3.1: The greenhouse in the Biological Science Department,	
University of Zimbabwe	50
Figure 3.2: Radiation Energy Balance (REBS) net radiometer	53
Figure 3.3: A tube solarimeter in the greenhouse	54
Figure 3.4: Wind, heated bead testo 425 anemometer	55
Figure 3.5 A Velleman K8000 interface card	60
Figure 3.6 A universal K6714 relay card	63
Figure 3.7 A setup for the integrity test.	68
Figure 3.8 A schematic diagram of the negative gain amplifying circuit	69
Figure 3.9: A flow chart for the computer control program	71
Figure 3.10: (a) an automatic outside weather station and (b) shows the bottom	part of
the automatic weather station inside a greenhouse	74
Figure 3.11: a stem heat balance sap flow gauge installed onto a tomato crop	75
Figure 3.12: A setup monitoring signals from data logger to the amplifying circuit	79
Figure 3.13: A flow chart for the irrigation control system	81
Figure 3.14: Integrated irrigation control	82
Figure 3.15: Connection between the K8000 card, relay card and the pump	83
Figure 3.15: A computer display of the running system.	84
Figure 3.16 : A setup of investigative crop treatments.	85

Figure 4.1: Temporal variation of radiation and air temperature on day 33, 2010	83
Figure 4.2 : Temporal variation of radiation and air temperature on day 38, 2010	83
Figure 4.3: Temporal variation of radiation and air temperature on day 39, 2010	84
Figure 4.4: Temporal variation of sap flow rate on day 32	84
Figure 4.5: Temporal variation of sap flow rate on day 33	85
Figure 4.6: Temporal variation of sap flow rate on day 38.	86
Figure 4.7: Temporal variation of sap flow rate on day 39	86
Figure 4.8: Temporal variation of sap flow rate and solar radiation on day 32,	87
Figure 4.9: Temporal variation of sap flow rate and solar radiation on day 33,	88
Figure 4.10: Temporal variation of sap flow rate and solar radiation on day 38	88
Figure 4.11: Temporal variation of sap flow rate and solar radiation on day 39	89
Figure 4.12: Correlation between sap flow rate and solar radiation on day 33	89
Figure 4.13: Correlation between sap flow rate and solar radiation on day 32	90
Figure 4.14: Correlation between sap flow rate and solar radiation on day 39	91
Figure 4.15: Correlation between sap flow rate and solar radiation on day 32	91
Figure 4.16: Temporal variation of sap flow rate & air temperature on day 32,	92
Figure 4.17: Temporal variation of sap flow rate & air temperature on day 33	93
Figure 4.18: Temporal variation of sap flow rate & air temperature on day 38,	94
Figure 4.19: Temporal variation of sap flow rate and air temperature on day 39	94
Figure 4.20: A summary of the variation of sap flow rate with weather variables	95
Figure 4.21:, Variation of sap flow rates and crop evapotranspiration	96
Figure 4.22:. Correlation between sap flow rate and crop evapotranspiration.	97
Figure 4.23:, Variation of the sap flow rate and weather variables	97
Figure 4.24 A comparison of the treatments 10days.	99
Figure 4.25: A summary of sap flow rate and solar radiation over 10 days	102
Figure 4.26: Variation of sapflow rate and evapotranspiration	106
Figure 4.27: Correlation of sapflow rate and crop evapotranspiration	102
Figure 4.28: Sap flow rate against weather variables over days	109
Figure 4.29: A bar graph comparison of the treatments	111

List of tables	Pages
Table 4.1 Calibration of relative humidity temperature sensor	79
Table 4.2: Calibration of radiation sensors with the CM11 Kipp solarimeter	
as the standard	80
Table4.3:Conversion of analogue signalstodigitalsignal	80
Table 4.4 : Results of an integrity test of the K8000 Velleman interface card	81
Table 4.5: Leaf dimensions used to calculate total leaf	82
Table 4.6: Readings used for calculating the stem cross sectional area	93
Table 4.7 : A summary of sap flow rate values & relative humidity for four days	98
Table 4.8: A summary of sap flow rates and solar radiation for four days	104
Table 4.9 : A summary of sap flow rates & air temperatures for four days	100
Table 4.10: Conversion of units method	100
Table 4.11: Summary of sap flow rate, crop evapotranspiration and the weather	103
Table 4.12: Climatic data outside the greenhouse	103
Table 4.13 : Climatic data inside the greenhouse	104
Table 4.14: Readings used to calculate the drip emitter rate pump	104
Table 4.15: Readings used to calculate the drip emitter rate from the Penman-Mo	nteith
based	105
Table 4.16: Daily water totals	107
Table 4.17: Daily potential totals of water used by the two systems	108
Table 4.18: Leaf temperatures on two treatments	108
Table 4.19: Water lost for the three treatments after over 6 days	108
Table 4.20: ETo values for the three treatments	110

List of annexes

Annex A: The irrigation control program	. 126
Annex B: The data logger program for outside greenhouse weather	130
Annex C: The data logger program for inside greenhouse weather	133
Annex D: The Day of Year (Julian) calendar	. 136

CHAPTER 1 BACKGROUND AND JUSTIFICATION

1.1 Introduction

Agriculture is one of the mainstays of the Zimbabwean economy and accounts for 20% of Gross Domestic Product (GDP) (Horticultural Promotion Council of Zimbabwe, 2000). The country has experienced phenomenal growth in horticultural exports over the past two decades and in 1999 alone, they trebled by volume and increased five-fold by value (Horticultural Promotion Council of Zimbabwe, 2000). Water is a chief input in horticulture that directly affects the quality and quantity of yield. Its management is therefore of importance to the farmer. The increasing worldwide shortages of water and costs of irrigation are leading to an emphasis on developing methods that minimize water use and maximize the water use efficiency (Jones, 2004). Irrigation scheduling has conventionally aimed to achieve an optimum water supply for productivity, with soil water content being maintained close to field capacity. Estimation of evapotranspiration, an indication of plant water use, is used to design irrigation schedules. Common schedules are based on evaporation pan measurements (Pruitt, 1966; Doorenbos and Pruitt, 1975), soil moisture measurements (Smith and Mullins, 2000; Dane and Topp, 2002) and meteorological measurements usually based on accumulated input solar radiation and calculation of reference crop evapotranspiration (ETo) based on the Penman Monteith equation.. These schedules have inherent flaws. Inadequate irrigation tends to waste water, nutrients and energy, and may cause soil degradation by waterlogging and salinisation (Baille, 1994). In addition challenges of labour, and response

time to offset moisture stress continue to inhibit the correct supply of water. In order to achieve higher levels of profitable and sustainable production, it is essential to modernize existing irrigation systems to improve water management. Automation of irrigation schedules holds a promise of efficiently optimizing the supply of water needed to satisfy the requirements of crops.

Jones (2004) observed that many features of the plant's physiology respond directly to changes in water status in the plant tissues, whether in the roots or in other tissues, rather than to changes in the bulk soil water content (or potential). As a result more precise irrigation schedules can be achieved with plant stress sensing or the speaking plant approach. To estimate plant water status, sensors like sap flow gauges (Granier,1987; Cohen et al.,1981; Cermak and Kucera,1981) have proved to be practical in use and, in most cases, are accurate to within 5% on a daily basis (Dugas,1990). Sap flow measurements of transpiration using both steady state heat flux (Sakuratani, 1981; Baker and van Bavel, 1987) and heat pulse technology (Cohen et al, 1981) remain a potential method for automating irrigation control based on direct physical plant measurements. Dendrometers that monitor the response of stem diameter to water stress (Huguet et al., 1992) can also be employed.

1.2 Problem statement

The use of such plant indicators, while being the ideal method for irrigation scheduling, is still hampered by the relatively low knowledge of the dynamic nature of plant water status and by the lack of suitable indicators, relative to established scheduling methods based on atmospheric and soil observations. In addition, the practical application of the researched theory in irrigation scheduling is very limited (Cohen, 2003; Garcia-Orellana et al., 2007).

1.2.1 Aim

This project seeks to design and implement a flexible plant based irrigation control with a more precise schedule using plant based responses as the indicator for determining the timing and amount of irrigation for greenhouse crops.

1.3 Objectives

- To monitor sap flow rates of greenhouse crops under different conditions,
- ii. To design an automated irrigation schedule based on transpiration rates measured by sap flow gauges,
- iii. To implement and compare this irrigation system with traditionally existing methods that are based on meteorological variables.

1.4 Expected benefits

- Conservation of water and increased water use efficiency.
- Enhanced crop productivity/yield through applying requisite amounts of water.
- Reduced labour, energy consumption and input costs.
- Flexible and user friendly system

1.5 Thesis layout

The project is made of five chapters. The first chapter deals with the introduction to the project under which the background and justification are discussed. The chapter gives an in-depth picture on the direction of the project and insight on the intended objectives.

The second chapter delves on the literature survey. This chapter reviews the theory on scheduling irrigation methods and aspects, crop water requirements and evapotranspiration estimation. It also sheds light on related topics to the project and works that have been done in the past by other researchers. The third chapter focuses on the materials and methodology. This chapter explains how the project was done or executed and the materials or apparatus employed to achieve the intended objectives. The location and geography of the area where the project was done are included in this section. The fourth chapter entails the analysis of results and discussion. Statistical interpretation using Microsoft Excel is done to give comprehensive scientific results. The fifth chapter concentrates on the lessons learnt, conclusions and recommendations.

CHAPTER 2 LITERATURE REVIEW

2.0 Introduction

The Zimbabwean horticultural export industry continues to experience phenomenal growth since inception in the mid 1980s and is now the third largest agricultural commodity after tobacco and livestock. In addition, horticulture is acknowledged as the second largest foreign exchange earner after tobacco and accounts for approximately 3.5 < 4.5 % of GDP. Foreign exchange earnings have increased by an average of 30 % per annum over the past ten years. The success of the industry has been based on free market situation requiring considerable entrepreneurial flair from producers. Most exporters employ agents who act on their behalf, and some growers access expertise in the form of consultants.

Horticultural production and exports have been the fastest growing sector in the Zimbabwean economy registering a growth rate in excess of 30 % per annum. In the last fifteen years horticultural exports have grown from US\$3.515 million in the season 1985/86 to US\$139.518 million in 2000/1. Prospects for continued growth are encouraging. Of significance is the fact that for all product groups, the most important export destination is the European community, with 99 % of cut flowers, 89 % of vegetables, herbs and spices, and 75 % of citrus.

The performance and success of horticulture is hinged on accurate water supplies assuming other farming management practices are in place. The supply of the required

water to the plant is of prime importance for its growth and economic production, especially in greenhouses, where irrigation is the only source of water for the plant. In this chapter the water requirements of greenhouse crops, physiological and/ or morphological effects of water on greenhouse crops, greenhouse microclimate, different irrigation methods and schedules, the automation of schedules, and the contemporary technologies being employed to automate schedules will be discussed.

2.1 Water requirements of greenhouse crops

Water is an essential plant component being a major constituent of plant cells, and ranging from about 10% of fresh weight in many dried seeds to more than 95% in some fruits and young leaves. Many of the morphological and physiological characteristics of land plants are adaptations permitting life on and by maintaining an adequate internal water status in spite of the typically rather dry aerial environment. The unique properties of water (Slayter 1967, Einsenberg & Kauzmann 1969, and Nobel 1991) form the basis of much environmental physiology. For examples it is a liquid at normal temperatures and is a strong solvent, thus providing a good medium for biochemical reactions and for transport (both short-distance diffusion and long-distance movement in the xylem and phloem). Water is also involved as a reactant in processes such as photosynthesis and hydrolysis, while its thermal properties are important in temperature regulation and its compressibility is important in support and growth.

2.1.1 The greenhouse water cycle

The main process involving the fate of water in the greenhouse, and hence the water requirements of crops, is evapotranspiration, a process that is driven by a constant inflow

of energy. In fact, the water balance is intimately and reciprocally related to the cycle and balance of energy (Boulard and Baille, 1993), since the state and content of water in the soil and its vegetative cover is affected by, and in turn, affects, the way the energy fluxes reaching the soil is partitioned and utilized. Control of the soil-plant-atmosphere system must therefore be based on simultaneous consideration of both the water and the energy balance. Two components of the greenhouse water cycle are important to measure and to control. The first one is the soil component (or artificial substrate), where the water balance is an account of all quantities of water added to, subtracted from and stored within the root zone during a given period of time.

For greenhouses, this general statement can be written as follows:

$$DS=W-(DR+E_s+TR)$$
 (2.1)

where DS is the quantity of water stored in the substrate, DR is the drainage, E_s is the soil evaporation and TR the actual transpiration of the crop. The last two variables are difficult to separate, and are generally lumped together and termed 'evapotranspiration' (ET= E_s +TR).It is still difficult to measure in practice the soil water balance. Often, the larger component of the losses side and the most difficult to measure directly, is the evapotranspiration, ET. To obtain the irrigation requirement, W, from the water balance equation (2.1), we must have accurate measurements of the other terms of the equation.

For long period, the change in water content of the root zone is likely to be small in relation to the total water balance. Soil evaporation is negligible if localized irrigation is practiced in soil less cultures or if the soil or substrate is covered by a mulch or plastic cover. If we neglect Es, W is approximately equal to the sum of TR plus the drainage, DR. TR is equal to the water uptake by the plant, A, minus the water stored in the plant organs, DW_p. Then:

$$W=TR+D=A-DW_{p}-DR$$
 (2.2)

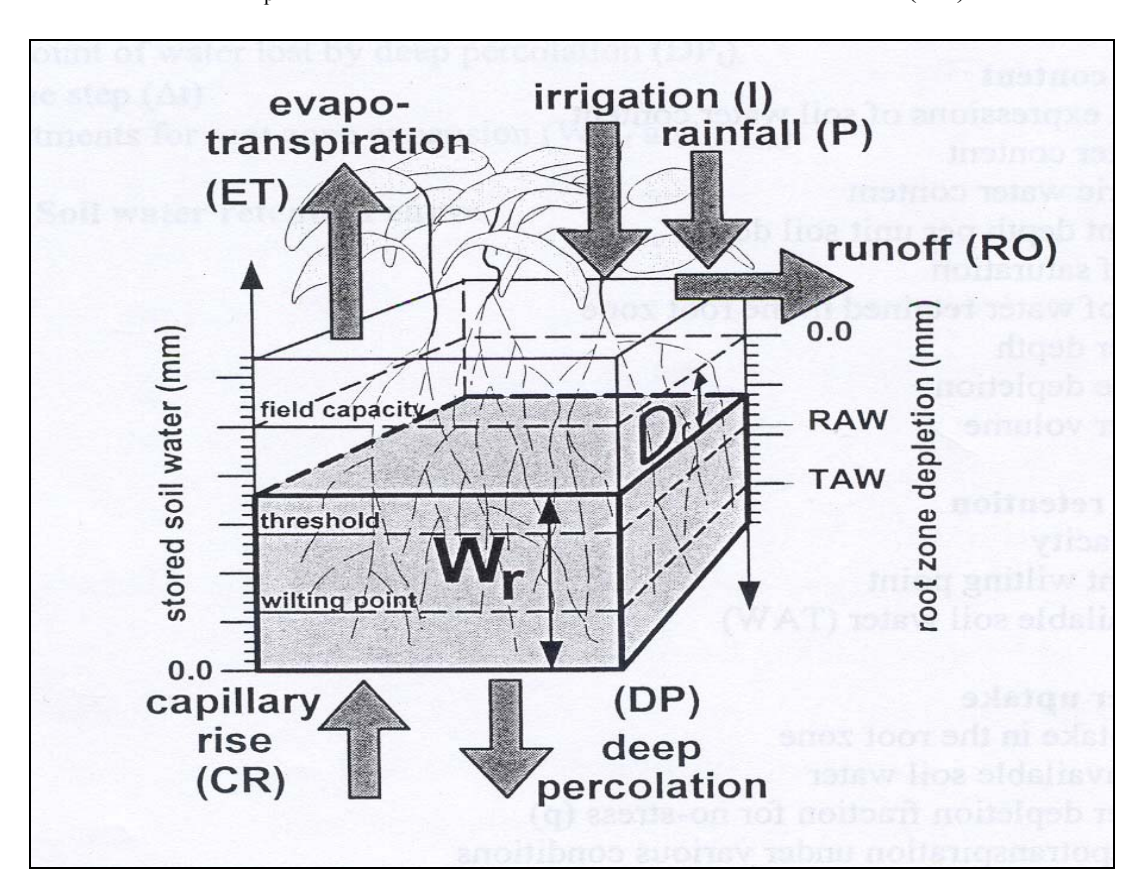


Figure 2.1: The water balance of a cropped soil (Allen et al., 1999)

2.1.2. Variation in water status in relation to greenhouse climatic factors

2.1.2.1 Dynamic behavior of leaf water potential

The diurnal variation in leaf water potential (Ψ_{leaf}) closely reflects the diurnal variation in transpiration and in its main driving forces, radiation and vapour pressure deficit (VPD), in field grown as well as in greenhouse grown tomato. A simple model for Ψ_{leaf} is the steady state equation using the Ohm's Law analogue(equation 2.3)

$$\Psi_{\text{leaf}} = \Psi_{\text{soil}} - E \times R_{\text{soil-plant}}$$
 (2.3)

which does not include any effects of variable hydraulic resistance, capacitance, coupled solute flow or volume for growth. Effects of the greenhouse climate act upon transpiration rate (TR) and Ψ_{soil} , while a factor like temperature of the root environment might affect Rsoil-plant. When E diminishes, Ψ_{leaf} will reach a maximum value, equal to Ψ of the root environment. In growing tissue, however, a small Ψ gradient will be maintained (Cosgrove, 1986). In the field the predawn Ψ_{plant} commonly approaches Ψ soil.

2.2 The microclimate of crops under a greenhouse

The changes in wind speed and turbulence that occur as a result of windbreaks affect the microclimate of the sheltered zone.

2.2.1 Radiation balance

Solar and net radiation may be significantly reduced in the areas shaded by windbreaks. This effect has not been found to be of major importance in north-south oriented windbreak systems, since only small areas are shaded during the course of the day, especially during the growing season when the sun is high. On a full day basis, the difference in radiation balance between areas near and areas remote from the barrier may

be entirely negligible. This follows; since an area shaded in the morning by a windbreak to the east will receive some additional radiation by reflection from the windbreak to the east will receive some additional radiation by reflection from the windbreak in the afternoon. East-west oriented windbreaks, on the other hand, may have a greater effect. Areas to the north, particularly during seasons when the sun is low, will be shaded for long periods. Areas to the south will be subject to reflection off the windbreak throughout the day. Shading depends, of course, on the height of the barrier, on latitude, season, and time of day. While severe shading may suppress photosynthesis and dry matter production, this effect can be offset by reduced evapotranspiration in the shaded zone.

2.2.2 Air temperature and humidity

It is usually observed in clear weather that daytime air temperatures are greater in shelter than in open fields. This is due, apparently, to the reduction of turbulent mixing of cold and warm air and the consequent reduction in the removal of sensible heat generated at the plant or soil surface. If evaporation is also suppressed in shelter, additional energy is available for sensible heat generation as well. When turbulent mixing is reduced, the aerial resistance r_a increases and the temperature gradients are intensified. Temperature inversions normally develop at night in both sheltered and unsheltered areas; then the plant and soil surfaces become the sink for sensible heat. Windiness mixes the nocturnal inversion layer. The reduction of windiness and effectiveness of turbulent mixing in shelter means that temperature inversions will normally be more intense there. Unless total calm prevails, the air will generally be colder at night in shelter than in open fields. The reduction of cooling near the windbreak could have been due to radiative exchange

with the trees. Probably the increased vapour content of the air in that zone may have reduced the rate of radiational cooling, as well. Humidity and vapour pressure gradients are also increased in shelter. Transpired and evaporated water vapour is not as readily transported away from the source, the evaporating surface, as in an unsheltered field. Vapour pressure remains higher in shelter throughout the night as well, since the surface usually remains the source of vapour, except during periods of dew deposition. Such intensified temperature and vapour pressure gradients in shelter have been observed under a wide range of climatic conditions with many types of vegetative and constructed barriers used to shelter many different types of crops studied. Despite the increased temperature the relative humidity is generally greater by day in shelter i.e. shelter prevents the escape of air molecules to the atmosphere.. The difference in relative humidity is generally greater by day in shelter. The difference in relative humidity between open and shelter is greater still at night because of the lower air temperatures in shelter. It is also important to recognize that the microclimate differences that develop in shelter vary with distance from the wind break, with weather conditions and with time of day.

2.2.3 Gradients and profiles

The changes in microclimatic conditions occur at more than one level above and within the sheltered crop. Since turbulent mixing is affected it is reasonable to expect that gradients of temperature, humidity, carbon dioxide, will also be changed.

2.3 Plant Physiology responses to shelter

Microclimate differences develop in shelter and the shelter microclimate influences crop growth and production. Often plants in shelter show more rapid vegetative growth and increase in size because of high temperatures that favour growth. This is manifested by greater total Leaf Area Index (LAI) and plant height. Plant growth and performance in shelter may also be favoured because the use of windbreaks reduces the incidence of mechanical injuries such as are caused by 'sandblasting'. Mechanical injuries may cause loss of production by defoliation, that is, loss of viable tissue, or by imposing short, high-intensity moisture stress on the injured plant. Both factors may combine to reduce productivity. Recent studies suggest, however, that the major influence of shelter on plant behaviour is due to a greater turgidity and lower stomatal resistance in the sheltered plants, especially during periods of water stress or strong evaporative demand. Wind tunnel studies show that transpiration increases with increasing wind speed. On the other hand, found, in a greenhouse study, that water use by beans and overall plant growth decreased when winds increased above 1ms⁻¹.

2.4 Evapotranspiration

Evapotranspiration of a crop indicates the rate at which water is lost from the crop to the atmosphere as transpired and evaporated water. Weather parameters, crop characteristics, management and environmental aspects are factors affecting evaporation and transpiration. Measurements of water loss are therefore important to the farmer to know how much water needs to be replenished to enhance a healthy crop growth.

2.5.1 Weather parameters

Crop evapotranspiration is influenced by weather parameters like radiation, air temperature, humidity and wind speed. The evaporation power of the atmosphere is expressed by the reference crop evapotranspiration, ET_o. The reference crop evapotranspiration from a standardized vegetated surface.

2.5.2 Crop factors

The crop type, variety and development stage should be considered when assessing the evapotranspiration from crops grown in large, well managed fields. Differences in resistance to transpiration, crop height, crop roughness, reflection, ground cover and crop rooting characteristics result in different evapotranspiration (ET) levels in different types of crops under identical environmental conditions. Crop evapotranspiration under standard conditions (ETc) refers to the evaporating demand from crops that are grown in large fields under optimum soil water, excellent management and environmental conditions, and achieve full production under the given climatic conditions.

2.5.3 Management and environmental conditions

Factors such as soil salinity, poor land fertility, limited application of fertilizers, the presence of hard or impenetrable soil horizons, the absence of control of diseases and pests and poor soil management may limit the crop development and reduce the evapotranspiration. Other factors to be considered when assessing ET are ground cover, plant density and the soil water content. The effect of soil water content on ET is conditioned primarily by the magnitude of the water deficit and the type of soil. On the

other hand, too much water will result in waterlogging which might damage the root and limit root water uptake by inhibiting respiration.

2.5.4 Reference crop evapotranspiration (ET₀)

The evapotranspiration rate from a reference surface, not short of water, is called the reference crop evapotranspiration or reference evapotranspiration and is denoted as ET₀. The reference surface is a hypothetical grass reference crop with specific characteristics. The concept of the reference evapotranspiration was introduced to study the evaporative demand of the atmosphere independently of crop type, crop development and management practices. As water is abundantly available at the reference evapotranspiring surface, soil factors do not affect ET. Relating ET to a specific surface provides a reference to which ET from other surfaces can be related. It obviates the need to define a separate ET level for each crop and stage of growth. ET₀ values measured or calculated at different locations or in different seasons are comparable as they refer to the ET from the same reference surface. The only factors affecting ET₀ are climatic parameters. Consequently, ET₀ is a climatic parameter and can be computed from weather data. ET₀ expresses the evaporative demand of the atmosphere at a specific location and time of the year and does not consider the crop characteristics and soil factors. The FAO Penman-Monteith method is recommended as the sole method for determining ET₀. The method has been selected because it closely approximates grass ETo at the location evaluated, is physically based, and explicitly incorporates both physiological and aerodynamic parameters.

2.6 Irrigation scheduling techniques in greenhouses

Estimation of crop water requirements or the response of plants to water stress can be indicated by the following methods which in turn are used to design irrigation schedules.

2.6.1 Meteorological based

2.6.1.1 ET computed from meteorological data

Owing to the difficulty of obtaining accurate field measurements, ET is commonly computed from weather data. A large number of empirical or semi-empirical equations have been developed for assessing crop or reference crop evapotranspiration from meteorological data. The FAO Penman-Monteith method is now recommended as the standard method for the definition and computation of the reference evapotranspiration, ET_o . The ET from crop surfaces under standard conditions is determined by crop coefficients (K_c) that relate ET_c to ET_o . The ET from crop surfaces under on-standard is adjusted by a water stress coefficient (K_s) and/or by modifying the crop coefficient.

2.6.1.2. Determination of ET₀ using FAO Penman-Monteith method

The FAO Penman-Monteith method is maintained as the sole standard method for the computation of ET_o from meteorological data. From the original Penman-Monteith equation and the equations of the aerodynamic and canopy resistance, the FAO Penman-Monteith equation ETo is as follows

ETo =
$$\frac{0.408 \Delta (Rn - G) + \gamma \frac{900}{T + 273} u^2 (e_s - e_a)}{\Delta + \gamma (1 + 0.34 u_2)}$$
(2.6)

Where ETo reference evapotranspiration [mm day⁻¹]

- R_n net radiation at the crop surface [MJm⁻²day⁻¹]
- G soil heat flux density [MJm⁻²day⁻¹]
- T air temperature at 2m height [°C]
- u₂ windspeed at 2m height [m s⁻¹]
- e_s saturation vapour pressure [kPa]
- e_a actual vapour pressure [kPa]
- e_s-e_a saturation vapour pressure deficit [kPa],
- Δ slope vapour pressure curve[kPa $^{\circ}$ C $^{-1}$]

The FAO Penman-Monteith equation determines the evapotranspiration from the hypothetical grass reference surface and provides a standard to which evapotranspiration in different periods of the year or in other regions can be compared and to which the evapotranspiration from other crops can be related.

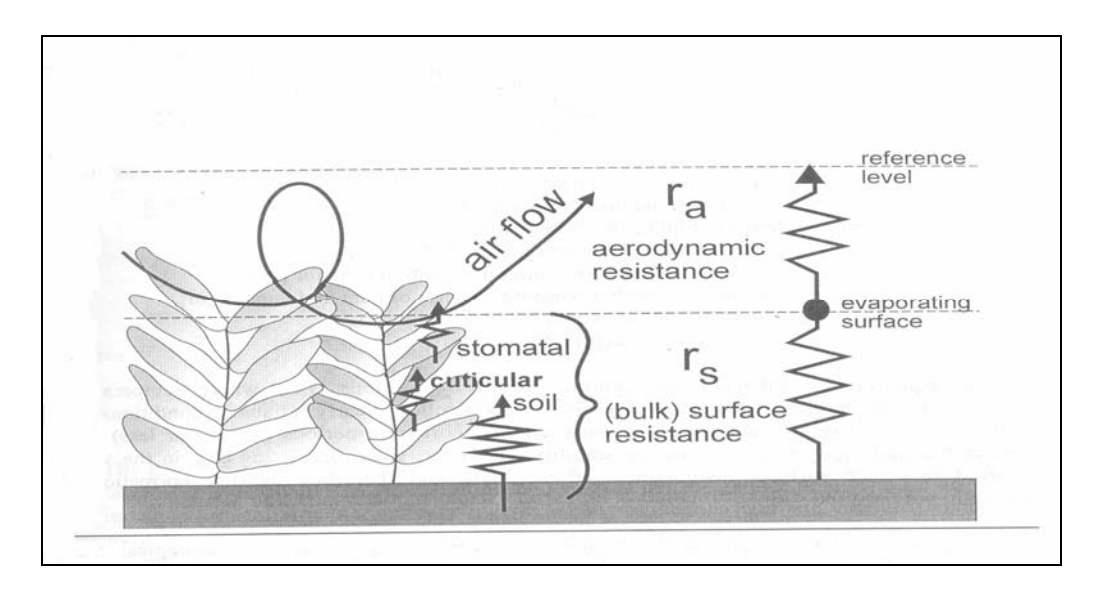


Figure 2.2: A simplified representation of the (bulk) surface and aerodynamic resistances for water vapour flow (Allen et al., 1999)

The resistance nomenclature distinguishes between aerodynamic resistance and surface resistance factors. The surface resistance parameters are often combined into one parameter, the 'bulk' surface resistance parameter which operates in series with the aerodynamic resistance, r_s, describes the resistance of vapour flow through stomata openings, total leaf area and soil surface. The aerodynamic resistance, r_a, describes the resistance from the vegetation upward and involves friction from air flowing over vegetative surfaces. Although the exchange process in a vegetation layer is too complex to be fully described by the two resistance factors, good correlations can be obtained between measured and calculated evapotranspiration rates, especially for a uniform grass reference surface. The Penman-Monteith form of the combination equation is:

$$\lambda E = \frac{\Delta (Rn - G) + \rho_a C_p \frac{(e_s - e_a)}{r_a}}{\Delta + \gamma (1 + \frac{r_s}{r_a})}$$
(2.7)

Where R_n is the net radiation, G is the soil heat flux, (e_s-e_a) represents the vapour pressure deficit of the air, ρ_a is the mean air density at constant pressure, c_p is the specific heat of the air, Δ represents the slope of the saturation vapour pressure temperature relationship, γ is the psychrometric constant, and r_s and r_a are the (bulk) surface and aerodynamic resistances.

2.6.1.3 Solar radiation based methods

The main role of solar of solar radiation in determining the evapotranspiration in a greenhouse (Morris et al., 1957, Lake et al., 1966), showing a strong correlation between daily evapotranspiration and solar irradiance. This constatation has given raise to the so called 'solar radiation' method or 'solarimeter' method, based on a simple relationship

giving the reference evapotranspiration under greenhouse if the outside global radiation, RG_0 and the greenhouse transmission, t, are known:

$$ET_o = K tRG_o/2.5$$
 (2.11)

(ET_o in mm day-1, RG_o inMJm⁻² day⁻¹)

Where K is an empirical coefficient, whose value is about 0.6 to 0.7

Crop coefficient based on this reference ET has been proposed for the main greenhouse species (Laberche et al 1977, De Graaf and van der Ende, 1981).

2.6.1.4 ET computed from pan evaporation

 ET_0 can also be estimated from the evaporation loss from a water surface.

Evaporation from an open water surface provides an index of the integrated effect of radiation, air temperature, air humidity and wind on evapotranspiration. However, differences in the water and cropped surface produce significant differences in the water loss from an open water surface and the crop. The pan has proved its practical value and has been used successful to estimate reference evapotranspiration by observing the evaporation loss from a water surface and applying empirical coefficients to relate pan evaporation to ET_o .

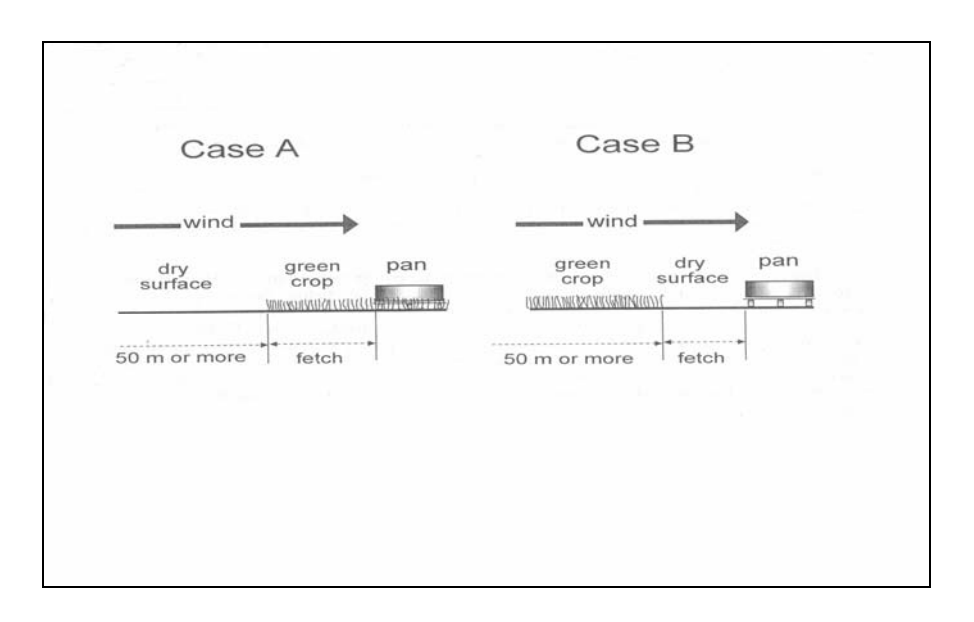


Figure 2.3: Showing surfaces used to compute evapotranspiration(Allen et al., 1999)

Pans of many shapes and sizes have been used to measure free water evaporation. Pans are inexpensive, relatively easy to maintain and simple to operate. However, care must be taken in relating evaporation from pans to actual ET, especially in arid climates. Because of the smaller aerodynamic roughness of water surfaces relative to vegetative surfaces, the former will extract less sensible heat energy from the passing air. Thus pans may at times, show less evaporation than ET from vegetation (Rosenberg, 1983).

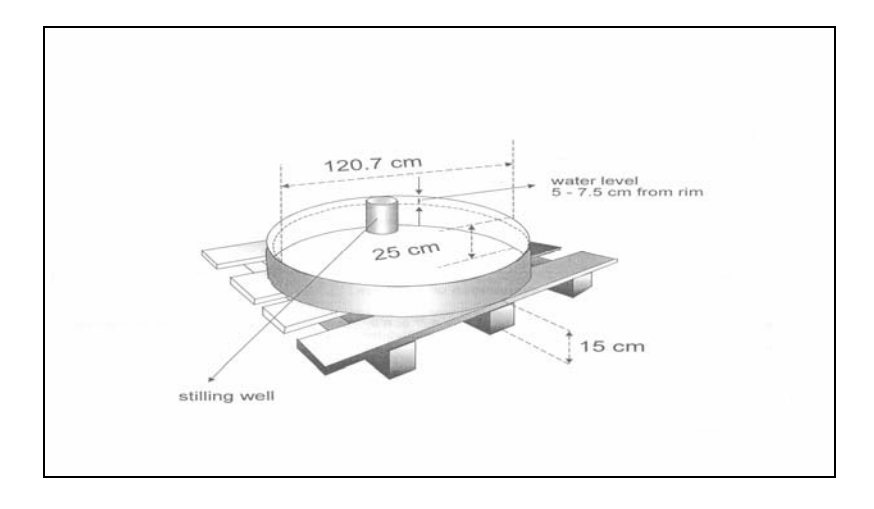


Figure 2.4: A Class A evaporation pan (Allen et al., 1999)

2.6.1.5 Problems related to ET estimation of greenhouse crops

The problem encountered in greenhouse crop ET estimation is that inside microclimate is affected by the outside climate, the type of greenhouse, the climate control strategy and the feedback between the crop and the inside microclimate. The concept of potential evapotranspiration for greenhouse crop often leads to misleading interpretations. Many authors have intended to propose calculation methods based on outside weather variables, eluding the fact that the outside climate is often poorly coupled to the internal microclimate. The concept of reference evapotranspiration is also somewhat difficult and delicate to be applied to greenhouse crops water requirements, because the two "reference" crops (grass, alfalfa) are not commonly grown in greenhouse production. The data from pan evaporimeters are affected by the spatial heterogeneity of greenhouse climate and the proximity and continuous evolution of the vegetation.

Another problem is inherent to the crop coefficient, K_c. Stanghellini et al.(1990) developed an analytical formulation of K_c, expressed as the ratio of the theoretical crop transpiration assuming maximal crop conductance to a given reference evapotranspiration . They showed for greenhouse tomato crops that this coefficient is a function of crop parameters, leaf area and prevailing weather, and that it is a coincidence that the crop coefficient in greenhouse crops was almost constant in its seasonal trend, due to the combination of two opposite effects. All these considerations suggest that the use of physically-based formulations of ET that take into account both crop parameters (such as maximal conductance) and the prevailing climatic regime in the greenhouse seem to be preferable to other empirical methods. However, these specific crop parameters are not

available for all the main species grown under greenhouses. That is why the classical methods based on a given reference ET and crop coefficient are still largely used for estimating water requirements of greenhouse crop, although their shortcomings are now well recognized.

2.6.2 Soil Moisture Based Methods

2.6.2.1 Available water capacity and plant available water

The available water capacity (AWC) defines the amount of water in a soil that is nominally available for plant growth. The upper limit is set by the field capacity (FC) and the lower limit as the value of θ at which plants lose turgor and wilt, that is, the permanent wilting point (PWP). In some extensive cropping systems, such as for vegetables, orchards and vineyards, the concept of readily available water (RAW) is also used. RAW is defined as the amount of water held between FC and matric potential (ψ m) values of -40 to -60 kPa, depending on the age of the plants and the soil texture.

2.6.2.1 .1 Lysimetry

Lysimeters are large blocks of soil isolated from, but as identical as possible with, surrounding soils. According to Pelton (1961), lysimeters were first used to study the percolation of water through soils. It was not until the twentieth century that modification in lysimeter design was made to permit the study of evapotranspiration. Different types of lysimeters range widely in the accuracy with which changes in the soil water content are detected. The most accurate lysimeters can detect losses as small as 0.01 mm of water and can be used to accurately detect ET rates over time periods shorter than 1h

(measurements over 5-10 min periods have been reported). Other lysimeters are only sensitive enough to detect changes that occur over a day or longer.

Lysimeters provide the only direct measure of water flux from a vegetative surface. As such, they provide a standard against which other methods can be tested and calibrated. To provide reliable measurement of ET, lysimeters should meet the following criteria (Pelton, 1961):

- 1. They should be constructed so that moisture relationships inside the lysimeter correspond closely to those of soils under natural conditions.
- 2. The lysimeters should be sufficiently deep to extend well below the plant root zone or should use a tensioning device at the bottom of the soil column to maintain moisture at or near the same level as surrounding areas.
- 3. Lysimeters should be managed in exactly the same manner as the surrounding area.
- 4. The ratio of the wall surface area to the enclosed lysimeter area should be small to avoid small-scale advection from the uncropped surface.
- 5. Common types of lysimeters are
 - potential evapotranspirometers
 - floating lysimeters
 - weighing lysimeters

2.6.2.1.2 Gravimetry

Soil wetness is characterized by the amount of water held in a certain mass or volume of soil; that is:gravimetric water content (θ_g), measured by drying the soil to a constant weight at a temperature of 105° C. θ_g is then calculated from

 θ_g = mass of water / mass of oven dry soil (2.23)

 θ_g (units of g H₂O/g oven dry soil) is often expressed as a percentage by multiplying by 100. Structural water, which is water of crystallization held in soil minerals, is not driven off at 105°C and is not measured as soil water.

2.6.3 Plant based methods

2.6.3.1 Sap flow gauges

2.6.3.1.1 Stem heat balance (SHB) theory

The SHB method requires a steady state and a constant energy input from the heater strip inside the gauge body. Therefore the stem section must be insulated from changes in the environment. For the same reason, the gauge time constant is limited from five minutes to an hour, depending on the flow rate and the stem size. The Dynamax loggers have a power down mode so that power is preserved from overheating. During the power down mode and at the transitions to power on, the sap flow is not computed to maintain the accumulated flow accurately during this unbalanced transition.

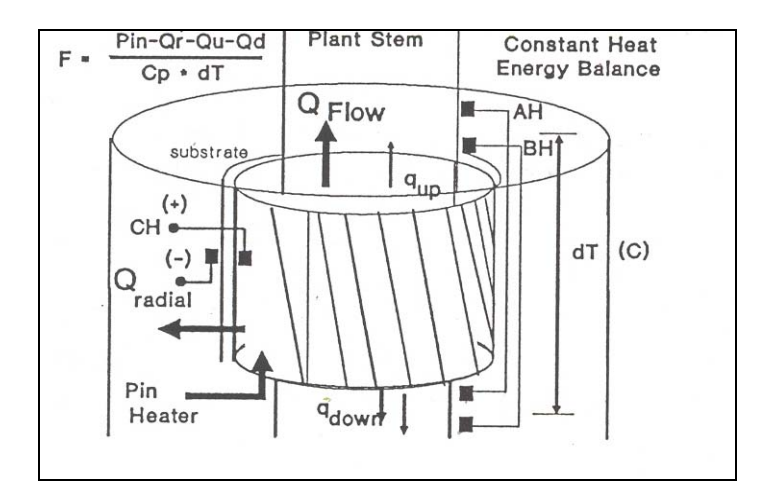


Figure 2.5: Stem Gauge Schematic (van Bavel, 1987)

Figure 2.5 shows a stem section and the possible components of heat flux, assuming no heat storage. The heater surrounds the stem under the stem under test and is powered by a DC supply with a fixed amount of heat; Qh. Qh is the equivalent to the power input to the stem from the heater, Pin. Qr is the radial heat conducted through the gauge to the ambient. Qv, the vertical or axial heat conduction through the stem has two components, Qu and Qd. By measuring Pin, Qu,Qd and Qr, the remainder, Qf can be calculated. Qf is the heat convection carried by the sap. After dividing by the specific heat of water and the sap temperature increase, the heat flux is converted directly to mass flow rate.

Energy balance equations:

The energy balance is expressed as:

$$Pin = Qr + QV + Qf(W)$$
....(2.12)

$$Pin = V^2/R$$
 from Ohms law.....(2.13)

Fourier's law describes the vertical conduction components:

$$Qv = Qu + Qd$$

Where
$$Qu=K_{st}AdT_u/dX$$
....(2.14)

$$Qd = K_{st}AdT_d/dX...(2.15)$$

Where Kst is the thermal conductivity of the stem (W/m*K); A is the stem cross sectional area (m2); the temperature gradients are dT_u/dX (K/m) and dT_d/dX ; dX is the spacing between thermocouple junctions (m). One pair of thermocouples is above the heater and one pair is below the heater as shown on the schematic in figure 2.6.

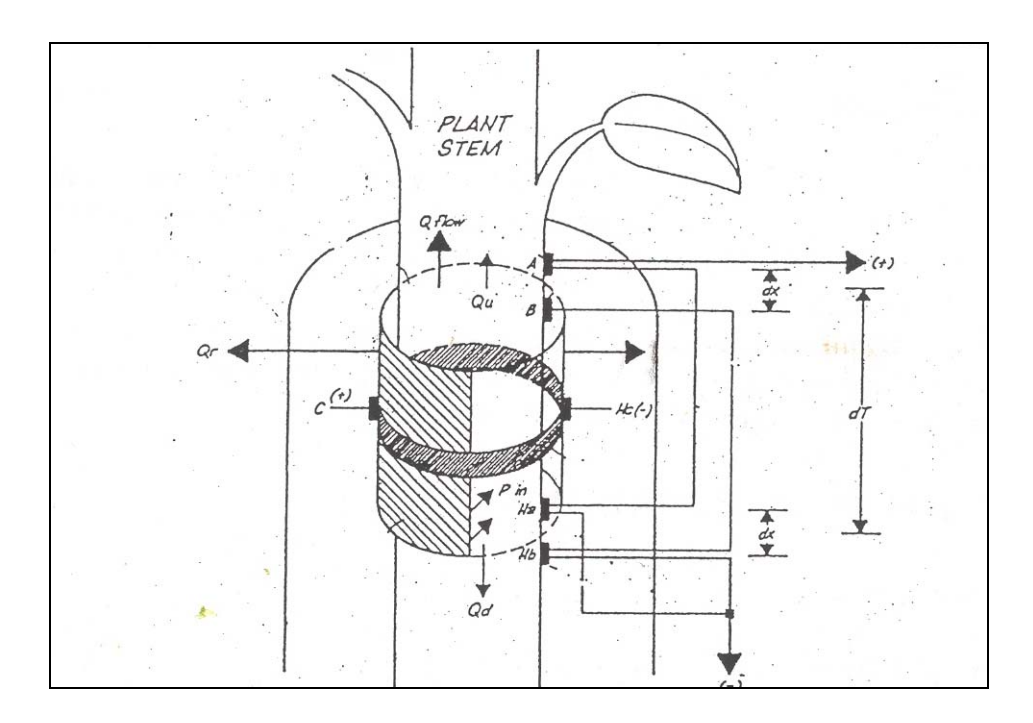


Figure 2.6: Dynagage schematic diagram (van Bavel, 1987)

There are two differentially wired thermocouples both measuring the rise in sap temperature. Channel AH measures the difference in temperature A-Ha (mV). Channel BH measures the difference in temperature B-Hb (mV). By subtraction of these two signals:

$$BH-AH = (B-Hb)-(A-Ha) = (B-A) + (Ha-Hb)$$
 (mV)

The result yields the two components of axial heat conduction out of the stem section, Qu and Qd. Since the distance, dX, separating the upper TC pair and lower TC pair are fixed by design for each particular gauge to the same value; the components of Qv are combined with a common denominator:

$$Qv = KstA(BH-AH)/dX*0.040 \text{ mV/C}$$

The factor 0.040mV/C converts the thermocouple differential signals to degrees C. Kst values are given for varying stem conductivity: 0.42 W m⁻¹K⁻¹ (woody stem), 0.54 W m⁻¹K⁻¹ (herbaceous), and 0.28 W m⁻¹K⁻¹ (hollow).

2.6.3.1.2 Sap thermodynamics

After solving equation (2.12) for Qf, the flow rate per unit of time is calculated from the equation for flow as described by Sakuratani (1981) and Baker-Van Bavel (1987). This equation takes the residual of the energy balance in Watts, and converts it to a flow rate by dividing by the temperature of the sap and the heat capacity of water. Water is 99% of the sap content and it is safe to assume the heat capacity, Cp, is constant to all stems. It is understood that a watt being 1 joule/second, will be converted to a flow rate when divided by 4.186 joules/ gram-deg C, and is divided by the temperature increase in C.

$$F = (Pin-Qv-Qr)/Cp*dT (g/s)....(2.16)$$

In equation 2.16 the radial heat loss is computed in by:

$$Qr = Ksh * CH.....(2.17)$$

Ksh is the thermal conductance constant for a particular gauge. Cp is the specific heat of water (4.186 J/g*C), and dT is the temperature increase of the sap. The temperature increase of the sap, dT is measured in mV by averaging the AH and BH signals, and then converted to degrees C by dividing by the thermocouples temperature conversion constant as follows:

$$dT = \frac{(AH + BH)/2(mV)}{0.040mV/C}$$

2.6.3.1.3 Ksh calculation

The sheath conductance is calculated when the user establishes a no-flow condition. The ksh algorithm is derived from flow calculation steps, and it is computed every scan period, then averaged every 30 minutes. Although the Ksh calculation is computed during the day, and may have high values at high flow and negative values when Qr heat is negative (inward heat flux), Ksh has no meaning except when the flow is zero. The

condition for Ksh is determined by solving equation (2.17) when setting Qf =0 as follows:

$$Pin = Qr+Qv$$

And
$$Qr = Ksh(CH) = Pin - Qv$$

So after computing Pin and Qv,

$$Ksh = (Pin - Qv)/(CH) (W/mV)....(2.18)$$

2.6.3.2 The trunk sector heat balance method

The trunk sector heat balance method of sap flow measurement is intended for use on tree trunks with diameters larger than 120 mm. like the stem heat balance method it is based on the principle that sap flow rates can be determined from the heat balance of heated stem tissue. However, in the trunk sector heat balance method, heat is applied internally to only a segment of the trunk, rather than superficially to the entire circumference. The measurement system can be purchased commercially.

2.6.3.2.1 Theory of operation

An alternating current (1.5 kHz) converted from a 12V Dc supply, is applied to the five electrodes embedded in the tree trunk, so that the electrical impedance of the woody tissue causes the four segments of sapwood bounded by electrodes to be heated. The use of an AC supply ensures that electrochemical effects in the tissue are avoided (Kucera et al., 1977). The trunk is insulated and shielded from radiation, so that the heat balance of the trunk sector is (Cermak et al., 1973)

$$P = q_v + q_r + q_l + q_f (2.19)$$

Here P is the electrical power dissipated as heat in the trunk sector, q_v is heat lost vertically by conduction, q_r is heat lost radially inwards to the non-conducting heartwood and outwards to the cambium and bark, q_l is the heat lost laterally into neighbouring sapwood by conduction; and q_f is heat loss by convection in the moving sap stream. The mass flow rate of sap is determined from the value of q_r for the two segments at the centre of the heated zone, which is evaluated by accounting for all other terms in equation 2.18.

Two versions of the instrument have been used (Cermak et al., 1984); in the first, which is the version available commercially, P is constant (Cermak et al., 1973), whereas in the second, a constant value of ΔT is maintained by automatic regulation of the power supply (Kucera et al., 1977). In both systems, P is determined by measurement of the potential drop across the electrodes and the current supplied (Cermak et al., 1976), while ql is assumed to be negligible because 'active thermal insulation' of the two central segments. Lateral heat losses are eliminated from the heat balance of these segments because the adjoining segments are heated to the same temperature, so that lateral temperature gradients do not occur and lateral heat losses by conduction are avoided (Cermak et al., 1973). The remaining heat losses by conduction, q_r and q_r , are accounted for together. In the constant power, q_v+q_r is found from

$$q_v + q_r = K_{vt} \Delta T \tag{2.19}$$

where K_{vt} is a thermal conductance coefficient which must be evaluated during periods when there is no sap flow. The value of K_{vt} accounts for the thermal conductivity of the tissue and insulation materials surrounding the heated zone, as well as the distance between thermocouples, so it must be evaluated for each new installation. From equation $2.18 \ q_v + q_r$ when sap flow is zero (assuming $q_1 = 0$), so that K_{vr} can be found from

$$K_{vr} = P_o / \Delta T_o \qquad (2.20)$$

where P_o and ΔT_o are values of P and ΔT measured when sap flow is zero. For the constant temperature system, ΔT is constant and so $q_v + q_r$ can be assumed to be constant, with a value of P_o .

With all other components of the heat balance of the trunk sector accounted for, qr is calculated by difference using equation 6 and converted to rate of mass flow through the central segments of the heated zone $(F_{m,c})$ by

$$F_{m,c} = q_f / c_s \Delta T \qquad (2.21)$$

where c_s is the specific heat capacity of sap, which is assumed equal to that of water, $F_{m,c}$ is then multiplied by the ratio of the width of the two central segments to the entire stem circumference to estimate sap flow for the whole tree (Cermak et al., 1976). Where there is substantial variation should be made at more than one location on the circumference of the trunk in order to reduce errors in estimates of flow for the whole tree (Cermak et al., 1995).

2.6.3.3 Heat-pulse method

With the heat method, rates of sap flow are measured by determining the velocity of a short pulse of heat carried by the moving sap stream, rather than the heat balance of a heated stem. The method is suitable only for use on woody stems. Heater and sensor probes must be installed by drilling holes into the sapwood, so that its use is limited to stems that are large enough to accommodate these, but not so large that the full depth of sapwood cannot be accessed; generally, it can be used on stems with diameters larger than about 30 mm. Two heat-pulse systems are commercially available.

2.6.3.3.1 Theory of operation

The heat pulse technique is based on the compensation principle; the velocity of sap ascending a stem is determined by compensation of the measured velocity of a heat pulse for the dissipation of heat by conduction through the matrix of wood fibres, water and gas within the stem (for a historical view, Swanson,1994) with modern instrumentation, this is accomplished by deploying the sensor probes at unequal distance upstream and downstream for the heater probe, with the upstream sensor placed nearer to the heater than the downstream sensor (Swanson and Whitfield, 1981; Swanson, 1994). Immediately after release of a pulse of heat of 1-2s duration, the temperature becomes higher at the closer, upstream sensor than at the downstream sensor because of conduction; but heat carried by the moving sap then quickly warms the downstream sensor, so that the temperature of the two sensors is again equal after a time (t_e) in the order of 60s. This is the time required for convection in the moving sap stream to move the peak of the heat pulse from the heater to the point midway between the two

temperature sensors, so that t_e decreases as sap velocity increases. The velocity of the heat pulse (v_h) is thus given by Swanson and Whitfield, 1981.

$$v_h = (x_d - x_u)/2t_e$$
 (2.22)

2.6.3.4 Leaf thickness

A number of instruments are available for the routine monitoring of leaf thickness, which is known to decrease as turgidity decreases. Approaches include direct measurement using linear displacement transducers (e.g. LVDTs [Burquez, 1987] or capacitance sensors or through measurements of leaf 'superficial density' using β-ray attenuation (Jones, 1973). Unfortunately, leaf thickness is frequently even less sensitive to changes in water status than is leaf water content because, especially with younger leaves, a fraction of leaf shrinkage is often in the plane of the leaves rather than in the direction of the sensor (Jones, 1973).

2.6.3.5 Stem and fruit diameter

Stem and fruit diameter fluctuate diurnally in response to changes in water content, and so suffer from many of the same disadvantages as other water status measures. The diurnal dynamics of changes in diameter, especially of fruits, have been used to derive rather more sensitive indicators of irrigation need, where the magnitude of daily shrinkage has been used to indicate water status, and comparisons of diameters at the same time on succeeding days give a measure of growth rate (Huguet et al., 1992; Li and Huguet, 1990; Jones, 1985). Although changes in growth rate provide a particularly sensitive measure of plant water stress, such daily measurements are not particularly useful for the control of high frequency irrigation systems. Several workers have

achieved promising results for low frequency irrigation scheduling by the use of maximum daily shrinkage (MDS). For example, Fereres and Goldhamer (2003) showed that MDS was a more promising approach for automated irrigation scheduling than was the use of stem water potential for almond tres, while differences in maximum trunk diameter were also found to be particularly useful in olive (Moriana and Fereres, 2002). The use of such dendrometry or micromorphometric technique has been developed into a number of successful commercial irrigation scheduling systems (e.g. Pepista 4000', Delta International, Montfavet, France); these are usually applied to the study of stem diameter changes. Selles and Berger (1990) reported that variations in trunk diameter or stem water potential were more sensitive as indicators of irrigation need than was the variation in fruit diameter.

2.6.3.6 γ -ray attenuation

A related approach to the study of changes in stem water content was the use of γ – ray attenuation (Brough et al., 1986). Although this was shown to be very sensitive, safety considerations and cost have largely limited the further application of this approach.

2.7 Different irrigation methods

Various methods of irrigation are used by farmers depending on water availability, the type of irrigated crop and the financial investment the grower is intending to make. A thorough knowledge regarding the irrigation techniques available can help give information on the different types of deficit irrigation.

2.7 .1 Drip irrigation

While drip irrigation may be the most expensive method of irrigation, it is also the most advanced and efficient method in respect to effective water use. Usually used to irrigate fruits and vegetables, this system consists of perforated pipes that are placed by rows of crops or buried along their root lines and emit water directly onto the crops that need it. As a result, evaporation is drastically reduced and 25% irrigation water is conserved in comparison to flood irrigation. Drip irrigation also allows the grower to customize an irrigation program most beneficial to each crop. Water high in salts should be filtered before use since they may clog the emitters and create a local buildup of high salinity soil around the plants.

2.7 .4 Spray irrigation

The more modern spray irrigation in all its various forms is a more expensive type of irrigation, requiring more complex machinery than flood irrigation, but it utilizes water more efficiently, reducing the amount of water needed to irrigate a field. Even more water is lost through evaporation in spray irrigation compared to flood irrigation and plant diseases due to excess moisture can occur at overwatering. In spray irrigation systems, a long hose is set to a water source on one side and on the side reaching the field, water is released through spray guns.

The center-pivot system is an efficient way to irrigate a large field with minimum machinery. This system is built of many triangular metal frames on wheels that hold the central hose above the field. The hose transports water from a pump at the center of the system and water is sprayed through sprinklers along the tube. The whole structure circulates the field spraying water, with the water source as the center of the circle. The disadvantages of this method, and other types of traditional spray irrigation, are the electric motors needed to help the system roll in a circle and the large amounts of water

(about 35%) that evaporate or get blown away by winds before they even reach the ground.

The Low Energy Precision Application (LEPA) center pivot system is a more efficient irrigation method than the conventional pivot system, boosting the irrigation efficiency from about 60% to more than 90%. This rise in effectiveness is also due to the decline in the electricity usage, but mostly because the water is applied directly onto the crops and not sprayed out into the air. This system also consists of a central hose, but instead of high power sprinklers, pipes hang from the central hose and attached to the bottom of each pipe, very close to the ground, is a nozzle that sprays water directly onto the crops. This way, less water is lost through evaporation compared to traditional spray irrigationmore than 90% of the water applied is used by the crop and less electricity is required.

2.8 Automation of irrigation controls

The most widespread use of automated irrigation scheduling systems is in the intensive horticultural, and especially the protected cropping, sector (Jones 2004). In general, the automated systems in common use are based on simple automated timer operation, or in some cases the signal is provided by soil moisture sensors. For timer-based operation many systems simply aim to provide excess water to runoff at intervals (e.g. flood-beds or capillary matting systems), although some at least attempt to limit water application by only applying enough to replenish evaporative losses (often calculated from measured pan evaporation; Allen et al., 1999). Much greater sophistication is required if an objective is to improve the overall irrigation water use efficiency or to apply an RDI (regulated deficit irrigation) system. Most of the remaining automated systems currently

in operation base control on soil moisture sensing; at least this approach has the potential for greater precision and improved water use efficiency (Jones, 2004).

The use of expert systems (Plant et al., 1992) which integrate data from several sources appears to have great potential for combining inputs from thermal or other crop response sensors and environmental data for a water budget calculation to derive a robust irrigation schedule. Among the various plant-based sensors that have been incorporated into irrigation control are stem diameter gauges (Huguet et al., 1992), sap-flow sensors (Schmidt and Exarchou, 2000) and acoustic emission sensors (Yang et al., 2003) though there has been most interest in the application of thermal sensors. For example Kacira and colleagues (Kacira and Ling, 2001; Kacira et al., 2002 have developed and tested on a small scale automated irrigation controller based on thermal sensing of plant stress. Similar approaches have been applied in the field: for example, Evanset al.(2001) and Sadler et al. (2202) mounted an array of 26 infrared thermometer (IRTs) on a centre pivot irrigation system which they used to monitor irrigation efficiency, but had not developed the system to a stage where it could be used for fully automated control. Coloaizzi et al. (2003) have tested another system that includes thermal sensing of canopy temperature on a large linear move irrigator (where the irrigator moves across the field). In another approach to the use of canopy temperature that makes use of the thermal kinetic window, Upchurch et al. (1990) and Mahan et al. (2000) have developed a 'biologically identified optimal temperature interactive console' for the control of trickle and other irrigation systems based on canopy temperature measurements. In this direct control system, irrigation is applied as canopy temperature exceeds a crop-specific optimum.

2.8.1 Irrigation control systems

In recent years, a variety of sophisticated features has been incorporated into residential irrigation controllers. A controller is an integral part of an irrigation system. It is an essential tool to apply water in the necessary quantity and at the right time to sustain agricultural production and to achieve high levels of efficiency in water, energy and chemical uses. An irrigation controller is responsible for selectively turning on and off a set of sprinkler valve stations. When properly utilized some of these features can contribute to an irrigation system that makes more efficient use of the available water resource. An irrigation controller is a device used to control, electrically or otherwise, operated valves, which control the flow of water to sprinkler heads and drip lines in an irrigation system. A single irrigation valve typically controls the flow of water to a specific area of a landscape. A computer-based control system consists of a combination of hardware and software that acts as a supervisor with the purpose of managing irrigation and other related practices such as fertigation and maintenance. This is done by the use of a closed control loop. A closed control loop performs the following tasks 1) monitoring the state variables, 2) comparing the state variables with their desired or target state, 3) deciding what actions are necessary to change the state of the system, and 4) carrying out the necessary actions. Performing these functions requires a combination of hardware and software that must be implemented for each specific application. The output device is interfaced with the control program to enable at least one specific functionality in response to a predetermined input received from the user through the input device.

2.8.3 Micro controller- based systems

The micro-controller based system includes an irrigation control processor. The control

processor consists of an input port, an output port, a memory element for storing a control

program and control parameters. The control program is responsible for implementing a

plurality of functionalities that are selectively enabled, a processing unit for executing the

control program, and a bus connecting the processing unit to the memory element and to

the input and output ports. An input device (sensor) is interfaced with the input port and

the output port provides an interface with the sprinkler valve stations for controlling the

turning on and off of the sprinkler valve stations. The operation of a microcontroller

depends entirely on a series of fetching, and then executing, the correct instructions from

the memory. The instruction decoder in the control unit decodes the instruction. Two or

more instructions can be fetched from different memory locations and certain arithmetic

or logic operations performed on them in the ALU. The result of which can be stored in a

different register. An instruction thus fetched from program memory must be decoded to

determine the assigned or user defined task that has to be executed.

KEY

INSTR: INSTRUCTIONS

ADDR: ADDRESS

ACC: ACCUMULATOR

PC: PROGRAM COUNTER

OSC: OSCILLATOR

I/O: INPUT/OUTPUT

WDT: WATCHDOG TIMER A/D: ANALOG-TO-DIGITAL

37

As instructions may within themselves contain assignments, which require different transfers of data from one memory into another, from memory onto ports, or some other calculations, the control unit is connected with all the other parts of the microcontroller through a data bus, a control bus and an address bus.

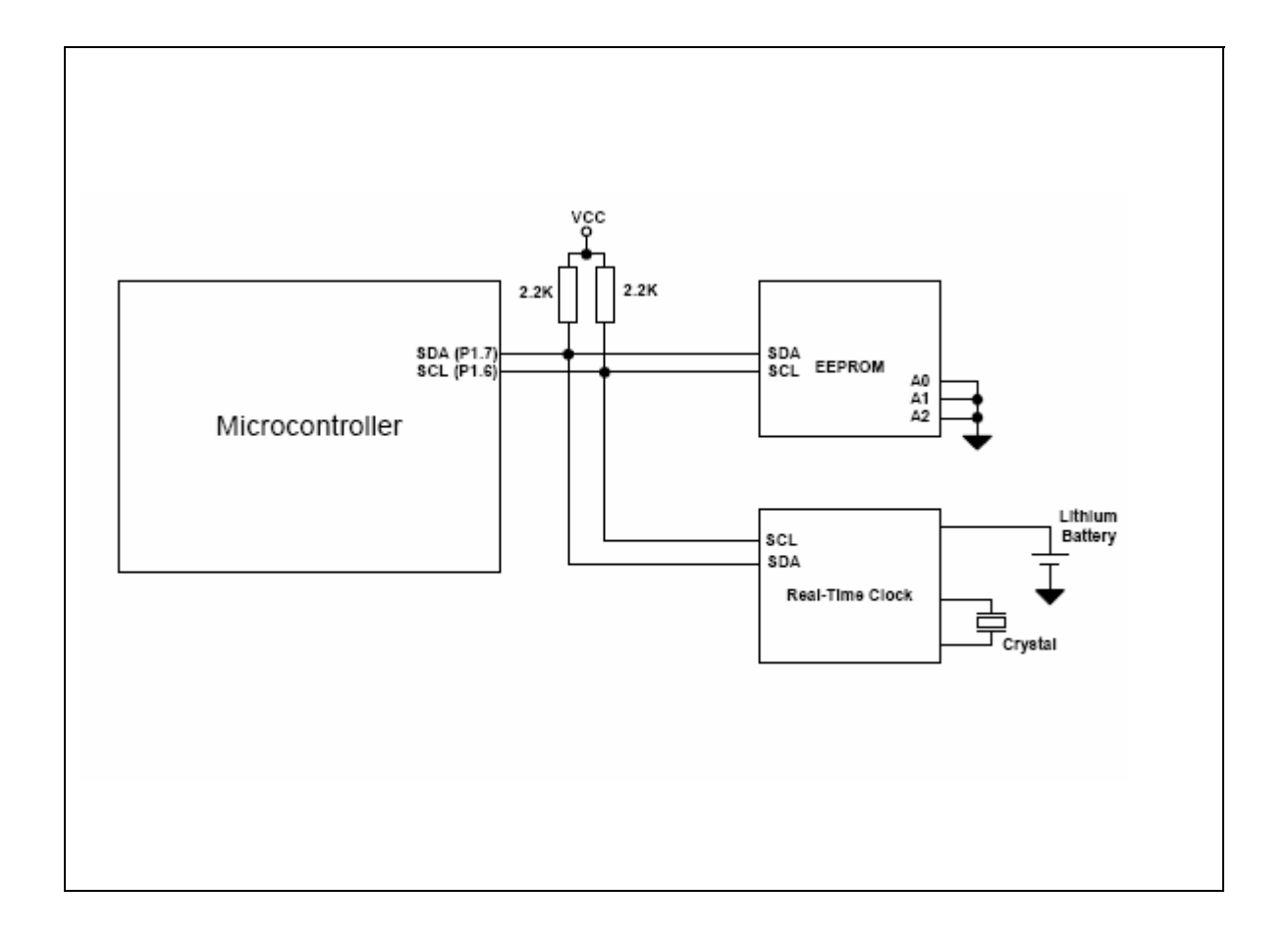


Figure 2.5: Micro-controller based systems

A clock from the oscillator that drives the microcontroller controls the execution of an instruction. The internal circuit of a microcontroller divides the clock into four even clocks Q1, Q2, Q3, and Q4. These four clocks make up one instruction cycle, called machine cycle, during which one instruction is executed. The execution of instruction

starts by calling an instruction from its memory location. The instruction is called from the program memory on every Q1 and is written in instruction register on Q4. Decoding and executing the instruction is done between the next Q1 and Q4 cycles

2.8.4 A computer based systems

Microprocessors have found great application in instrumentation, industrial control and aerospace. Microprocessors are used to handle a set of tasks that control one or more external events or systems. Microprocessors substitute programmed logic for hard-wired logics. The programmed logic can be placed into a semiconductor read only memories (ROMs), which have a very regular structure and hence offers even greater functionality per chip. It has been shown that a ROM can replace a large number of standard logic gates. Once the basic microprocessor module is built, a large number of logic power can be added with only a few additional integrated circuits. The other or older technique of implementing the logic product in the inter-connection of the standard hardware, is with the logic stored in a ROM. This has permitted the designer to place nearly all of his product logic in a very small portion of the design tool. That is, the logic is in a few integrated circuits rather than diffused throughout the design in wiring. With the logic concentrated in only a few components, a high degree of design flexibility is possible⁴. Applications, problem-oriented architectures with an optimum instruction set for each use are in great demand to improve system performance and efficiencies. The Central Processing Unit (CPU) usually contains an execution core with two or more pipelines, a data and address bus, a dedicated arithmetic logic unit (ALU, also called the math coprocessor), and in some cases special high-speed memory for caching program instructions from RAM .

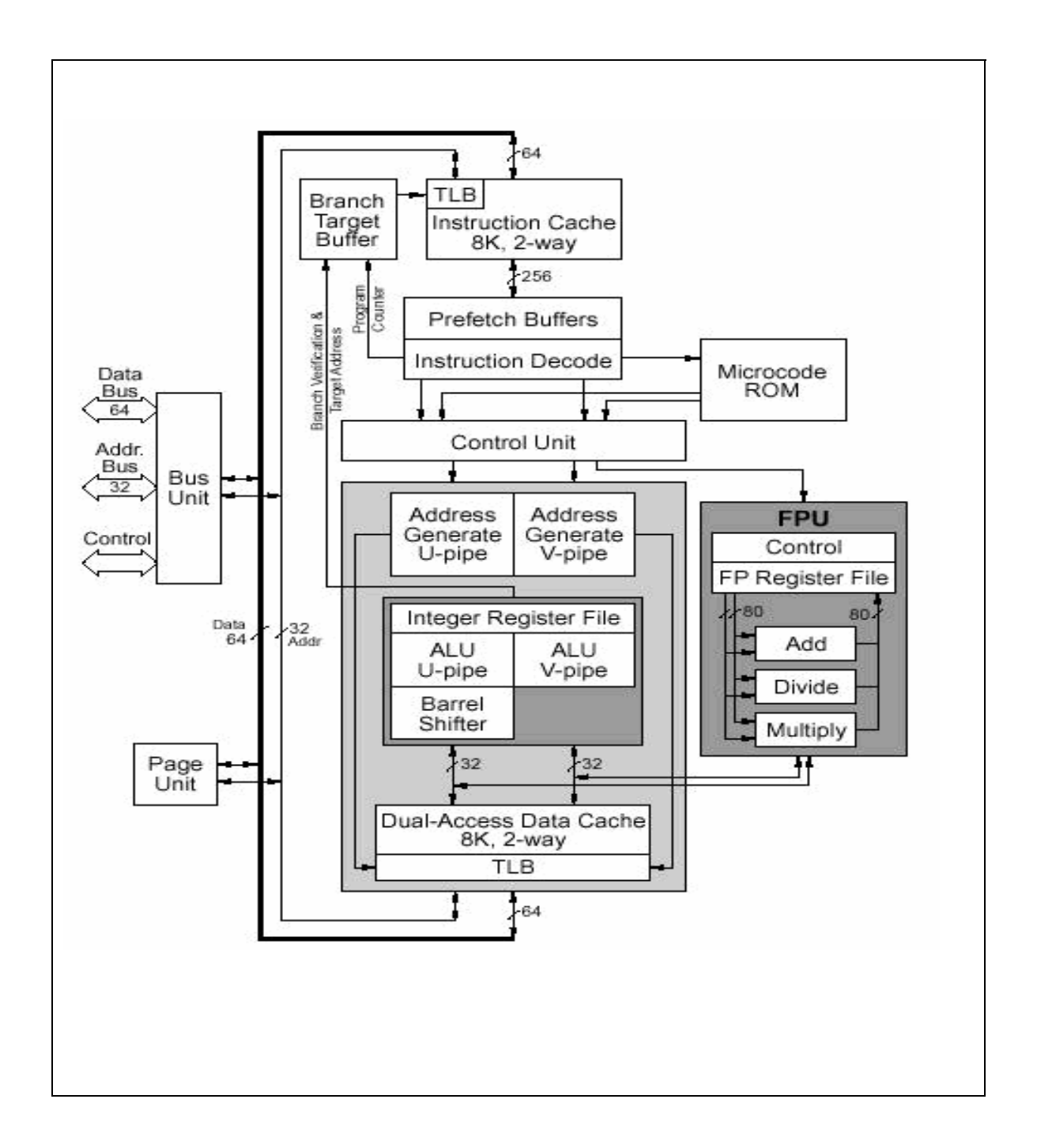


Figure 2.6: Pentium block diagram

2.8.1 Wireless technology in Greenhouse monitoring

Using wireless sensor networks within the agricultural industry is increasingly common. Gravity fed water systems can be monitored using pressure transmitters to monitor water tank levels, pumps can be controlled using wireless I/O devices, and water use can be measured and wirelessly transmitted back to a central control center for billing. Irrigation automation enables more efficient water use and reduces waste.

Wireless sensor networks are also used to control the temperature and humidity levels inside commercial greenhouses. When the temperature and humidity drops below specific levels, the greenhouse manager must be notified via e-mail or cell phone text message, or host systems can trigger misting systems, open vents, turn on fans, or control a wide variety of system responses. Because some wireless sensor networks are easy to install, they are also easy to move as the needs of the application change.

2.9 Analogue to digital signal conversion

2.9.1 Resolution

The resolution of the converter indicates the number of discrete values it can produce over the range of analog values. The values are usually stored electronically in binary form, so the resolution is usually expressed in bits. In consequence, the number of discrete values available, or "levels", is usually a power of two. For example, an ADC with a resolution of 8 bits can encode an analog input to one in 256 different levels, since $2^8 = 256$. The values can represent the ranges from 0 to 255 (i.e. unsigned integer) or from -128 to 127 (i.e. signed integer), depending on the application.

Resolution can also be defined electrically, and expressed in volts. The voltage resolution of an ADC is equal to its overall voltage measurement range divided by the number of discrete intervals.

Where:

Q is resolution in volts per step (volts per output codes less one),

 E_{FSR} is the full scale voltage range = $V_{RefHi} - V_{RefLow}$,

M is the ADC's resolution in bits.

N is the number of intervals, (one less than the number of available levels, or output codes), which is: $N = 2^M - 1$

Some examples may help:

• Example 1

- Full scale measurement range = 0 to 10 volts
- o ADC resolution is 12 bits: $2^{12} = 4096$ quantization levels (codes)
- \circ ADC voltage resolution is: (10V 0V) / 4095 steps = 10V / 4095 steps

• Example 2

- \circ Full scale measurement range = -10 to +10 volts
- o ADC resolution is 14 bits: $2^{14} = 16384$ quantization levels (codes)
- \circ ADC voltage resolution is: (10V (-10V)) / 16383 steps = 20V / 16383

• Example 3

- Full scale measurement range = 0 to 7 volts
- \circ ADC resolution is 3 bits: $2^3 = 8$ quantization levels (codes)

o ADC voltage resolution is: (7 V - 0 V)/7 steps = 7 V/7 steps = 1 V/ step = 1000 mV/step

In practice, the smallest output code ("0" in an unsigned system) represents a voltage range which is 0.5Q, that is, half the ADC voltage resolution (Q), as does the largest output code. The other N-2 codes are all equal in width and represent the ADC voltage resolution (Q) calculated above. Doing this centers the code on an input voltage that represents the M th division of the input voltage range. Doing this the "1" code spans a voltage range from 0.5 to 1.5 V, the "2" code spans a voltage range from 1.5 to 2.5 V, etc. Thus, if the input signal is at 3/8 ths of the full-scale voltage, then the ADC outputs the "3" code, and will do so as long as the voltage stays within the range of 2.5/8 ths and 3.5/8 ths. This practice is called "mid-tread" operation. The exception to this convention seems to be the Microchip PIC processor, where all M steps are equal width. This practice is called "Mid-Rise with Offset" operation. In practice, the useful resolution of a converter is limited by the best signal-to-noise ratio that can be achieved for a digitized signal. An ADC can resolve a signal to only a certain number of bits of resolution, called the effective number of bits (ENOB). One effective bit of resolution changes the signalto-noise ratio of the digitized signal by 6 dB, if the resolution is limited by the ADC. If a preamplifier has been used prior to A/D conversion, the noise introduced by the amplifier can be an important contributing factor towards the overall SNR.

2.9.2 Response type

2.9 2.1 Linear Analogue to digital conversions (ADCs)

Most ADCs are of a type known as linear. The term linear as used here means that the range of the input values that map to each output value has a linear relationship with the output value, i.e., that the output value k is used for the range of input values from

$$m(k+b)$$
 to $m(k+1+b)$,

where m and b are constants. Here b is typically 0 or -0.5. When b=0, the ADC is referred to as mid-rise, and when b=-0.5 it is referred to as mid-tread.

2.9.2.2 Non-linear ADCs

If the probability density function of a signal being digitized is uniform, then the signal-to-noise ratio relative to the quantization noise is the best possible. Because this is often not the case, it is usual to pass the signal through its cumulative distribution function (CDF) before the quantization. This is good because the regions that are more important get quantized with a better resolution. In the dequantization process, the inverse CDF is needed. This is the same principle behind the companders used in some tape-recorders and other communication systems, and is related to entropy maximization.

For example, a voice signal has a Laplacian distribution. This means that the region around the lowest levels, near 0, carries more information than the regions with higher amplitudes. Because of this, logarithmic ADCs are very common in voice communication systems to increase the dynamic range of the representable values while retaining fine-granular fidelity in the low-amplitude region. An eight-bit A-law or the μ -



CHAPTER 3: MATERIALS AND METHODS

3.1 Introduction

In this chapter, the experiments and the materials or apparatus used to achieve the intended objectives are discussed. The project was divided into three parts. The first part involves the setting up of automatic weather stations outside and inside the greenhouse. Under the first part was the monitoring of sap flow rates under different conditions. The second part of the project consists of the designing and the implementation of the automatic irrigation control system. The last part of the project comprises the investigative treatments in which the control system was compared with traditional methods of measuring evapotranspiration rate in crops.

3.2 Experimental site

The experiments were all carried out at the University of Zimbabwe (UZ) in Harare (17.8°S, 31.1°E and altitude 1483 m). The project was done in two places: the Agricultural meteorology laboratory in the Physics Department and at an experimental greenhouse in Biological Science Department. Calibrations of sensors and the preliminary tests were carried out in the laboratory. The implementation of the control system and the assessment of its performance were done at the greenhouse.

3.2.1 The greenhouse

The experimental greenhouse Figure 3.1 was located at the Biological Science department, UZ and was a single-span, Venlo-type greenhouse whose cladding material was single-layered glass. The floor was concrete. The greenhouse structure and its

orientation are shown in figure 3.1. It was oriented along North-South direction and half of it was used for the experiments. The greenhouse had a floor area of 10 m x 12 m and the roof has centre beam height of 4.46m from the ground and side height of 2.90 m from the ground.



Figure 3.1: The greenhouse in the Biological Science Department, University of Zimbabwe

3.3 Plant material and agronomic operations

Tomato plants, species Nemo Netta were planted on the 14th of September 2009. The seedlings were planted in a soilless medium, Vermiculite. Vermiculite was specifically

used for advantages, which, among others include:

- 1) enhanced control of water and fertilizer applications,
- 2) optimal moisture in the substrate,
- 3) optimal nutrient supply and,
- 4) Disinfecting between growing seasons.

However Vermiculite also has several disadvantages which include, among others the following:

- 1) low root volume
- 2) low nutrient and
- **3)** Fast changes in pH and salinity control.

The Vermiculite was put in 20litre buckets. Altogether, 128 buckets were used covering the northern half of the greenhouse. Fertilizers were applied according to a schedule given in Table 3.1.

Table 3.1: Program for the application of fertilizers

WEEK	Quick	QUICK	BEST	CALCIUM	AMMONIUM	Nutrifoil
	START	GROW	BLOOM	NITRATE	NITRATE	NO1
3-6	1.125	1.25	0	0.25	0	4ml/L
7-10	0.4375	0	2.125	3.125	0.5	0
11-14	0	5	1.25	5.875	0.5	4ml/L
15-25	0	0	10	5.875	0.625	4ml/L
26-30	0	5	1.25	1.25	0.625	4ml/L

3.4 Instruments used

3.4.1 Meteorological instruments

The following instruments were used in this study:

- REBS (Radiation Energy Balance Systems) net radiometer,
- A tube solarimeter,
- HMP 45C Vaisala temperature-humidity sensor,
- Wind, heated bead testo 425 anemometer,
- A matrix sensor,
- Photosynthetically active radiation (PAR) quantum sensor,
- A CR23X Campbell Scientific (CSL) datalogger,

3.4.2 Radiation Energy Balance (REBS) net radiometer

The Q-7.1 is a high-output thermopile sensor which measures the algebraic sum of incoming and outgoing all-wave radiation (i.e. short-wave and long-wave components). Incoming radiation consists of direct (beam) and diffuse solar radiation plus long-wave irradiance from the sky. Outgoing radiation consists of reflected solar radiation plus the terrestrial long-wave component. Specifications: 60-junction thermopile with low electrical resistance (4 ohms nominal) to reduce susceptibility to noise; Nominal calibration factors 9.6Wm⁻²mV⁻¹ (for positive values), 11.9 W m⁻²mV⁻¹ (for negative values); Spectral response 0.25 to 60µm; Uncorrected wind effect : up to 6% reduction at 7ms⁻¹ for positive fluxes, up to 1% reduction at 7ms⁻¹ for negative fluxes; Time constant: Approximately 30 seconds; Top and bottom surfaces painted black and protected from

convective cooling by hemispherical heavy-duty polyethylene windshields (0.25 mm thick) and a dessicant contained in support arm; volume of dessicant tube 45cm³; breather port on the end of the support arm.



Figure 3.2: Radiation Energy Balance (REBS) net radiometer

3.4.3 Tube solarimeter

Tube solarimeters are designed to measure average irradiance (in W m⁻²) in situations where the distribution of radiant energy is not uniform e.g. amongst foliage, in greenhouses etc. Their tubular construction provides the necessary spatial averaging, while minimising disturbance to the foliage of plants.

Specifications (Delta- T Devices Ltd, 1993):

- thermopile: Copper-constantan;
- Tube: Pyrex borosilicate glass; overall length 970mm, tube diameter 26mm,
- element size 858 x 22mm;
- number of junction pairs 60;
- typical internal resistance ≈25 ohms;
- approximate response time for 63% change 40s;
- approximate response time for 99% change 3min;

- sensitivity (Diffuse light 15mV/ kWm⁻²;
- Spectral range (50% points) 0.4-2.2μm;
- absolute accuracy $\pm 10\%$ (solar spectrum, sun angle $> 30^{\circ}$ relative to tube axis)



Figure 3.3: A suspended tube solarimeter in the greenhouse

3.4.5 HMP45C temperature and relative humidity probe

The HPM45C temperature and relative humidity probe (Campbell Scientific Inc. (2007) was designed to measure air temperature and relative humidity. Temperature measurement was based on a platinum resistance thermistor (PRT). Humidity measurement was based on Vaisala's Humicap 180 capacitive humidity sensor, and this, together with the precision temperature sensor, were mounted in the removable probe head. The probe was designed to be housed in a URS1 or 41004-5 radiation shield. A 3m cable length was fitted as standard.

Specifications (Campbell Scientific Ltd, 2007):

Relative Humidity:

measurement range 0.8 to 100% RH; Output Scale 0 to 100 % RH equals 0 to 1V DC; accuracy (in clean air at 20° C, including non-linearity and hysterisis): Against factory references ± 1 % RH, against field references ± 2 % RH, to 90%, ± 3 % RH, 90 to 100%,

temperature dependence $\pm 0.05\%$ RH/°C; typical long term stability \pm better than 1% RH per year; response time (at 20 °C, 90 % response) 15 s with membrane filter; humidity sensor Vaisala Humicap 180.

Temperature- Measurement range $_$ -39.2°C to +60 °C; operating scale $_$ -40 °C to +60 °C equals 0 to 1V; accuracy at 20 °C $_$ ±0.2 °C; temperature sensor $_$ Pt 1000 (IEC 751 1/3 class B).

3.4.6 Wind, heated bead testo 425 anemometer

The anemometer measures wind speed in m/s, and give the air temperature in either °C or °F. The heated bead anemometer was based on the fact that the rate at which the heated bead dissipates heat to the environment was proportional to the wind speed causing the heat loss. It was typically used in glasshouses where wind speeds are very low. Other details: Testo GmGH and Co- Testo Strasse 1_D – 79853 Lenzkirch and its made in Germany.



Figure 3.4: A Wind, heated bead testo 425 anemometer

3.4.7 PAR (Photosynthetically active radiation) sensor

A PAR is quantum sensor (LI-COR, Lincoln, Nebraska USA, 1986) that has been developed to provide accurate estimates of photosynthetically active radiation by measuring the flux of photons in the 400 to 700 nm wavelength range.

Specifications

- Sensitivity: Typically 8μA per 1000 μmol m⁻²s⁻¹
- Linearity: Maximum deviation of 1% up to 10.000 µmol s⁻¹m⁻².
- Absolute calibration: ±5% traceable to the U.S National Bureau of Standards
 (NBS)
- Stability: $<\pm 2\%$ per annum
- Temperature dependence : -0.15 %/ °C maximum
- Azimuth error: $<\pm 1\%$ over 360° at a 45° elevation.
- Response time : 10µs

Dimensions

- Cable length: 3.0m (10ft)
- Weight: 28g (1oz)
- Attachment: via an M3 screw in base
- Connection : Bare Wire Termination
- Sensor housing: black anodized aluminium case with acrylic diffuser and stainless steel hardware.

 Weather proofing: waterproof to 1m depth of water (10m versions available on request)

3.4.8 A matrix sensor

A matrix sensor is an instrument for measuring the solar irradiance. The sensor construction is such that it measures the solar energy that is received from the whole hemisphere (180° field of view). The output is expressed in Watts per metre square.

3.5 Physiological instruments

3.5.1 Copper constantan (T type) thermocouples

Thermocouples of diameter 122 µm were used for measuring leaf temperatures in the greenhouse. These were clipped onto the underside of the leaves by plastic paper clips. The sensitivity curves for each type of thermocouple are pre-recorded in the data logger so that outputs were displayed in ${}^{\circ}C$.

3.5.2 Sap flow gauge

The sap flow gauge used was a stem heat balance gauges (model SG10WS, Dynamax, Inc., Houston, USA). Sap flow gauges also known as dynagages have a soft foam collar that surrounds the electronics. The unit is installed on a stem having an axial length of at least the gauge height which is cleared of branches and smoothed. A weather shield is installed for outdoor applications and radiation shielding. The O-Rings are installed and the user must allow it enough room for its height above and the same distance below the gauge. If only can be installed, the upper O-ring should be installed to provide insulation

from the rain. The specification for the gauge diameter is the determining factor for selection of a gauge which fits properly.

Mechanical specifications

- SGA 10-ws
- Gauge height 70mm
- Shield height 180mm
- Minimum stem diameter 9.5mm
- Maximum stem diameter 13mm
- Typical stem diameter 10mm
- TC Gap dX 4.0mm
- Number of TC pairs 2
- Input voltage 4.0V
- Input power 0.10 Watts

Electrical specifications

- Minimum input voltage D.C measured at device terminals 3.5
- Typical input voltage D.C measured at device terminals 4.0
- Maximum voltage D.C measured at device terminals 5.0
- Minimum heater input power 0.06watts
- Typical heater input power 0.12 watts
- Maximum heater input power 0.15 watts

3.6 Electronic instruments

3.6.1 A Zener diode

A Zener diode is a semiconductor device which has a p-n junction which conducts in the two regions. When the p region is at a higher potential than the n, holes in the p region flow into the n region and electrons in the n region into the p region, so both contribute substantially to current. When the polarity is reversed, the resulting electric fields tend to push electrons in the p region, only those associated with intrinsic conductivity and some that diffuse over from the n region. A similar conduction prevails in the n region, and the current is much smaller than with the opposite polarity.

Specifications (RS components Midrand S.A 1999)

- Type UDZ 4-7B
- Minimum voltage 4.55V
- Maximum voltage 4.75V
- Test current 5mA
- Dynamic impedance 100Ω

3.6.2 The Velleman K8000 interface card

. Sap flow gauges are the transpiration rate indicators and they give analogue signals which cannot be read by a computer. The Velleman K8000 interface card (shown in Figure 3.5) was used to establish a link and convert the analogue signals to digital form for the computer to read and after the signals had been processed by the computer the card then changes them back to analogue for the relay switch to be actuated.

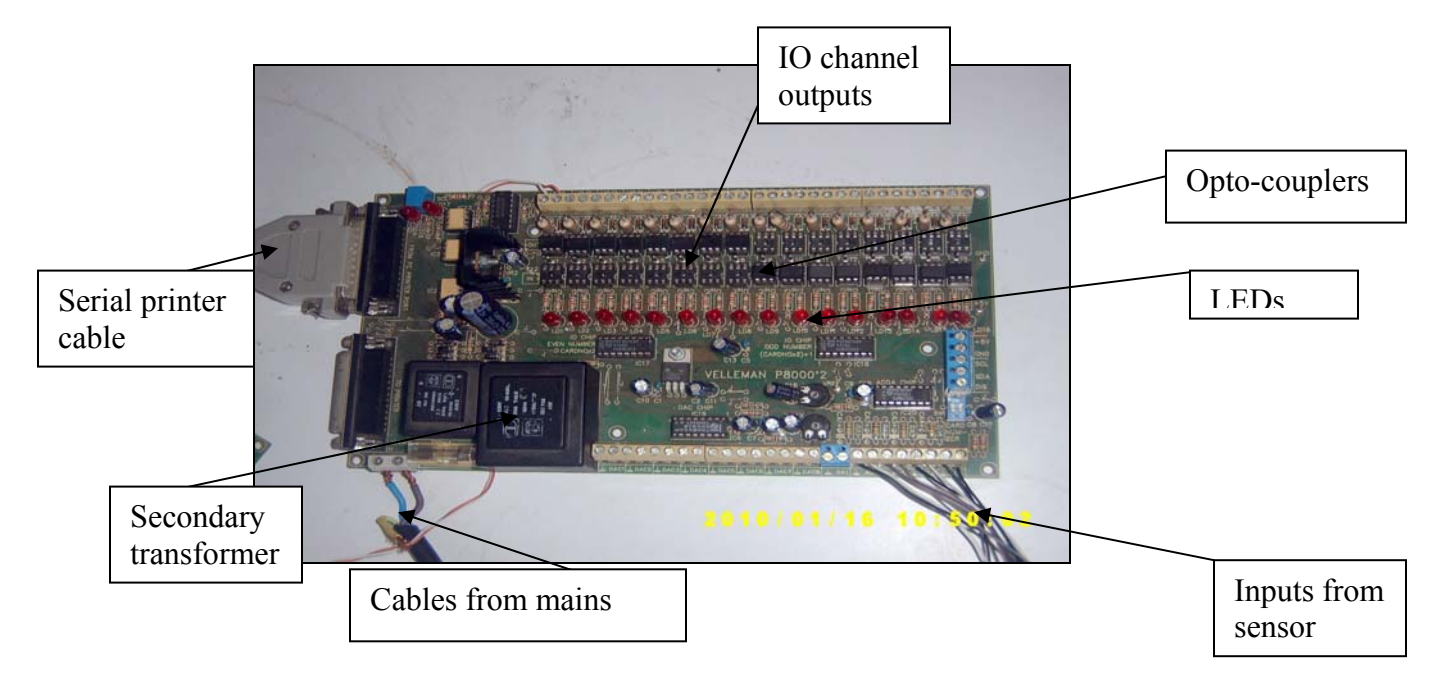


Figure 3.5: A Velleman K8000 interface card

The Velleman K8000 is a computer interface card that allows one to control electric/electronic devices with a computer. The card has some electrical inputs and outputs. The K8000 runs on IBM compatible computers, and can be connected to a computer through a standard parallel cable. The card can be programmed in any programming language, such as Visual Basic, C/C++, Q Basic, Turbo, Pascal e.t.c. In addition, a software called Power WinPLC can be used to program the card. Power WinPLC provides a good environment to create applications for the K8000 card. The K8000 card provides 16 I/O channels, which can be configured as in- or output. Digital inputs can read the state of switches. The outputs can set relays etc. the K8000 had also 9 analogue inputs and 4 analogue outputs.

Features

- Optically isolated from computer
- 16 optically isolated digital connections
- 9 analogue outputs, of which one was high precision and 4 analogue inputs.
- A simple way of controlling using Visual Basic, C/C++, Q Basic, Turbo Pascal
- Printer bypass connector on board,
- Simple connection with printer port

Specifications

Digital outputs:

Optocoupler, open collector output; 50mA- max.30VDC

Analogue inputs:

Optocoupler input: 5V/%mA, max.20V/40mA,

Analogue outputs

- 8 outputs DAC1 to DAC 8, resolution: 64 steps
- Minimum output voltage 0.1V at 2mA
- Maximum output voltage 11.5V adjustable at 2mA
- Resolution per step from 0.1 to 11.5V: 160mV +/- 90mV,
- 1 precision output voltage DA1, resolution: 256 steps.
- Minimum output voltage :0V
- Maximum output voltage: 4.5V adjustable at 0.5mA
- Resolution per step from 0 to 4.5V: 17.5mV

Analogue Inputs

- 4 analogue inputs AD1 to AD4, resolution: 256 steps
- Minimum input voltage :0V
- Maximum input voltage 5V
- Input impedance : 50ohms
- Resolution: 19.5mV

Other features

- Communication protocol: I2C bus
- LED indication for each I/O.
- 25 pin D series connector for computer
- 25 Pin D series connector for printer
- Supply voltage :230Vac

PCB dimensionas: 237 x 133mm(9.3"x5.2")

(http:/bvsystems.be/k8000)

3.6.3 A universal K6714 relay card

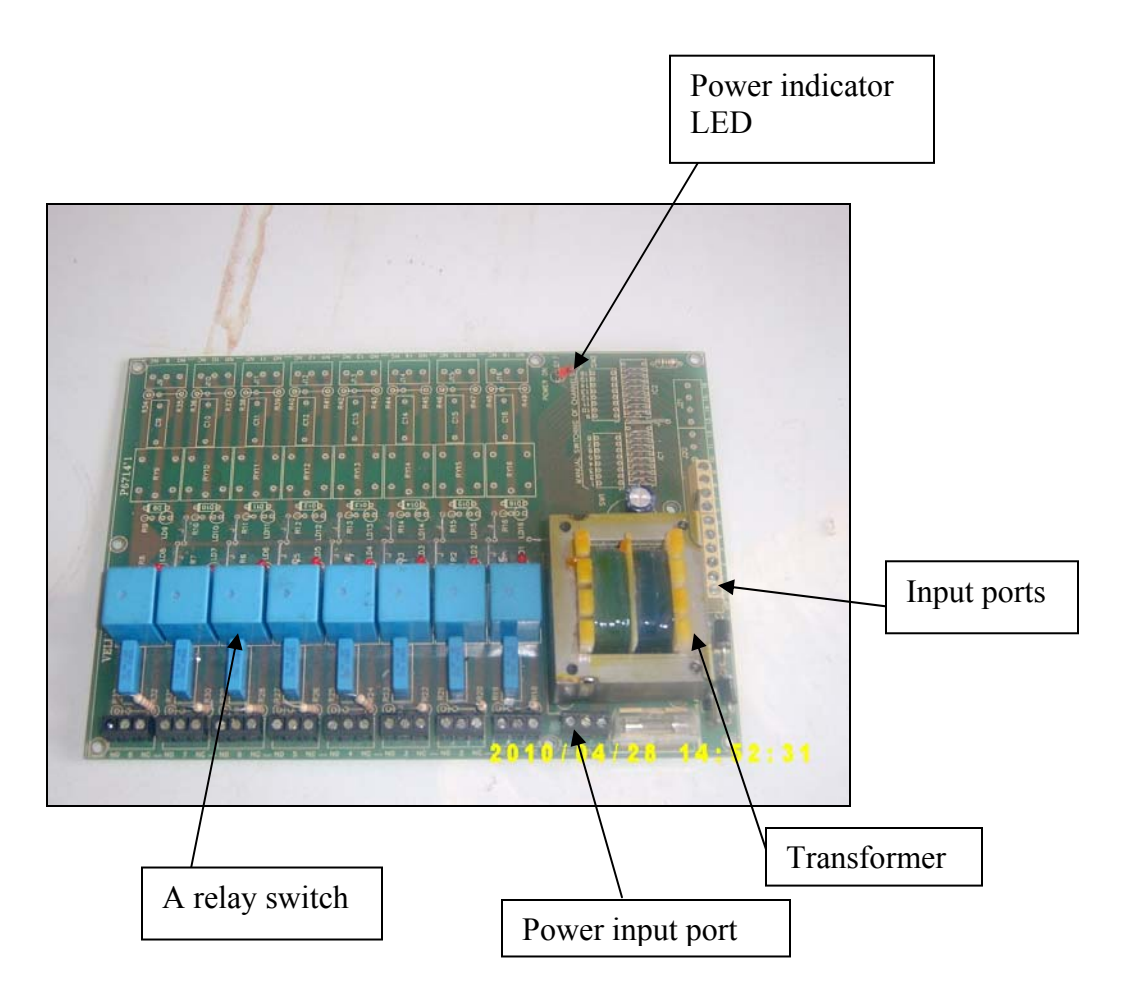


Figure 3.6: A universal K6714 relay card

The K6714 Universal Relay Card (8 Relays) self-assembly electronic construction kit was ideal for switching large electric currents using an electronic control while controlling isolation at the same time. The circuit board is powered by 125-230 Vac mains. Power supply transformer was included and provides a 12V DC output that can be used as a power supply for other kits e.g., K8023. Every output of the print can be equipped

with a noise suppressor network. It provides 16 channels but components to populate only the first 8 channels are provided.

Features

- 8 relays included (extendible to 16)
- the relays can be controlled in different ways:
 - o direct control from open-collector outputs, TTL or CMOS level
 - o other kits like K8000, K8023, K6711, ...
- Contact: 1 x inverter: 10A / 28VDC or 125VAC, max. 5A at 230VAC
- Relay switch-over contact: max. 5A at 220V

Specifications

- output voltage: 12V / 250mA for power supply
- power supply: 220 or 115VAC / 12VA
- PCB dimensions: 150 x 212mm (5.9" x 8.4")
- recommended housing: WCAH2507
- Product format: self assembly electronic construction kit

3.6.4 Electric pump

The pump used was the Pedrollo San Bonifacio (VR) type of pump and made in Italy. It ejects water at a rate of 0.125 litres per minute.

3.7 Computer software used

3.7.1 Power WinPLC

Power WinPLC was a software tool to control the Velleman Interface card K8000. The program helps to construct applications very quickly, with as little commands as possible. Setting an I/O channel only takes a single line with WinPLC, doing the same in Visual Basic requires dozens of lines. WinPLC had 10 groups with several commands one can use in applications. They vary from special commands like IF ...THEN to networking commands, allowing one to connect to other computers very quickly. The language for the programming was a sort of scripting language. It includes subroutines, labels, IF-statements, I/O basic operations, DAC basic operations, time functions. To run K8000 applications, WinPLC always must be started.

3.7.2 Visual Basic, VB. Net Studio 2005

A programming language called VB. Net Studio 2005 was used to code the control program. The program and commands are given in annex A. Installation of the VB.Net software was done and the computer had Windows XP as the operating system. Some commands of the WinPLC language were used within the program to call, set and clear the channels on the K8000 card.

3.8 Calibration of sensors

All meteorological and physiological sensors lose accuracy with time after they have been manufactured. It was essential that before these sensors are taken for field use they are calibrated against standard ones and the accuracy limits should be within those stipulated by the manufacturer. Several experiments were carried out in the Agrometeorology laboratory and on the roof top of Physics department, University of Zimbabwe to obtain readings from the temperature- humidity sensors and radiation sensors.

3.8.1 Experiment 1: Calibration of temperature humidity sensors (Vaisala type)

The temperature humidity sensors calibrated were the Vaisala HMP45AC type and the Delta-T type and the Walz system (Dewpoint system TS-2, Mess-unit and GegelTechnik) was used as a standard. The experiments were done separately since the two types of sensors use different dataloggers and due to limited resources. Two Vaisala HMP45AC type sensor (serial numbers A0640010, A0130013) were tied together with a platinum resistance thermometer and a Walz system tube and inserted into a hollow cylinder in which the air temperature was presumed to be similar to the water bath temperatures if there were no energy losses. A program was designed using PC208W Campbell computer package with consultations from the sensors' manuals available and fed into the Campbell datalogger CR10X and CR23X (serial number 14397 and 4081 respectively) from a laptop. The program made it possible for the logger to record temperature and humidity readings from the Vaisala and the Walz sensors every minute and also gave averages and standard deviations. A fixed temperature was set on the water bath and about five temperatures were set on the Walz dewpoint generator but the latter temperatures had to be below the former always to avoid condensation inside the pipes of the Walz system that occurs when temperatures equalled. For each dewpoint temperature set the system was left to stabilize for at least 10 minutes to allow for accuracy in the

measurements. This procedure was done for water bath temperatures from 1° C to 40° C. The data was downloaded later to a laptop for analysis. The multipliers obtained from the straight line figures gave evidence to the accuracy of the sensors. The accuracy proposed by the manufacturer must be within \pm 0.2 % of the original multiplier otherwise the new multiplier had to be adopted.

3.8.2 Experiment 2: Calibration of radiation sensors

Radiation sensors which comprise the CM11 solarimeter (Kipp and Zonen Delft, Netherlands) and one tube solarimeters (serial numbers 24) were set up on the Physics department open air rooftop and connected to a Campbell CR23X datalogger (serial number 4081). The CM11 solarimeter was used as the standard against which all the other radiation sensors were compared. The sensors were all leveled and checked for dryness before they were left to run. The tube solarimeters was oriented along the north-south direction to increase surface area of incident radiation according to Monteith (1993). A program was written with consultations from the manuals of corresponding sensors using a keypad on the logger. The sensors were left to give readings for four days and four nights (20 August to 24 August 2009) after which the data was downloaded and read in excel spreadsheets. The multipliers obtained from the regression line gave evidence to the accuracy of the sensor.

3.9 Preliminary measurements and tests

3.9.1 The integrity test

The integrity test was done to calibrate the analogue input AD channels using the nominal values from a power supply with regulated d.c.voltage outputs. A program was

coded using Visual Studio 2005 language to read the voltages of the channels. Each channel was subjected to nominal voltages and checked if it was reading true values. The results for the four channels are shown in Table 4.4.

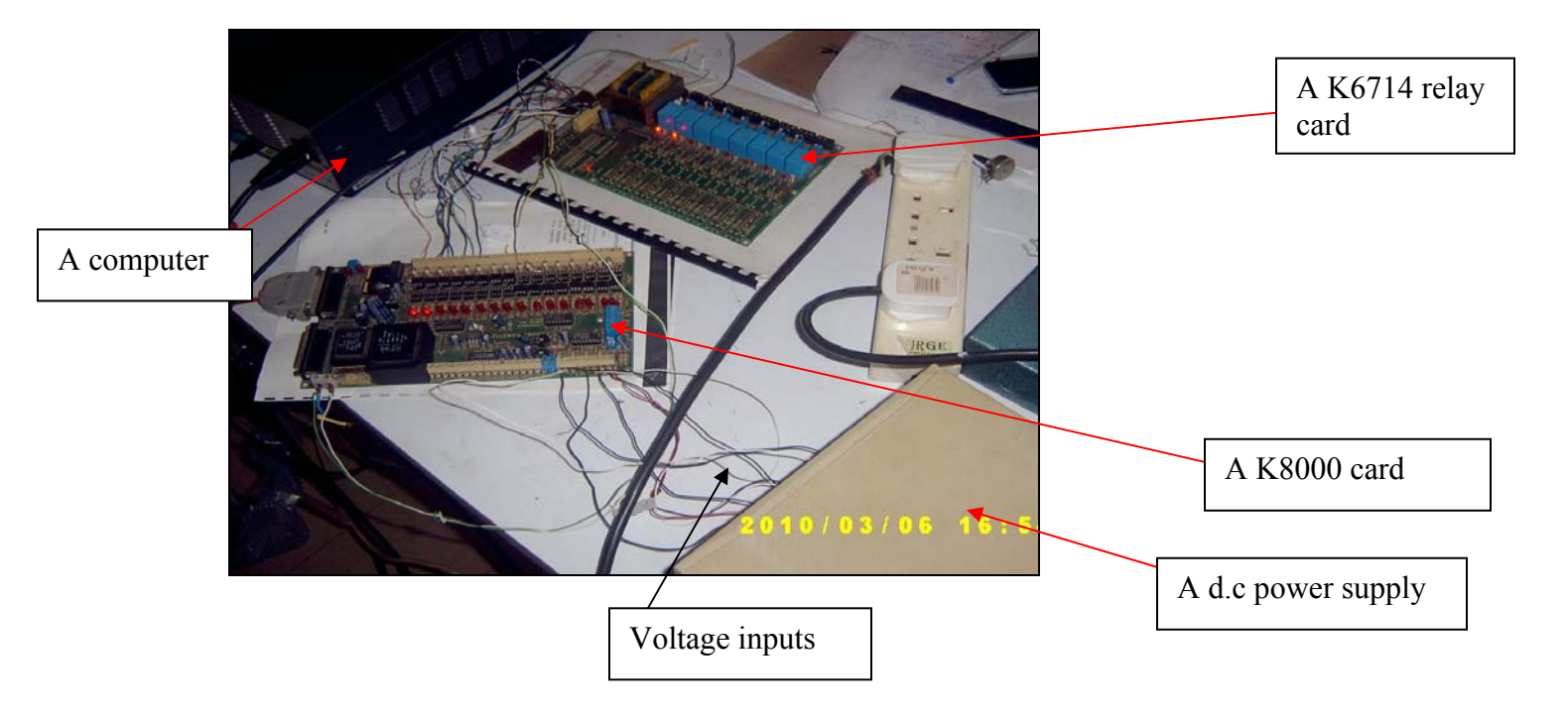


Figure 3.7 A setup for the integrity test

3.9.2 Analogue voltage signal conversion to digital signal resolution test

An experiment was carried out in the Agro-meteorology laboratory in which the set up was similar to the one for the integrity test. A simple program was coded in VB.Net language which read voltage inputs on the analogue input port of the K8000 card. A voltage regulated power supply was used as the source for analogue signals and the program when run displayed the corresponding digital values for the input signals. Sixteen values for the analogue signals were sent in and the corresponding digital signals are as tabulated in Table 4.3. A regression curve for the two signals was subsequently plotted to show the degree of agreement between the two.

3.9.3 Amplification of sap flow gauge signals

The three output signals from the sap flow gauges i.e. AH, BH and CH are too low (i.e. range from 0 to 0.4mV) to be accepted and processed by the K8000 card, amplification was necessary. To amplify, three CA3201E operational amplifiers were employed and assembled as shown in figure 3.5. The gain of the amplifier was set using the external resistors combination i.e. a preset feedback resistor of 25 k Ω and an input resistor of 22 Ω to determine the gain for each amplifier. A preliminary experiment was carried out in which the amplified voltage signals were recorded against the actual voltages from the sensor. This experiment was done in order to provide the computer program with known voltages that can be read in the program as millivots. Small changes in millivolt ranges were registered as well in the amplified voltages.

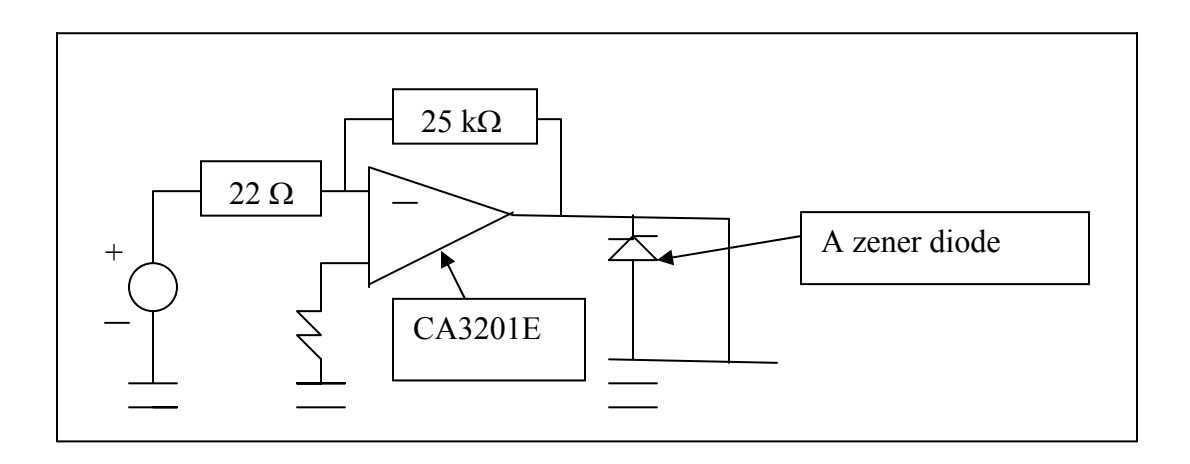


Figure 3.8 A schematic diagram of the negative gain amplifying circuit

3.9.4 Designing of a computer program

The computer program was coded using VB.Net 2005 (Visual Basic language). The program accepted inputs that were coming from a sap flow gauge sensor as voltages. It

calculated the amount of water lost from the crop and then sent a command to the relay switch to turn on the irrigation pump to replace the lost water.

3.9.4.1 A flow chart for the control program (algorithm)

The program was written using Visual Basic .NET 2005 version language. The flow chart in figure 3.9 shows the sequence of events in the program

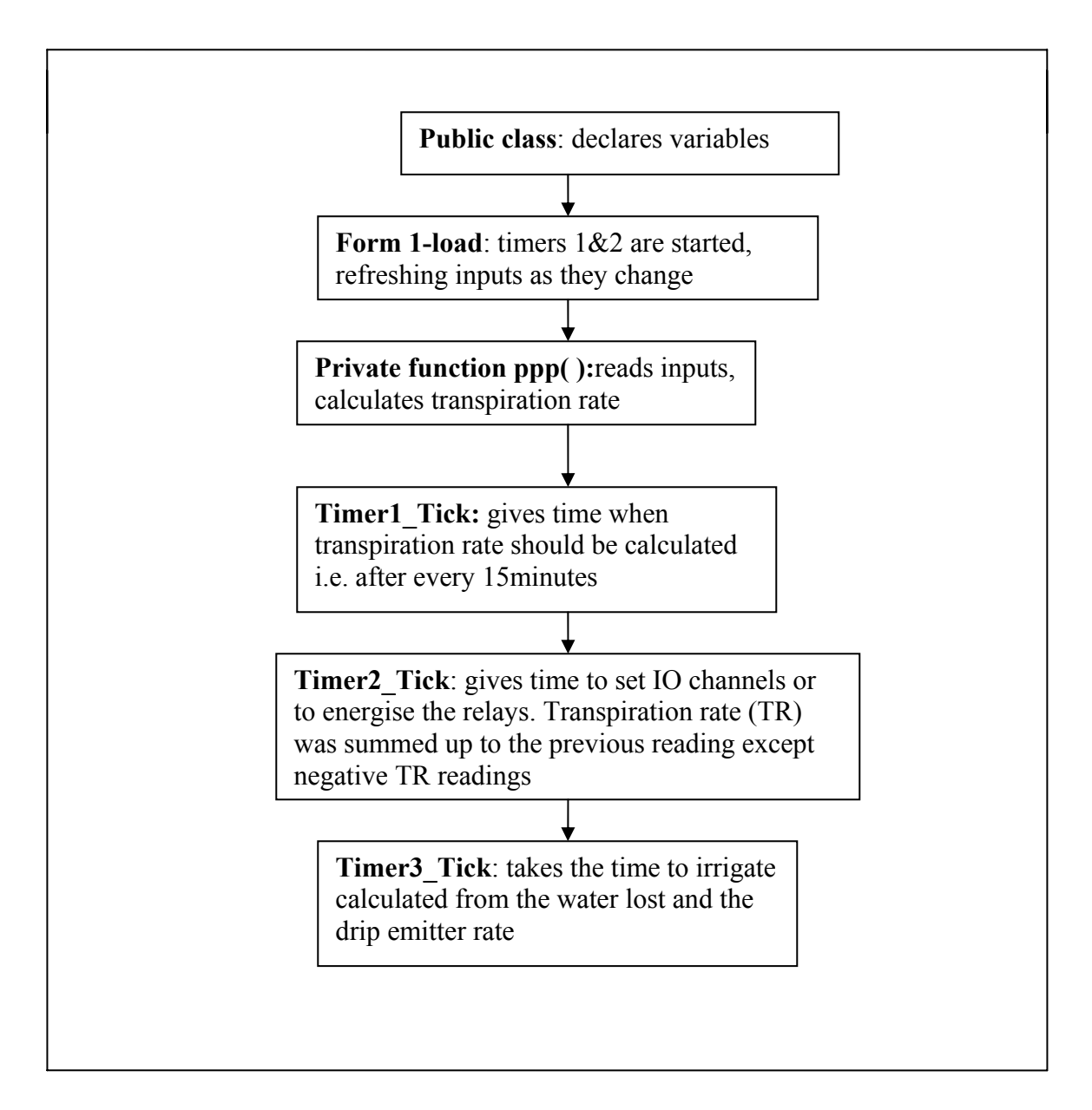


Figure 3.9: A flow chart for the computer control program

The computer program was made of five parts. The first was entitled the 'Public Class Form 1'. Under this class are declarations of global variables (variables that can be used in any sub class). The second part of the program comprise of a function given a name 'ppp'. Under the function are some declarations of certain variables made followed by WinPLC statements (i.e. winplc.getADState) that are meant to read the analogue input channels of the K8000 card. The next part of the function was made of mathematical

equations to compute the water lost estimated by a sap flow gauge sensor. The last part of the function was made of commands for textboxes which display the input signals from the sensor when the program was running. The function was followed by timers. Under the first timer dubbed 'Timer1' was a command that starts the ticking of the timer as soon as the application (program) starts running. When Timer1 ticks the function 'ppp' was called and everything under the function was executed. Timer 1 determines the time when transpiration rate of the crop was measured and that was after 15 minutes. Transpiration (TR) was added only when it was greater than zero. Timer 2 sub class follows. Timer 2 ticks as soon as the application starts running and was executed after 24 hours. Timer 2 determines the time to switch on the irrigation pump to replace the lost water. The third timer which was Timer 3 takes the time calculated from the water lost and the drip emitter rate. Under timer 3 was a command to energize the relay switch i.e. set IOch and a command that switches the relays off i.e. clear IO ch when irrigating interval had elapsed. The program was given in Annex C.

3.10 Field measurements

3.10.1 Setting up of an automatic weather station inside the greenhouse

An automatic weather station shown in figure 3.1 was set up at the greenhouse in the Biological Science department, University of Zimbabwe. The station measures both meteorological and physiological variables and the sensors were all sending readings to a CR23X Campbell Scientific (CSL) datalogger. Weather parameters measured include

solar radiation (measured by CM3 pyranometer), photosynthetically active radiation (using a PAR sensor), air temperature and relative humidity (measured by a Vaisala temperature-humidity sensor) and net radiation (measured by a REBS (Radiation Energy Balance Systems) net radiometer. Other variables measured were the sap flow rate of tomato crops (measured by a stem heat energy balance gauge), soil temperature (using soil temperature probe) and leaf temperatures (using chrome-constantan type thermocouples).

3.10.2 Setting up of an automatic weather station outside the greenhouse

The station measured fewer variables and these are only meteorological. It comprise sensors like CM3 pyranometer, a Vaisala temperature-humidity sensor estimating same variables mentioned for the inside station on common sensors. All the sensors were sending readings to a CR23X CSL datalogger.



A temperature-humidity sensor (Vaisala type)



A tomato crop in greenhouse

A Campbell scientific datalogger (CSL)

Figure 3.10 (a) an automatic outside weather station and (b) shows the bottom part of the automatic weather station inside a greenhouse at the Biological Science Department, UZ

3.10. 3 Data collected from the sensors

Programs 1 and 2 given in annexes B and C were loaded onto the outside and the inside greenhouse loggers respectively. The inside automatic weather station datalogger (CR 23 X) sampled data every 5 seconds and averaged it every 15 minutes. Data was downloaded as *.DAT files* and processed in the Excel spreadsheet.

The data for the outside the green house weather station was sampled by a CR 10X datalogger every 5 seconds and averaged over 30 minutes. It was as well processed in Excel spreadsheets. Solar radiation was in units of W/m², net radiation was read in units of W/m², air temperature in °C, relative humidity as % and PAR in µmol m⁻² s⁻¹

3.10.3.1 Installation of sap flow gauge sensors

The sap flow gauge was mounted as shown in figure 3.8. A straight stem was selected carefully from a tomato crop. The branch's diameter was measured with vernier calipers and found to have an average of 9.1mm which corresponded to the inscribed gauge diameter of 10mm. A cloth was used to clean the branch and some canola oil was sprayed onto the branch to prevent the shoots or buds from emerging during the experiment as this will damage the gauge or result in the gauge giving erroneous readings. Before installing the gauge, the voltage which was meant for heating of the gauge had to be regulated by a voltage regulator to the required level, which in this case was 4V dc. The data logger was programmed to allow for the recording of sap flow measurements every 15 minutes. An automatic weather station measured weather parameters such as air temperature, humidity and radiation: variables which had influence on the rate of sap flow and ultimately on the transpiration rate.



Figure 3.11: Showing a stem heat balance sap flow gauge installed onto a tomato crop

3.10.3.2 Determination of Ksh

The stem heat balance sap flow gauges to be used with the card had a sheath coefficient (Ksh) which was a property of how the sheath conducts heat and these coefficients were calculated after an experiment was done. Two sap flow gauges were mounted around tomato crops in the greenhouse at the Biological Science department, University of Zimbabwe. The gauges were connected to a Campbell CR23X, Z10 datalogger and were left to give readings for two days and two nights. It was experimentally proved that transpiration rate for many greenhouse crops was zero or very close to zero just before dawn (between 4am and 6 am) the component Qf will be zero and Ksh will be calculated from equation (2.17)

3.10.3.3 Determination of stem diameters and cross sectional areas

A micrometer screw gauge with an accuracy of 0.01 mm was used to measure the stem diameters of two tomato crops on which the sap flow gauges were mounted. For each plant three measurements were done to minimize the random error on the results. The

results were used in the calculation of the stem cross sectional area for the calculation of the flow rates for the sap flow gauges. Results for these measurements are tabulated in Table 4.5

3.11 Monitoring of transpiration rates from sap flow rates

Transpiration rates differ with changes in the microclimate of a greenhouse. Sap flow rates under different conditions were monitored by having two sap flow gauges to record the transpiration rates for the tomato crops in the greenhouse for ten days (day 32 to 41 in 2010). The data was downloaded and analysed in Excel spreadsheets. The data was important in one way that it set some limits or gave an idea of the amount of water lost under certain conditions. This information helped in the designing of the computer program and ultimately had a bearing on the irrigation schedule. A comparison of the transpiration rates registered by the sap flow gauges and those computed from weather data according to the FAO Penman-Monteith equation was done. The analyses for these comparisons are given in form of a graph in Figure 4.36.

3.11.1 The scaling up of the estimated evapotranspiration

Transpiration rate estimated by sap flow gauges was upscaled to be representative of the whole cropped area where it was measured using the method suggested by Katsoulas et al in 2001. In this method the leaf area index L_A in m^2 (leaf) m^{-2} (ground) was estimated from leaf length measurements L in m, using the relationship : $S = 0.26L^2$, linking the area S in m^2 of a leaf to L .

3.12 Monitoring of transpiration rates using the FAO Penman –Monteith equation

The FAO Penman-Monteith method employs meteorological variables to estimate crop evapotranspiration. Ten consecutive days (day 32 to day 41, 2010) data from the automatic weather station inside the greenhouse was read and analysed in the Excel spreadsheet to compute ETo. The variables that were of interest in this method were the relative humidity, the air temperature, solar radiation, and net radiation. The wind speed was estimated manually using a hot wire anemometer and an average for every hour was recorded. Equation 2.6 was used to compute hourly ETo and it was given in mm per hour as units. A table of results and Figures were plotted to show how the calculated ETo varied with the weather parameters.

3.12.1 Determination of the wind speed using the hot wire anemometer

A hot wire anemometer was used to estimate the windspeed inside the greenhouse. Sampling method was used in which readings were taken randomly at different places inside the greenhouse. About 25 readings were taken and averaged out to give the mean windspeed inside the green house. The results of the exercise were seen to be very irregular and an average value of 0.4 ms⁻¹ was used in the estimation of ETo using the FAO Penman-Monteith equation.

3.13 Monitoring of the system signals with the data logger signals

The three signals (AH, BH and CH) sent to the K8000 card had to be the same as the signals read by the datalogger. A setup as shown in figure 3.12 was put in place and the computer program was designed to register 15 minute interval data. The set up was made to run for ten hours during daytime from which the data was collected and analysed. Data

from the data logger was downloaded and read in an Excel spreadsheet in which a regression analysis between logger data (standard) and the system was done.

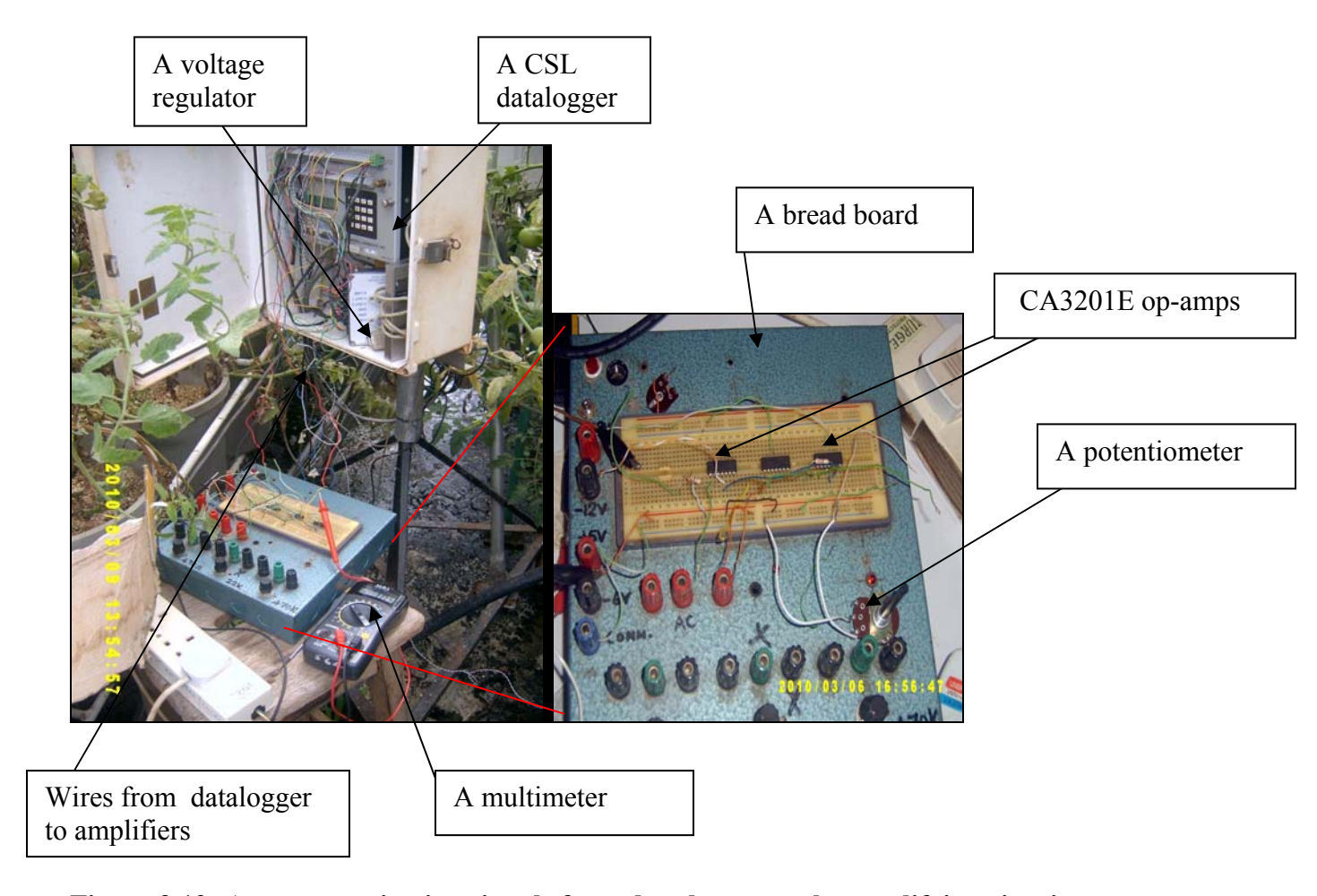


Figure 3.12: A setup monitoring signals from data logger to the amplifying circuit

3.14 Measurement of the drip emitter rate

An experiment was carried out in the greenhouse to measure the drip emitter rate when the pump was supplying water. Four drip pipes were inserted into a 2 litre container and were timed for the filling of the container with water when the pump was switched on. The experiment was done three times on different pipes to minimize error and the results were tabulated in Table 4.7 the emitter rate was used to calculate the time allocated for the pumping of water from the reservoir tank.

3.15 Integration and implementation of control system

The electrical pump was connected onto the relay card and was controlled by the computer program which after calculating the transpiration rate gives the time the pump had to run. The outline of a sequence of steps was given in the flow chart given in figure 3.13.

3.15.1 The flow chart of the control system (algorithm)

This flow chart will show a sequence of events in the irrigation control system

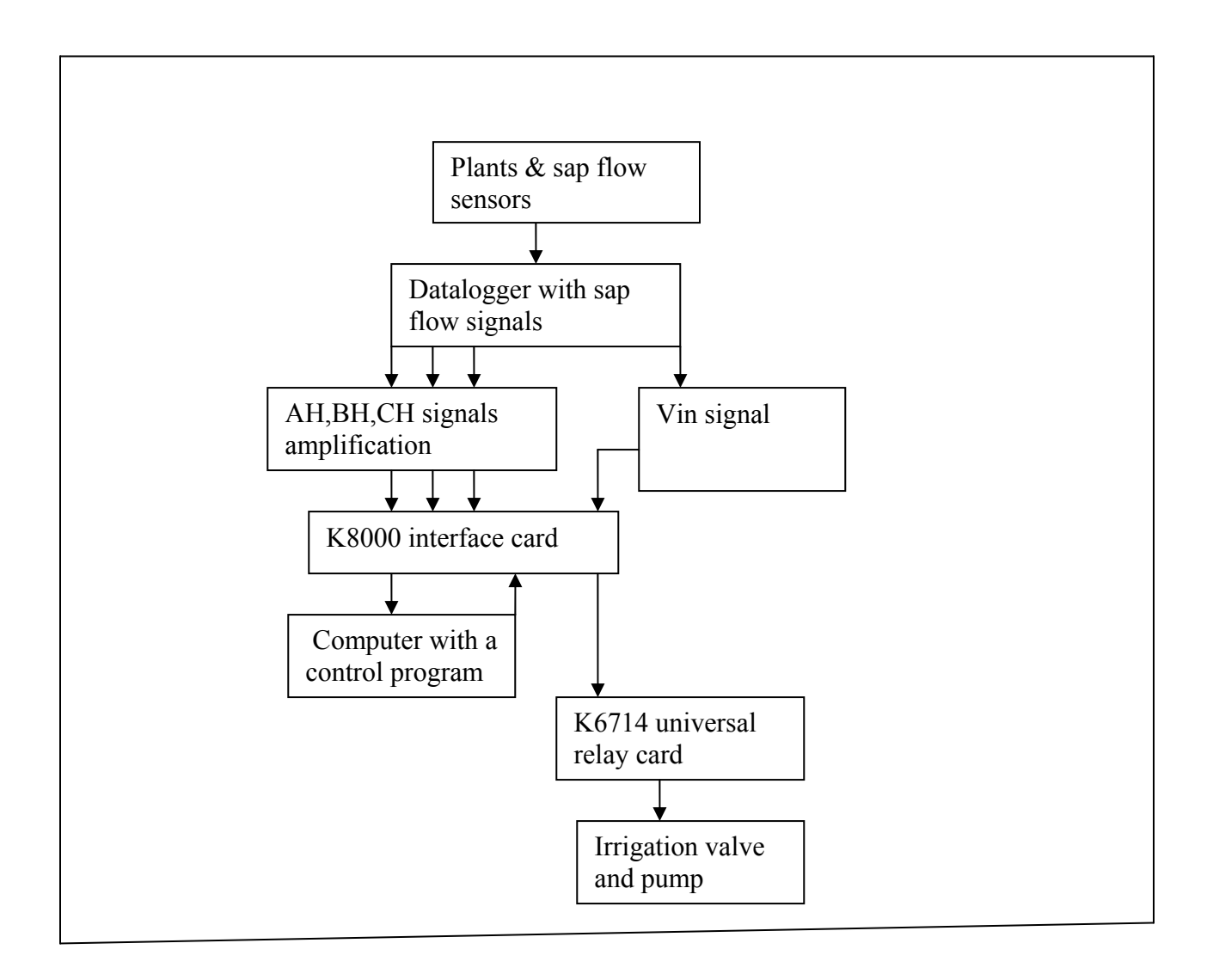


Figure 3.13: A flow chart for the irrigation control system

3.15.2 The irrigation control system

Computer

monitor

Figure 3.14 is showing the proposed irrigation control system when it was implemented in the greenhouse with a tomato crop.

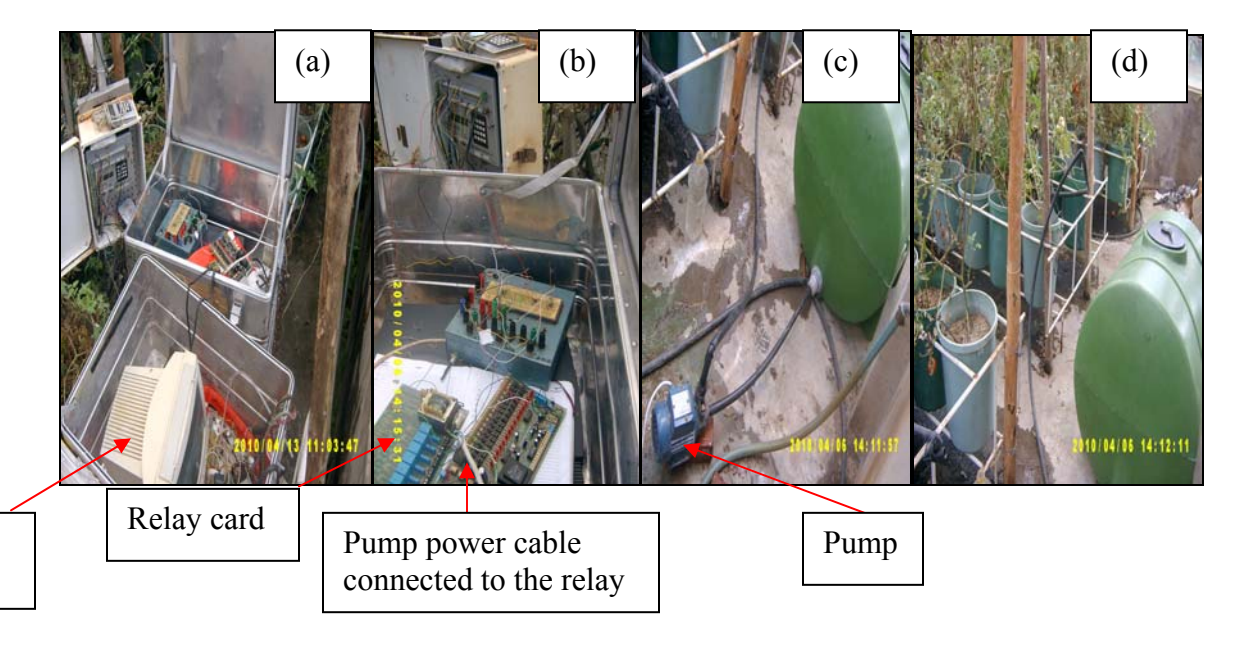


Figure 3.14: (a) An irrigation control system (b) connections from the datalogger to the cards (c) A pump connected to the water tank (reservoir) and supplying water to the crops, (d) A pipe from the pump leading to the potted plants.

3.15.2.1: Connection between the K8000 card, relay card and the pump

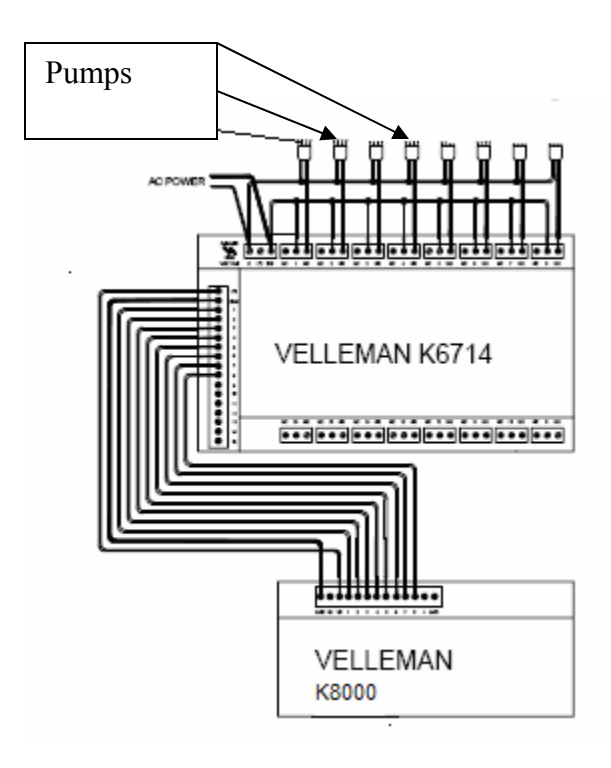


Figure 3.15: Connection between the K8000 card, relay card and the pump

One pump was used in the project so one relay switch was used. The setup in figure 3.15 is used when more than one pump is used.

3.15.3 A computer display of the running system

Figure 3.16 shows a page of the application interface for the program. In the page were textboxes indicating the four input voltage signals i.e. Vin, AH, BH and CH, give the transpiration rate computed every 15 minutes and 24 hours, and finally had list boxes that

show the daily water loss, the time given to the pump and the day on which the irrigation took place.

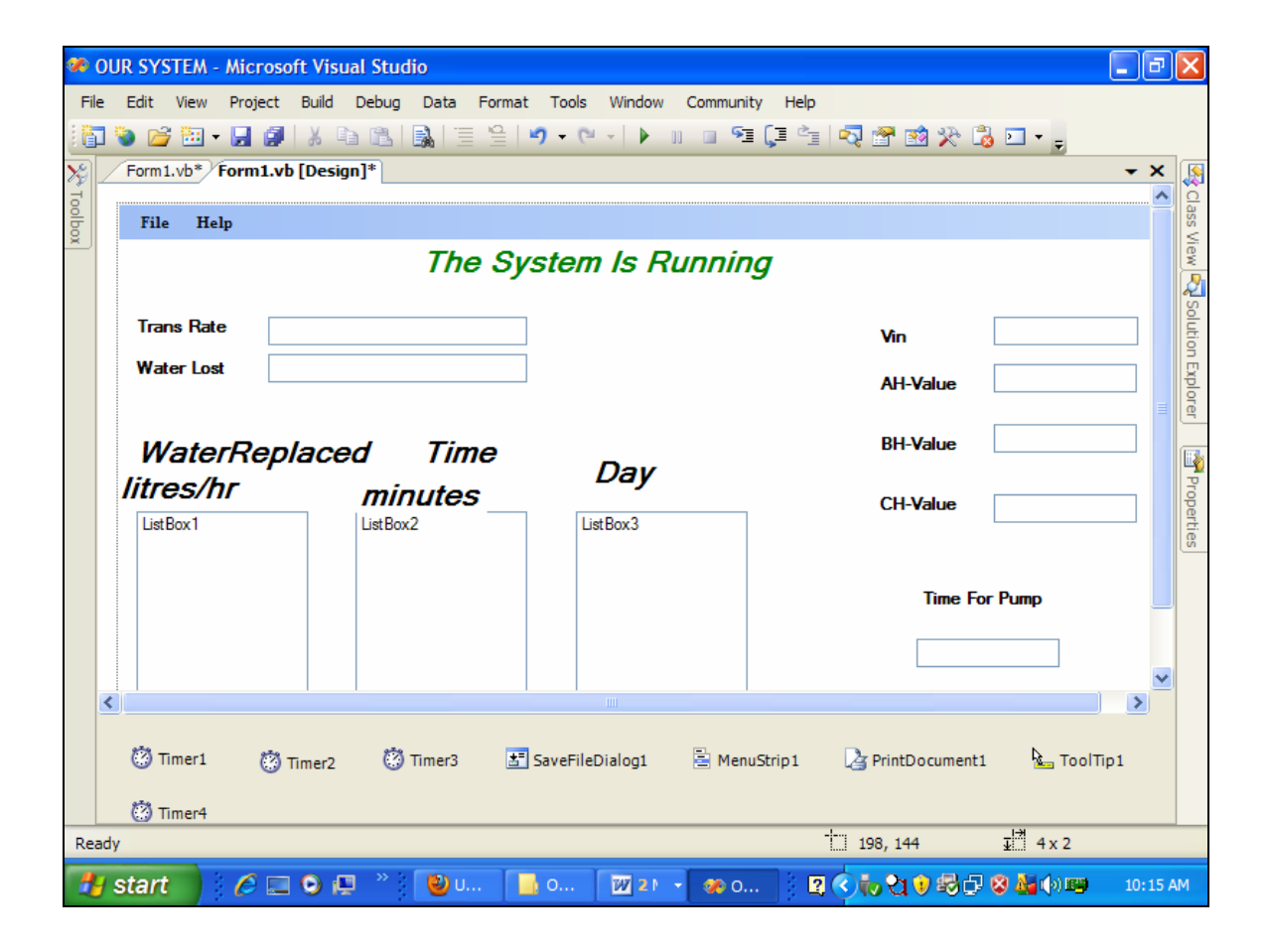


Figure 3.16: A computer display of the running system

3.15.4 Investigative crop treatments

Three treatments were set up as shown in figure 3.17. The first treatment was made of a tomato crop bed whose evapotranspiration rate was to be estimated from the FAO Penman–Monteith equation (equation 2.6) which was the current grower practice. The second treatment was an automated one with sap flow gauges measuring the evapotranspiration and sending the signals to a computer to determine how much water to

be replaced. The last treatment was a stressed one which was used in principle as the control and evapotranspiration was estimated using the FAO Penman –Monteith equation again.

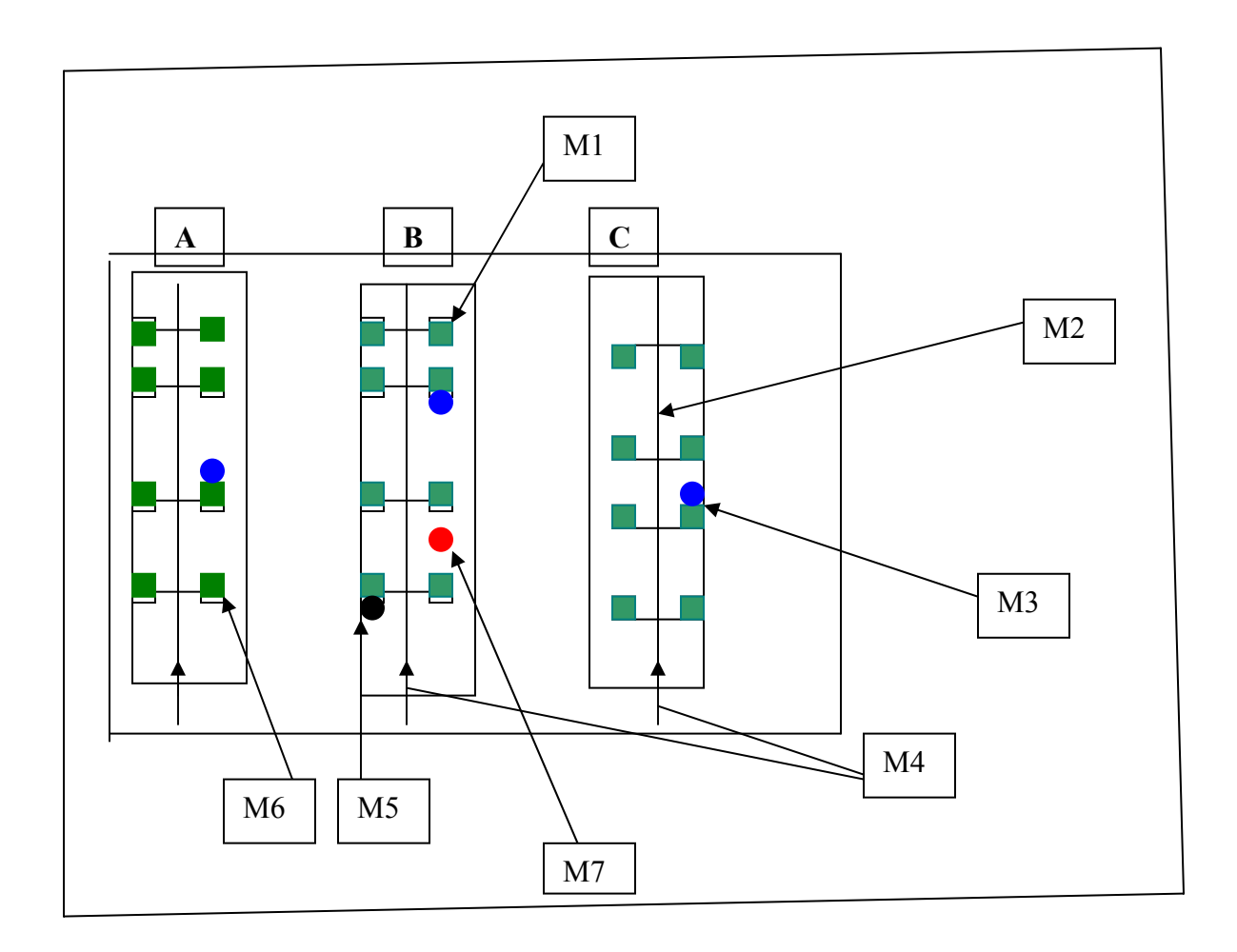


Figure 3.17: A setup of investigative crop treatments

Key

M1 A potted tomato plant

M2 A drip line

M3 A T type thermocouple

M4 A water supply pipe

M5 A sap flow gauge

M6 A T type thermocouple

M7 An automatic weather station inside the greenhouse

Copper constantan (T-type) thermocouples were attached to leaves of the three treatments since loss of water has a strong bearing on the leaf temperatures. Variation of the leaf temperatures was monitored for the stressed treatment and the current grower's practice treatment. Reference crop evapotranspiration in all the treatments was finally read in mm/day units and compared to see how they varied. Cooling of the greenhouse was achieved by employing a fan that was electrically driven.

CHAPTER 4

RESULTS AND DISCUSSION

4.1 Introduction

This chapter is composed of calibration of instruments used; data analysis for the monitoring of sap flow rates under different weather conditions; the testing of the system results and the comparison of the control system in terms of total water used with the two other treatments. The chapter in addition had an in depth discussion on all the results obtained.

4.2 Calibrations

Table 4.1: Calibration of relative humidity temperature sensor

Sensor	Serial number	Calibration equation
HMP 45C (RH output)	A0130013	$RH_{(walz)} = 0.733*RH_{600}$
HMP 45C(Temp output)	A0130013	$TM_{(walz)} = 0.92*TM_{600}$
HMP 45C (RH output)	A0640010	$RH_{(walz)} = 1.017*RH_{602}$
HMP 45C(Temp output)	A0640010	$TM_{(walz)} = 0.96*TM_{602}$

The HMP 45C calibration have a high accuracy value for the temperature component as the multiplier values are 92% and 96% and have a less accuracy for the relative humidity component with 73.33 % and 101.7 % for the calibration multipliers.

Table 4.2: Calibration of radiation sensors with the CM11 Kipp solarimeter (serial number 997082 and multiplier $5.22\mu\text{V/Wm}^{-2} \pm 0.5\%$) as the standard

Sensor	Serial number	Calibration equation
Tube solarimeter	24	TSL ₂₄ = 0.72313*CM11-
		0.3176

The calibration multiplier for the tube solarimeter was 72.313 %. This was adopted as its new multiplier for the readings obtained from it.

Table 4.3: Voltage results used to convert analogue signals to digital signals (resolution test)

Analogue voltage signal (V)	Digital voltage signal (V)
0.05	10
0.95	51
1.03	58
1.51	88
2.00	105
1.99	108
2.35	128
2.83	149
3.00	158
3.28	172
3.90	208
4.00	211
4.14	220
5.00	255

Table 4.3 shows the results of a resolution test that was carried out to see the conversion of analogue signal to digital signal. It was clearly observed that there was strong agreement between the two variables. The analogue voltage signal of 5 volts corresponded to the maximum digital equivalence of 255 volts.

Table 4.4: Results of an integrity test of the K8000 Velleman interface card

AD1 Cha	nnel	AD2 Cha	nnel	AD3 Cha	nnel	AD4 Cha	nnel
Nominal	Observed	Nominal	Observed	Nominal	Observed	Nominal	Observed
(V)	(V)	(V)	(V)	(V)	(V)	(V)	(V)
0.50	0.491	0.99	0.945	0.80	0.782	1.00	0.964
1.01	0.964	1.50	1.436	0.99	0.945	1.51	1.455
1.52	1.455	2.05	1.964	1.10	1.054	1.80	1.727
2.02	1.927	2.56	2.455	1.66	1.600	1.90	1.818
2.65	2.545	3.06	2.927	1.75	1.673	2.08	2.000
3.00	2.873	3.50	3.345	2.00	1.909	2.61	2.491
3.51	3.364	3.91	3.745	2.50	2.400	3.06	2.927
4.02	3.836	4.04	3.873	3.11	2.964	4.03	3.855
4.50	4.291	4.47	4.273	4.00	3.818		

Table 4.4 show results obtained from calibration of the AD channels. Input voltages of values from 0.49 to 4.5 volts were used. Using the conversion of analogue signal to digital from resolution test a factor of 1/55 was used to get the equivalent analogue readings from the card. These results show that there is high correspondence between the compared variables and the card can be used to give precise readings.

4.3 The computation of sap flow rates

Table 4.5: Leaf dimensions used to calculate total leaf area from a theory postulated by Katsoulas et al (2001)

Leaf number	Leaf length (m)	Total leaf area(m ²)_0.26L ²
1	0.085	0.00187850
2	0.083	0.00179114
3	0.065	0.00109850
4	0.070	0.00127400
5	0.057	0.00084474
6	0.067	0.00116714
Average to	tal	
leaf area		0.26846733

Table 4.6: Readings used for calculating the stem cross sectional area

	Stem diameter_ plant 1	Stem diameter_ plant 2
	10.05mm	9.03mm
	10.31mm	9.41mm
	10.42mm	9.36mm
	10.26mm	9.27mm
Average diameter	0.01026 m	0.009268 m
Cross sectional area	$8.27E-05 \text{ m}^2$	$6.75E-05 \text{ m}^2$

4.3 Monitoring of sap flow rates

Monitoring of sap flow rates under different weather conditions was done using results that were taken from a ten day (day 32 to day 41, 2010) recording with a Z10 CR 23X CSL data logger. The results are based on one sap flow gauge. Four days were chosen to give graphical picture of how the sap flow rate varied with other weather parameters i.e. days 32, 33, 38 and 39.

4.3.1 Temporal variation of weather parameters on different days inside the greenhouse

Temporal variation of weather parameters entails time variation of weather variables inside the greenhouse. Weather variables influence its microclimate and most importantly the crop evapotranspiration rate of crops.

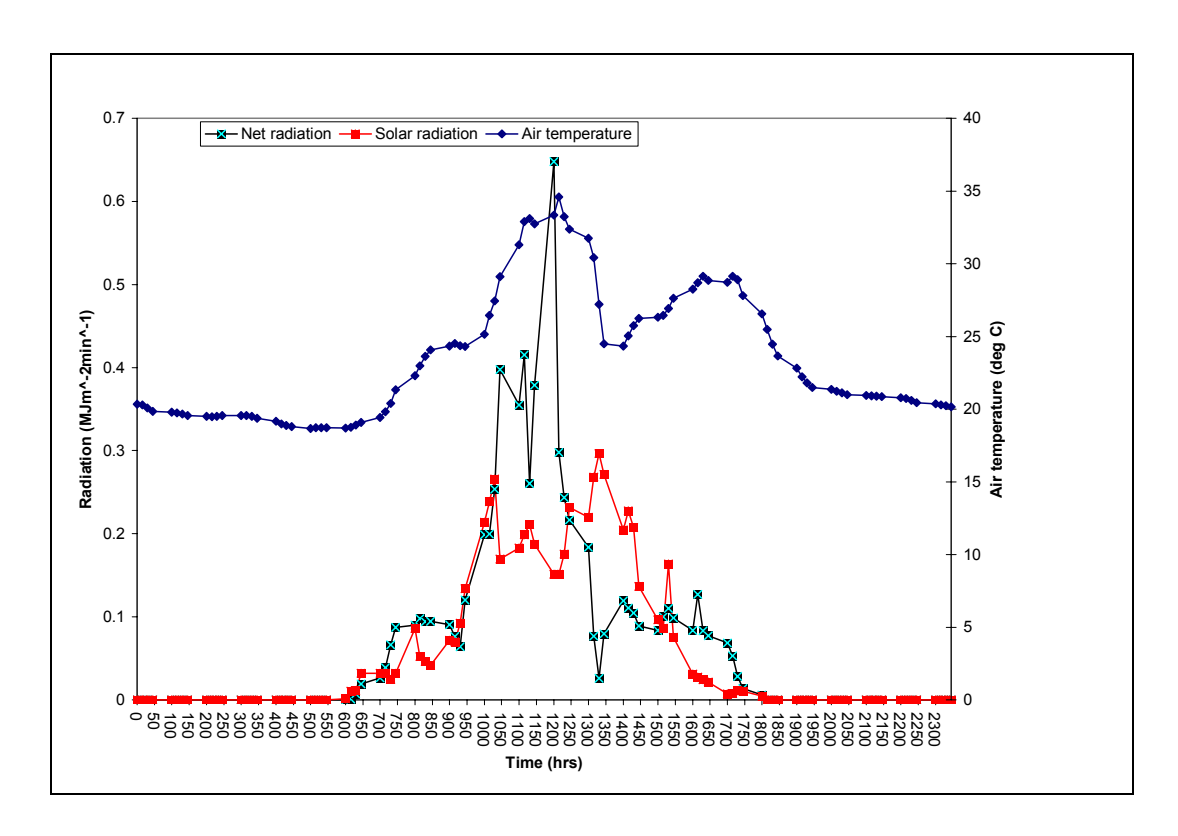


Figure 4.1: Temporal variation of radiation and air temperature on day 32, 2010

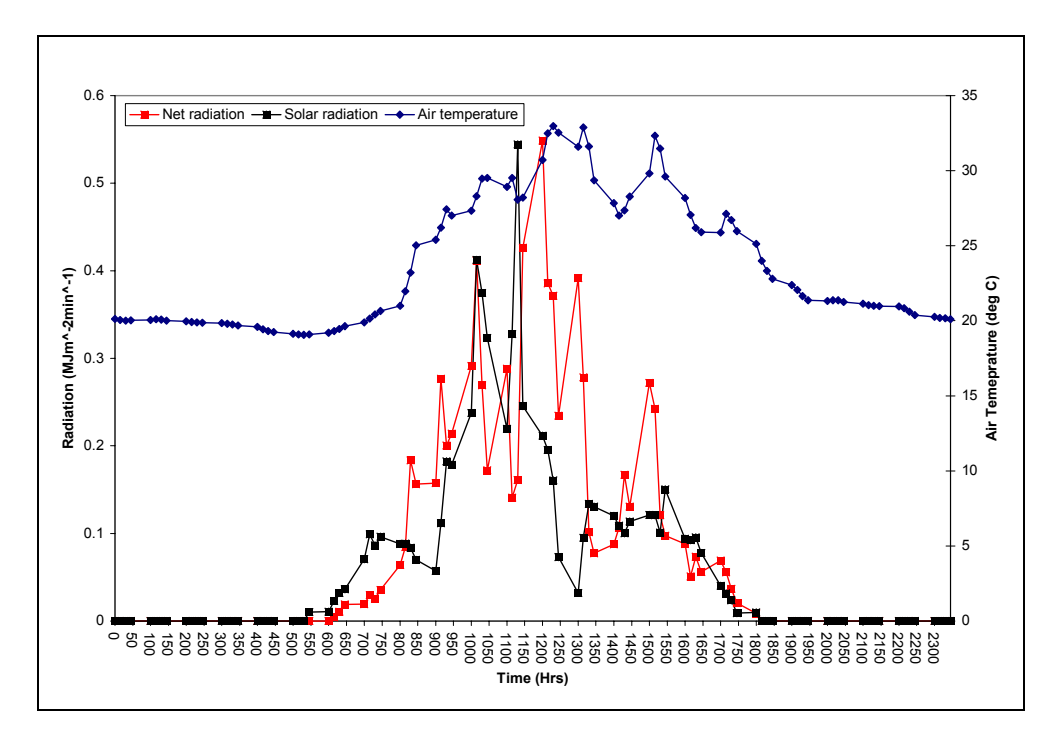


Figure 4.2: Temporal variation of radiation and air temperature on day 33, 2010

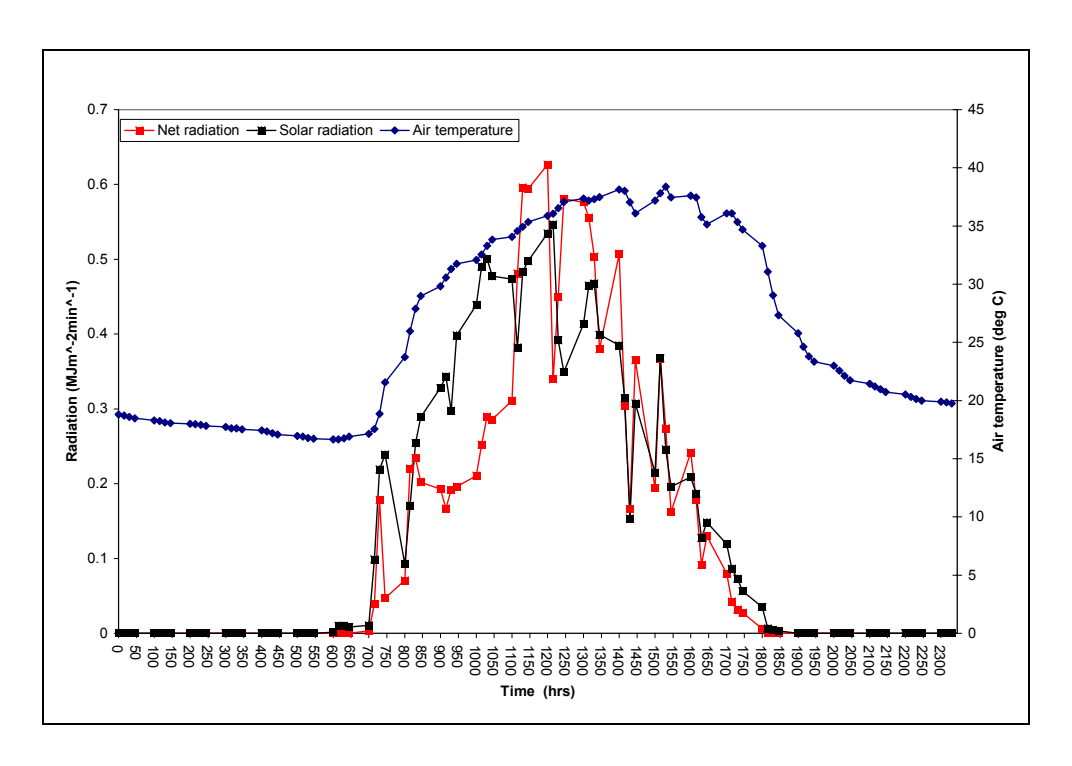


Figure 4.3: Temporal variation of radiation and air temperature on day 38, 2010

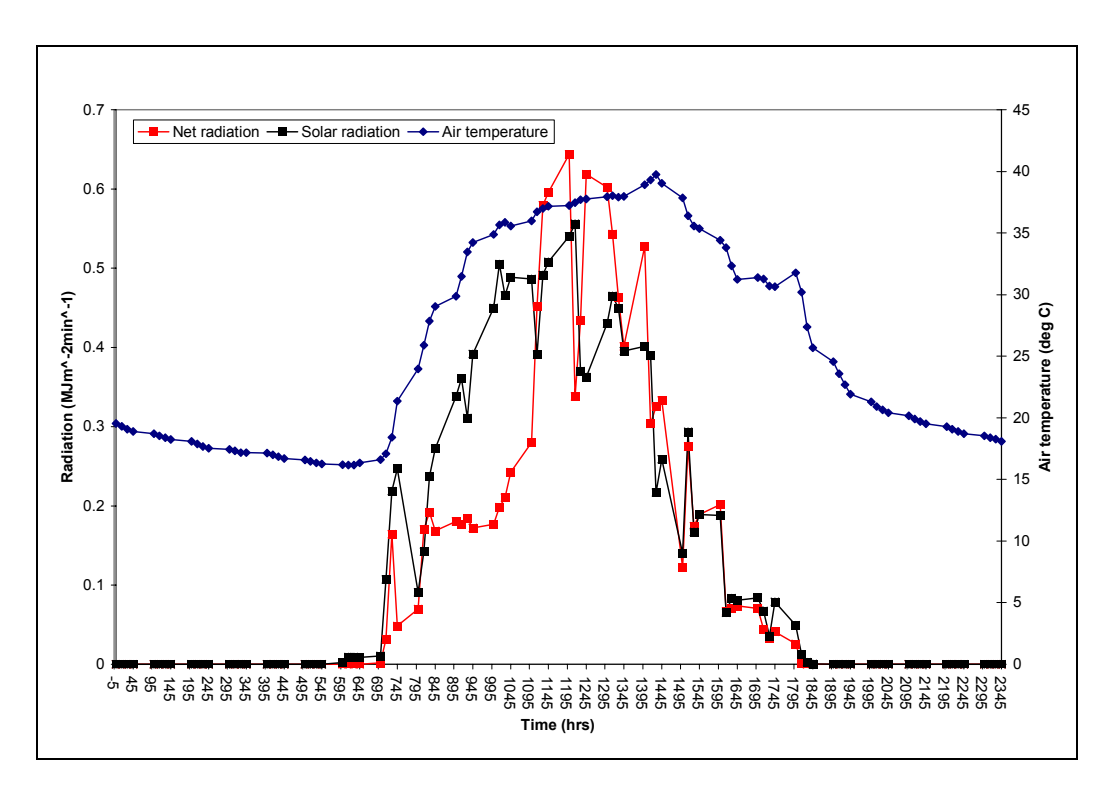


Figure 4.4: Temporal variation of radiation and air temperature on day 39, 2010

Figures 4.1 to Figure 4.4 are showing diurnal variations of solar radiations, net radiations and air temperature. The general forms of the curves are similar for the three variables with minimum values attained at night and maximum values between noon and 2 pm. Air temperatures attain their peak values an hour or two after the radiations and this was normal since temperature was a response to incoming radiation i.e. high radiation result in high temperature and less radiation in low temperatures. In addition air had a low heat capacity hence the time delay in attaining the peak value. Partially cloudy skies caused fluctuations in net radiation and solar radiation wave forms.

4.3.2 Temporal variation of sap flow rate on different days

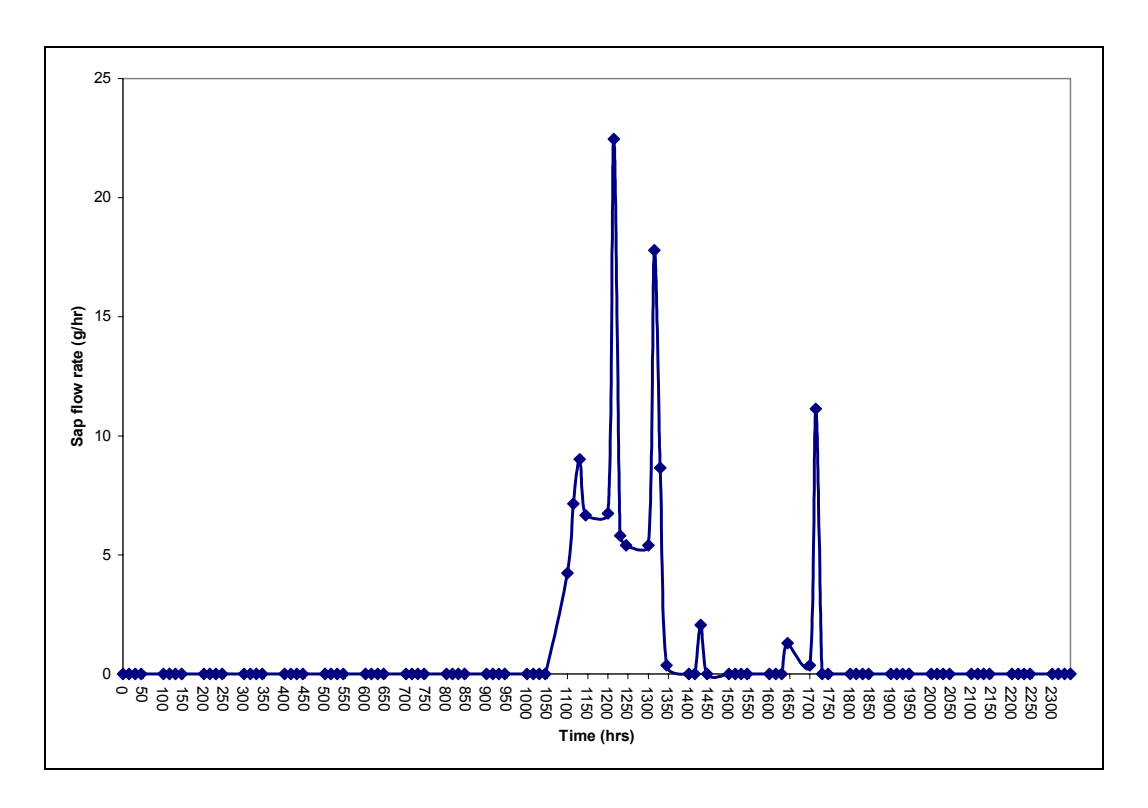


Figure 4.5: Temporal variation of sap flow rate on day 32

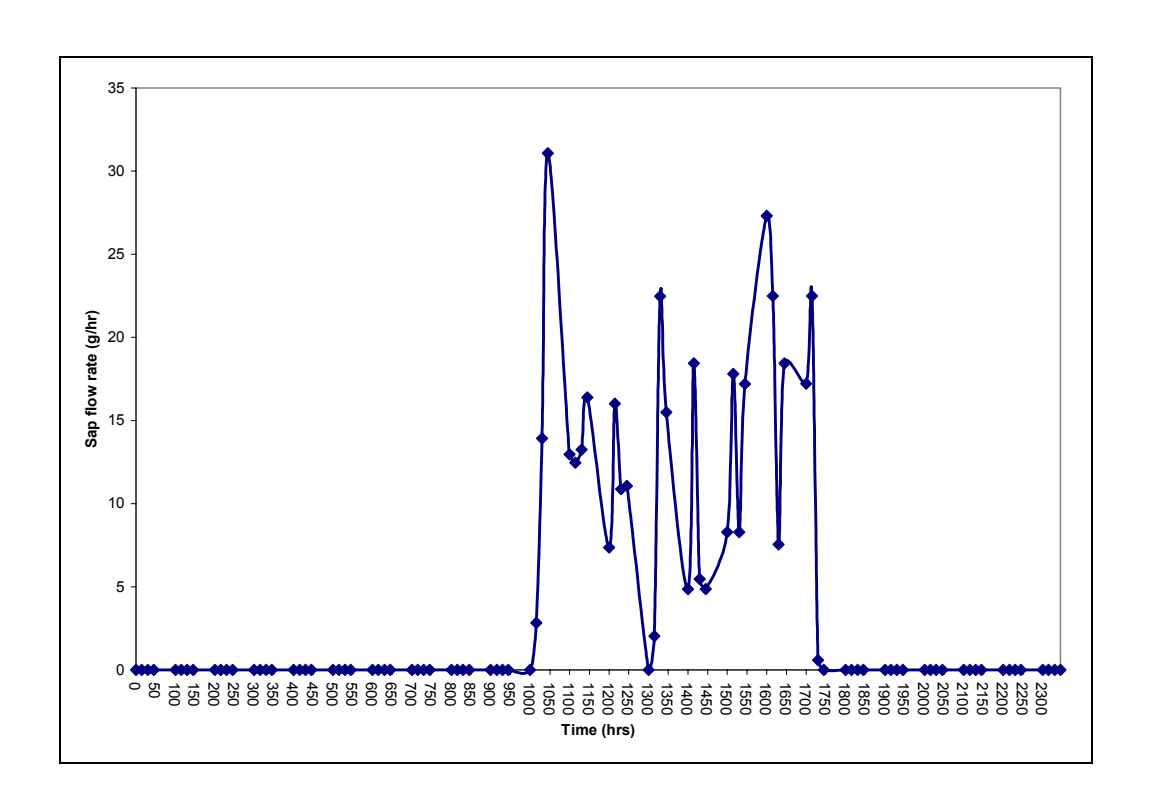


Figure 4.6: Temporal variation of sap flow rate on day 33

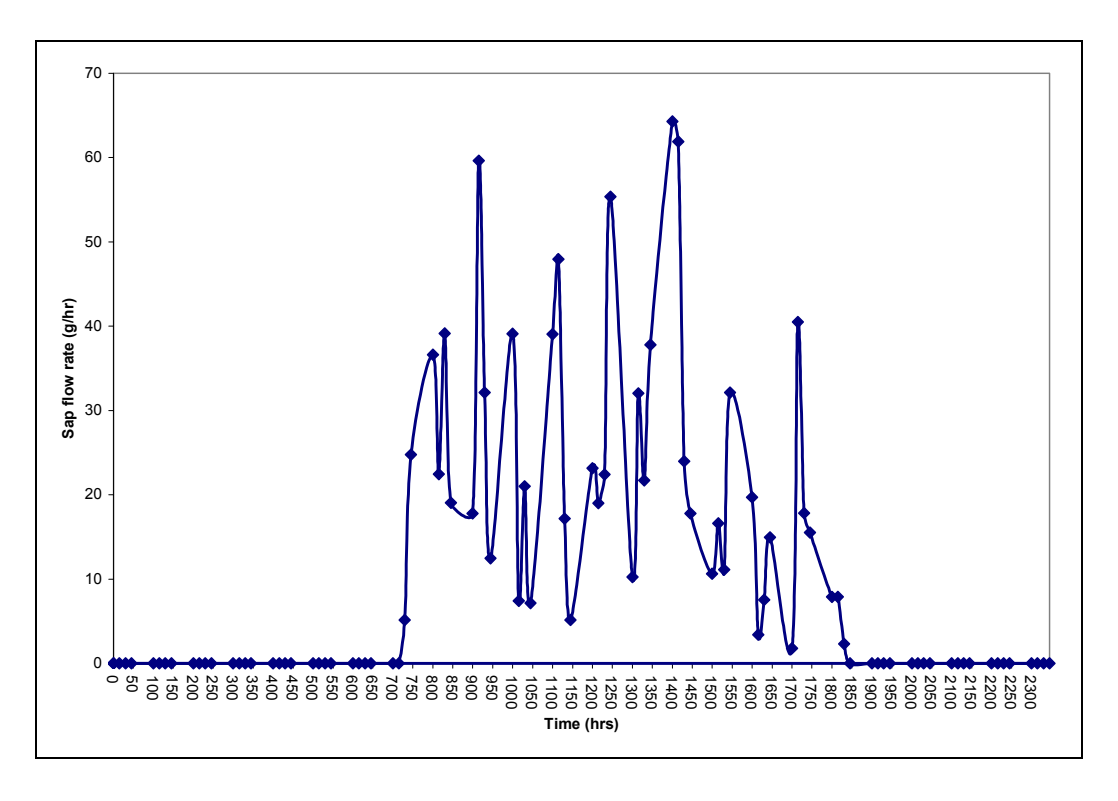


Figure 4.7: Temporal variation of sap flow rate on day 38

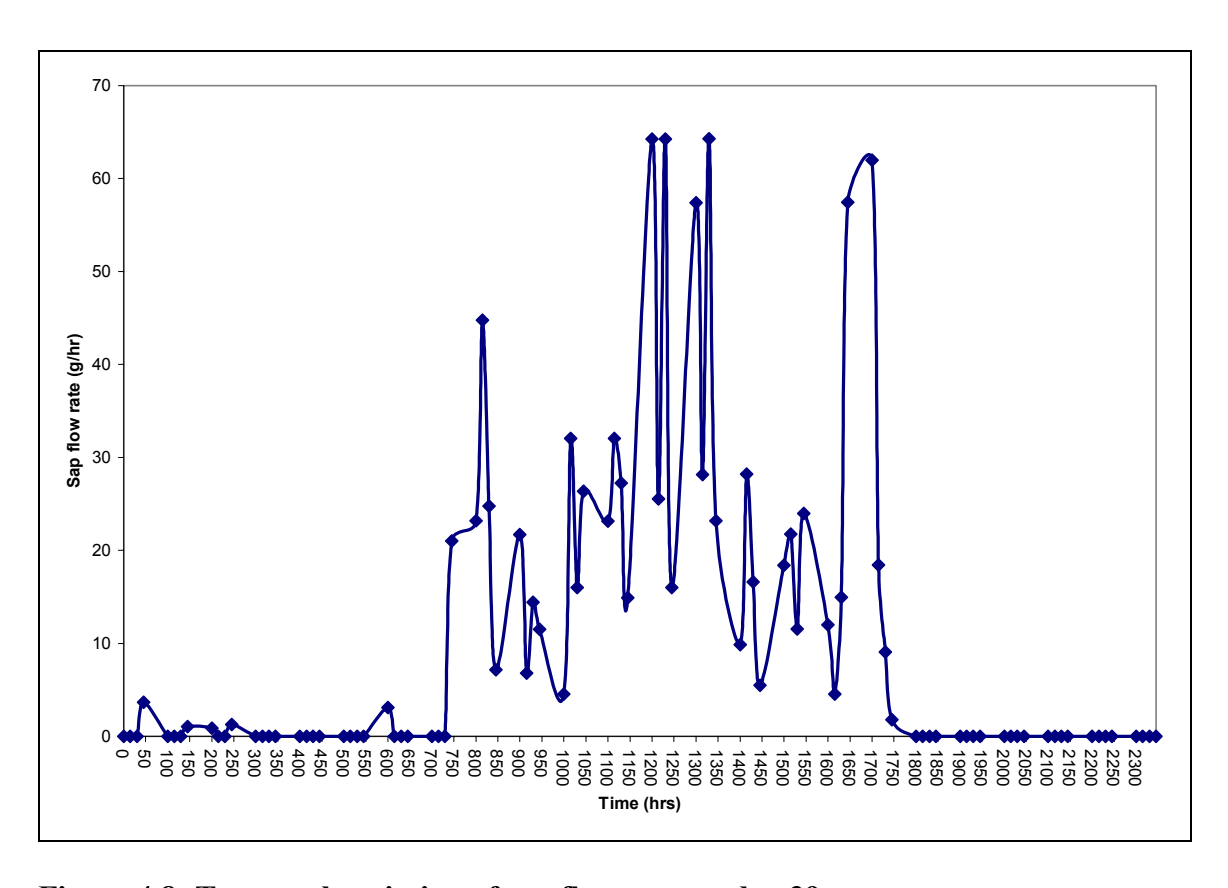


Figure 4.8: Temporal variation of sap flow rate on day 39

Figures 4.5 to Figures 4.8 show diurnal variations of sap flow rates on four different days. All the figures show the same form as they attain their minimum values at night, early morning hours and late afternoon hours. Some uncharacteristic drops of sap flow rates readings to zero around noon time could be attributed to technical problems in the gauges which sometimes arise due to poor shielding or brief power cuts or due to midday stomatal closure. Early morning and nighttime readings were recorded as negative values but in principle should be read as zero flow rates. The variation of sap flow rate was in line with the theory in which transpiration rate was induced by the incoming solar radiation and thermal radiation trapped by the green house.

4.3.4 Variation of sap flow rate with solar radiation

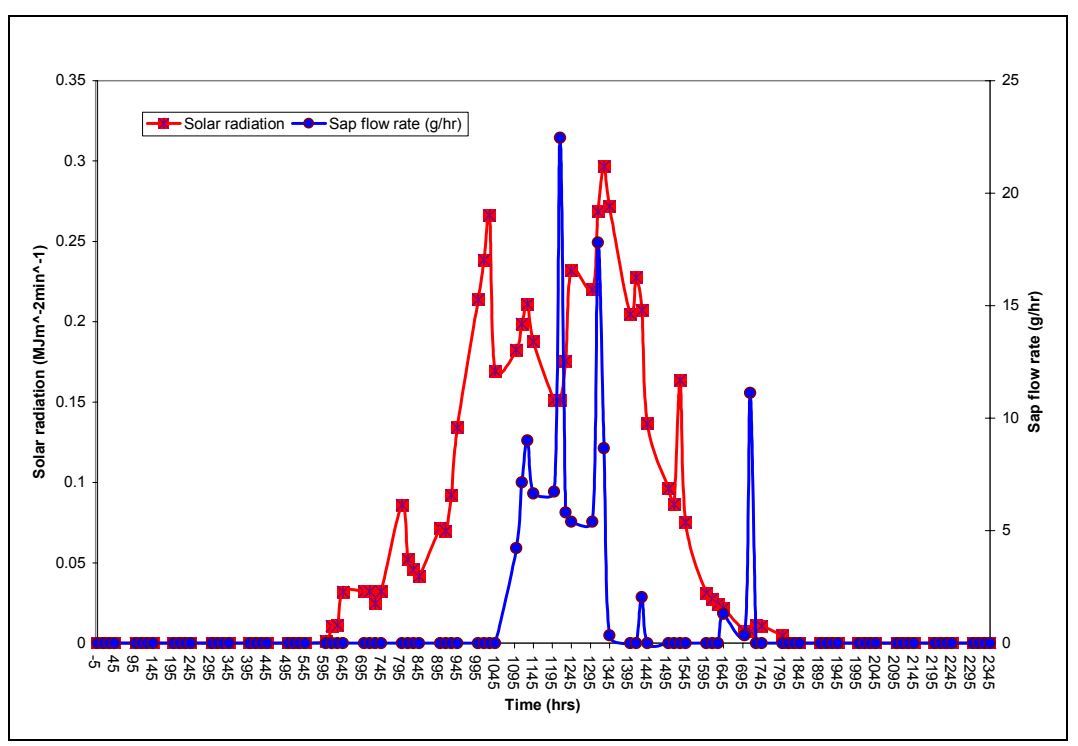


Figure 4.9: Temporal variation of sap flow rate and solar radiation on day 32, 2010

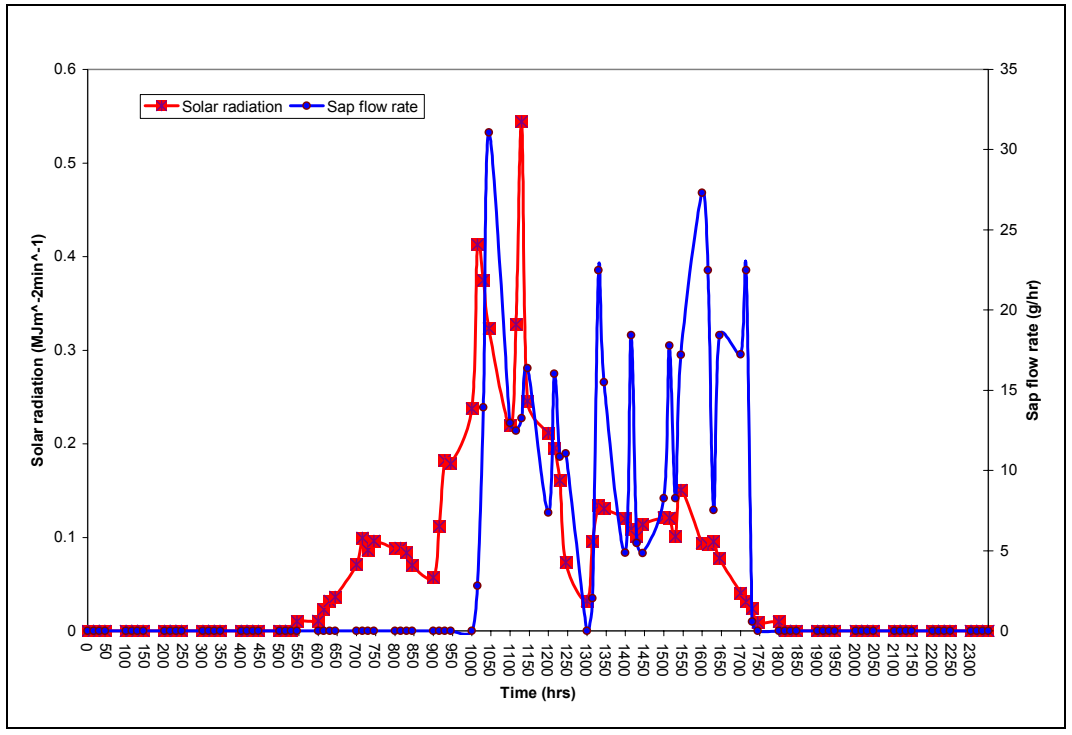


Figure 4.10: Temporal variation of sap flow rate and solar radiation on day 33, 2010

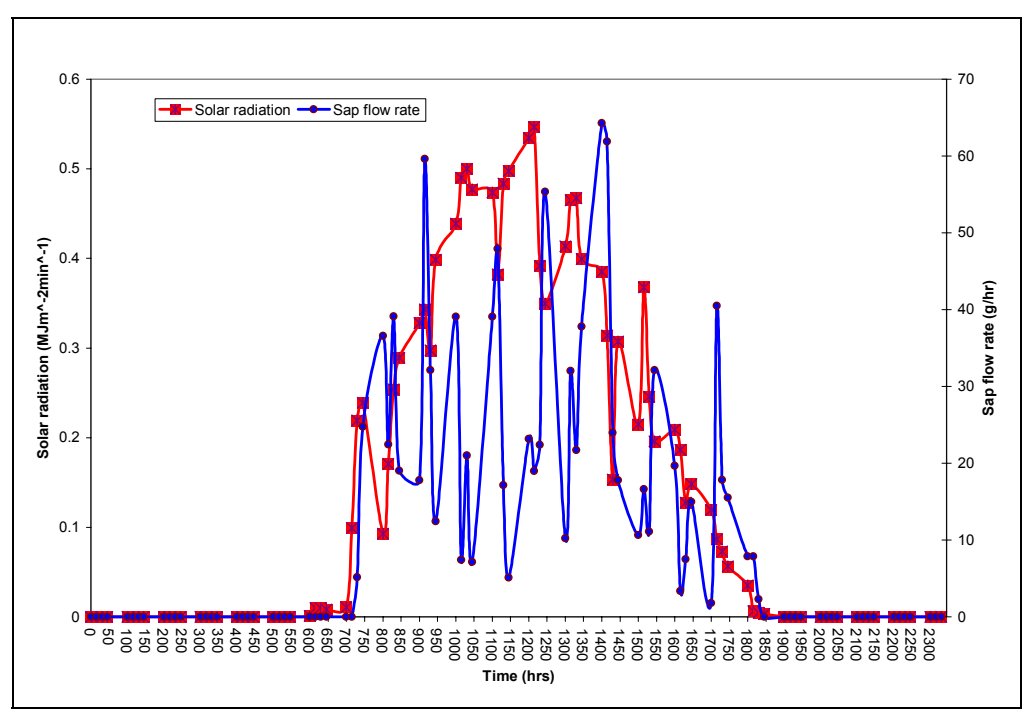


Figure 4.11: Temporal variation of sap flow rate and solar radiation on day 38, 2010

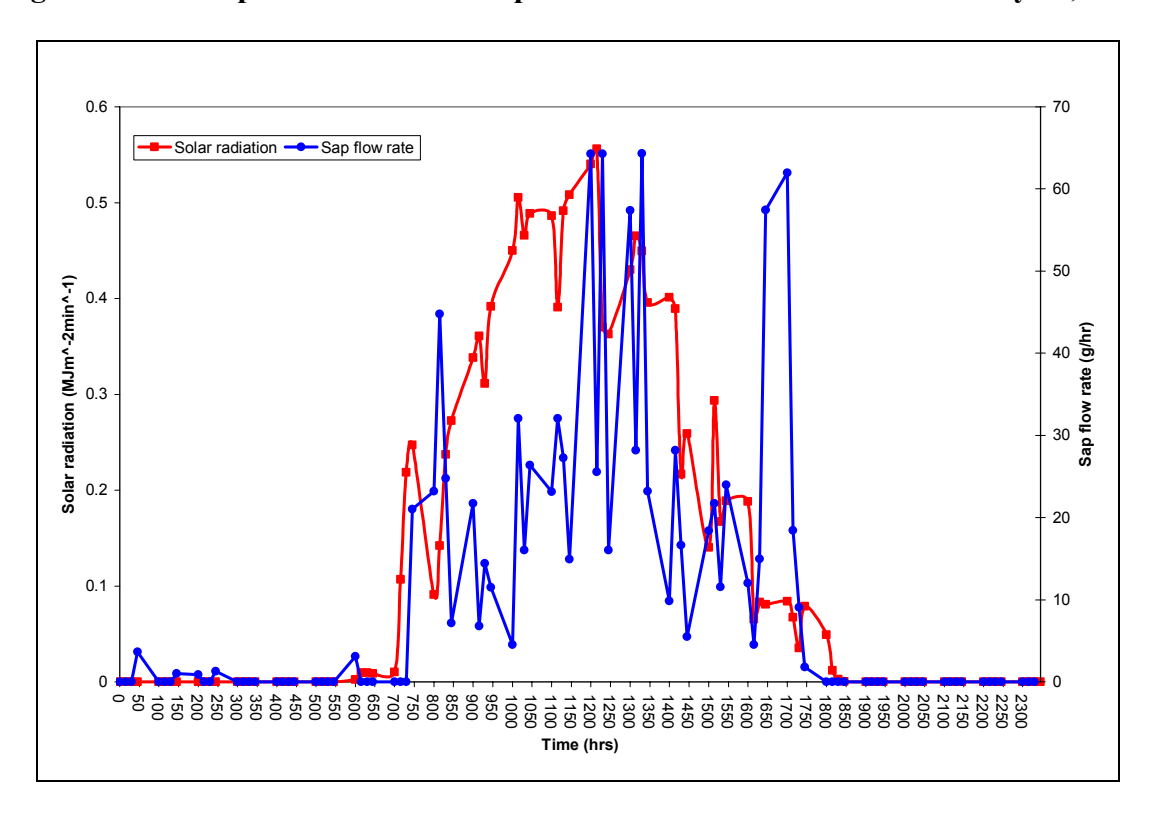


Figure 4.12: Temporal variation of sap flow rate and solar radiation on day 39, 2010

Figure 4.9 to figure 4.12 are showing diurnal variation of sap flow rate with solar radiation. It is quite apparent the sap flow rate graphs followed the shape of the solar radiation which shows that solar radiation is the driving factor of water loss in these crops. There is a time lag though between the time when the sun rises and the beginning of sap movement as with day 39 and 38 showing a short time lag of a few minutes just after sunrise and on day 32 and 33 there is a significant time lag of a few hours.

4.3.5 Variation of sap flow rate with relative humidity

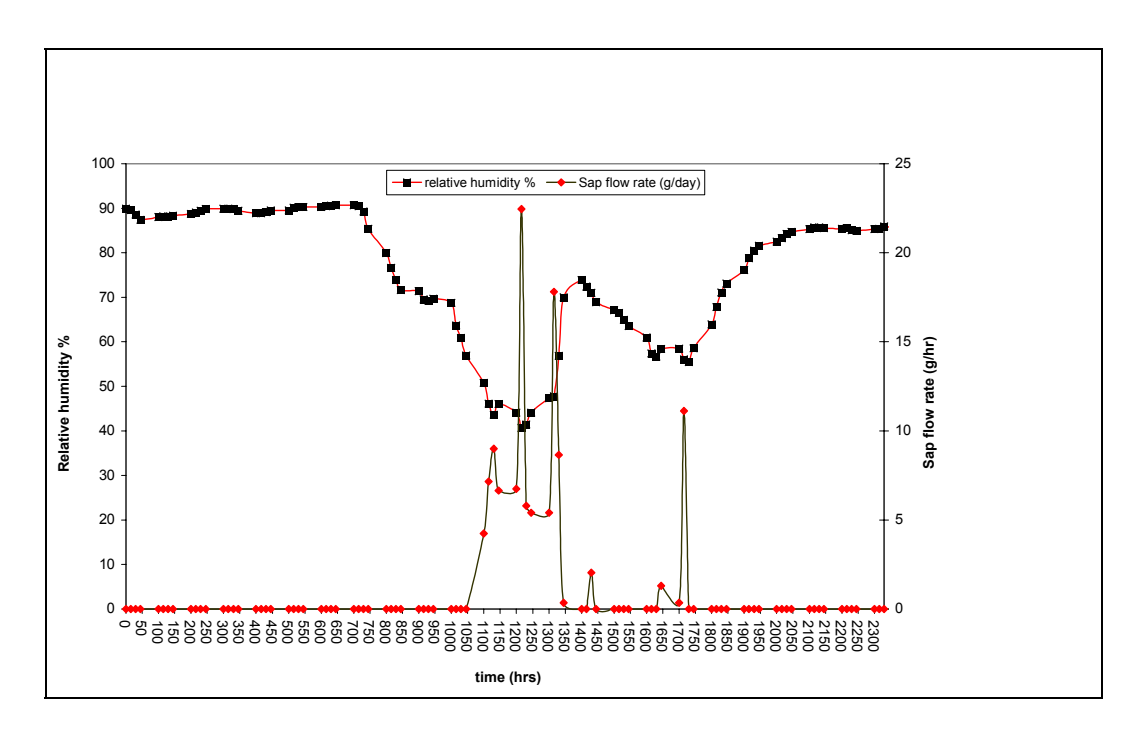


Figure 4.13 Temporal variation of sap flow rate and relative humidity on day 32, 2010

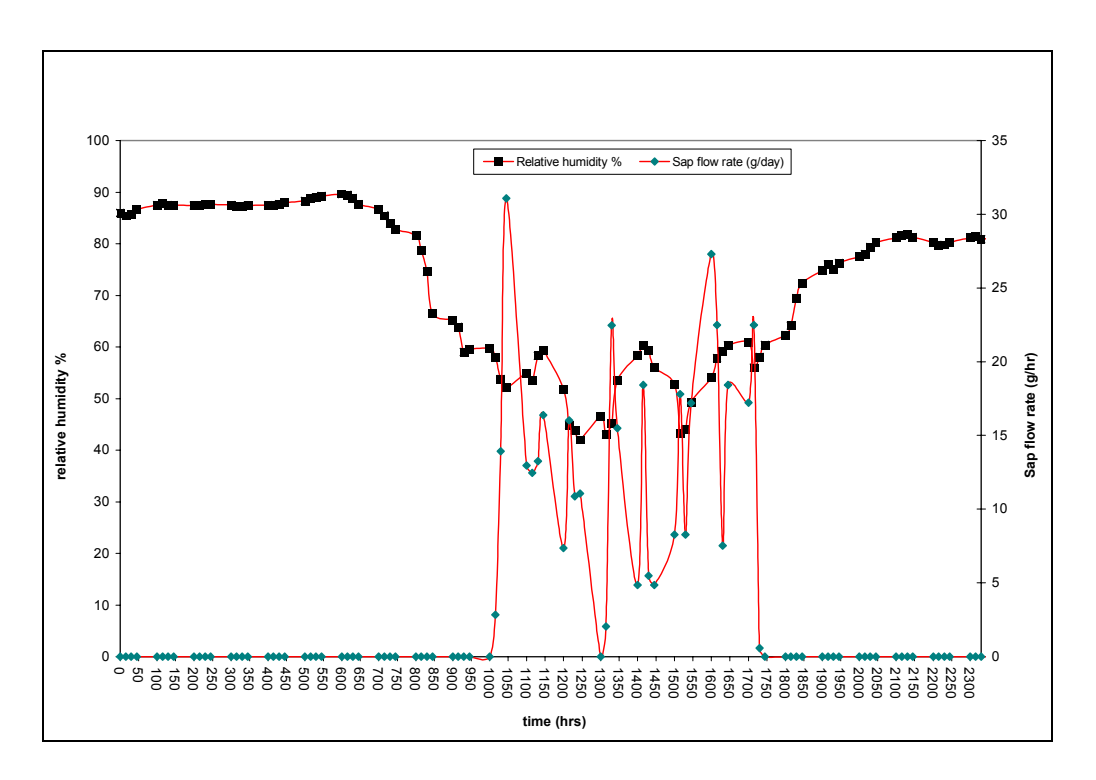


Figure 4.14: Temporal variation of sap flow rate and relative humidity on day 33, 2010

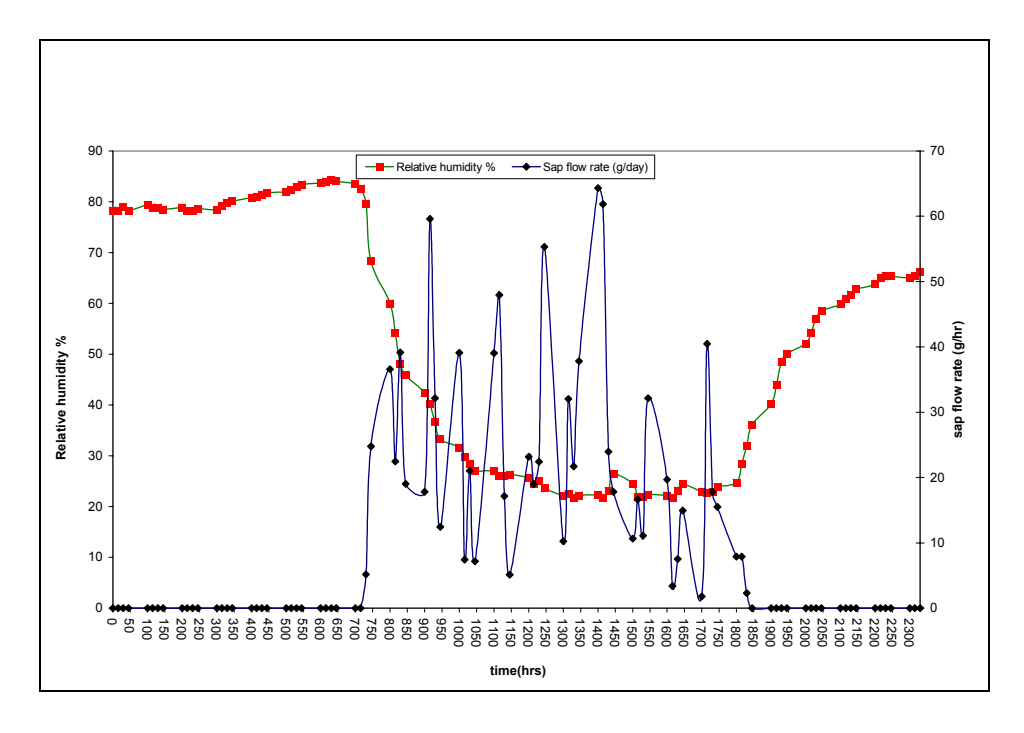


Figure 4.15: Temporal variation of sap flow rate and relative humidity on day 38, 2010

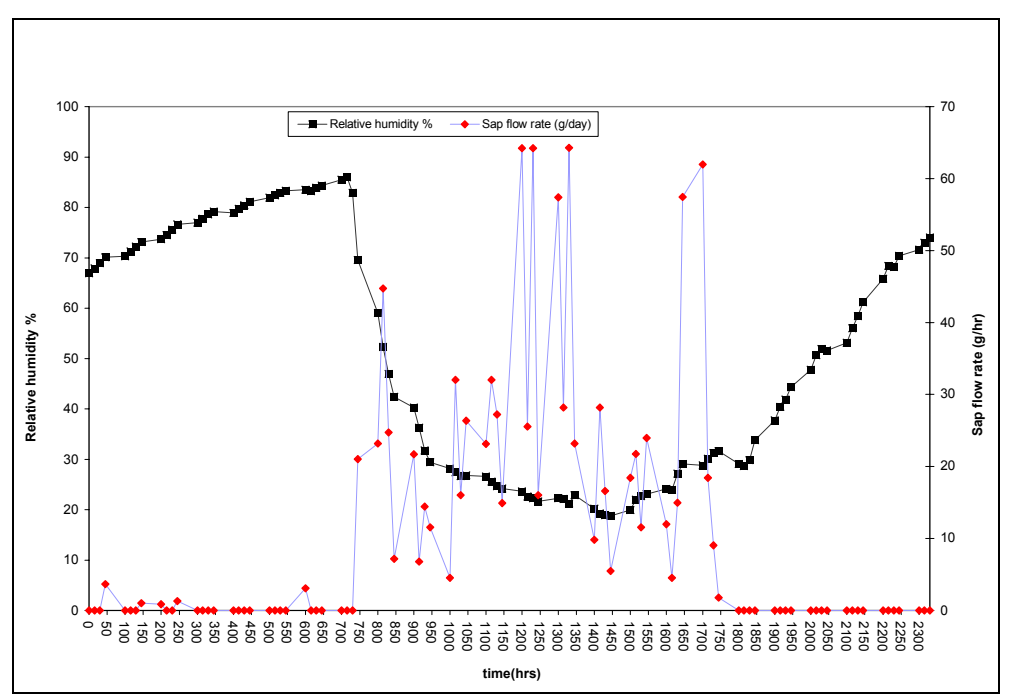


Figure 4.16: Temporal variation of sap flow rate and relative humidity on day 39, 2010

Figure 4.13 to Figure 4.16 show diurnal variations of sap flow rates and relative humidity on four different days. The wave forms of relative humidity have contrasting shapes with the sap flow rate attaining their minimum during the night, early morning hours and late afternoon hours. Relative humidity on the other hand attained its maximum at night and minimum during the day.

4.3.6 Correlation between sap flow rate and weather parameters

Regression analysis was done between sap flow rate results against solar radiation and to give a statistical interpretation of the level of agreement.

 $\begin{tabular}{ll} Table 4.7: A summary of sap flow rate values and relative humidity values for four days \end{tabular}$

Day of year in 2010	Relative humidity %		Sap Flow g/hr
	Maximum	Minimum	sum
32	90.7	10.10188	10.10188
33	89.6	18.63174	18.63174
38	84.3	38.96096	38.96096
39	86	43.27104	43.27104

4.3.5 Variation of sap flow rate with daytime solar radiation

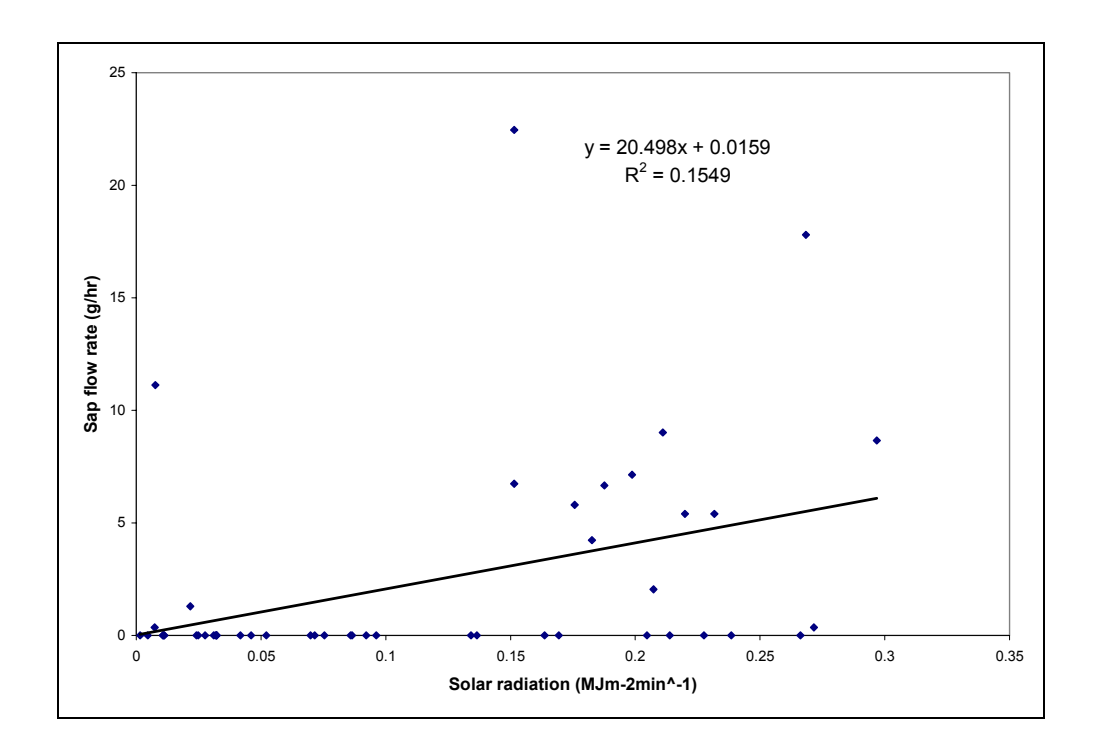


Figure 4.17: Correlation between sap flow rate and solar radiation on day 32

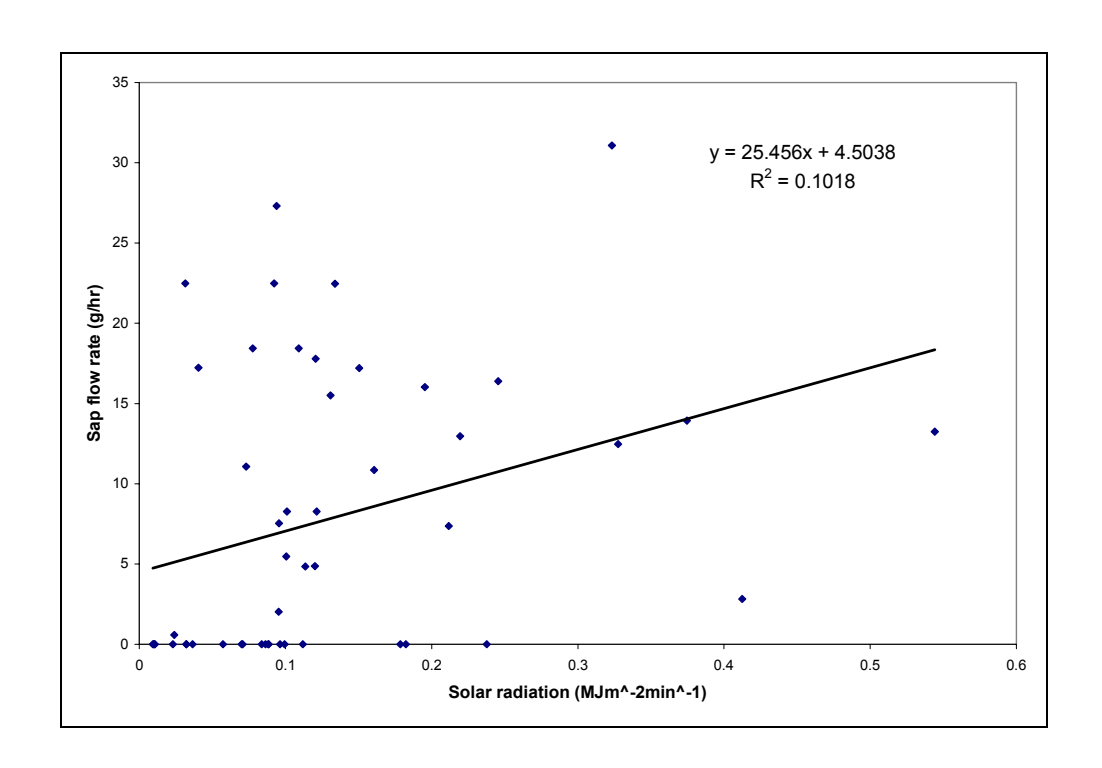


Figure 4.18: Correlation between sap flow rate and solar radiation on day 33

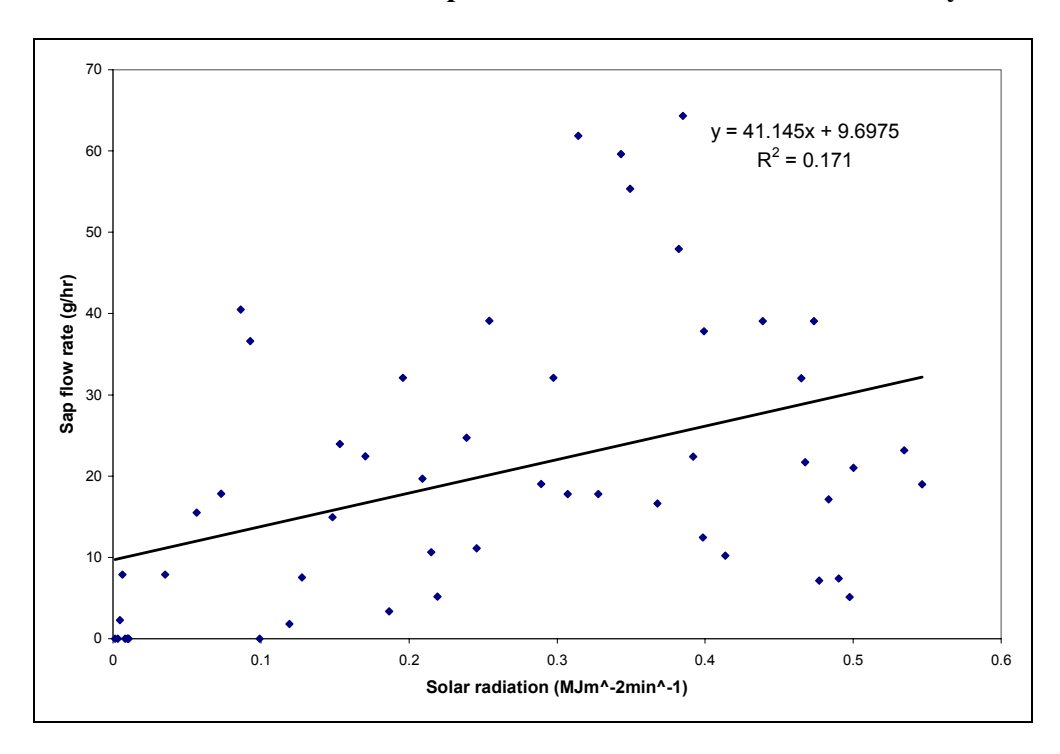


Figure 4.19: Correlation between sap flow rate and solar radiation on day 38

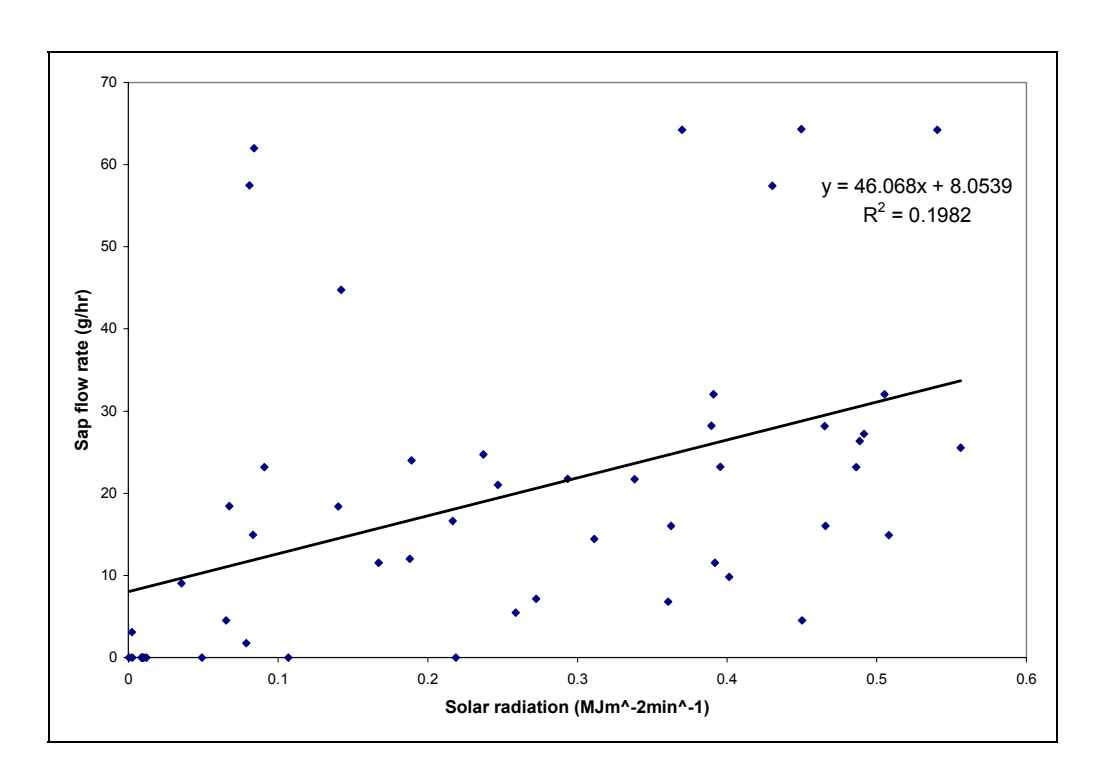


Figure 4.20: Correlation between sap flow rate and solar radiation on day 39

Figure 4.17 to 4.20 show regression analysis between the sap flow rate and solar radiation on four days. It is clearly observed that the linear regression coefficient was weak with 19 % as the highest R^2 value. A positive gradient though of the curve that solar radiation has effect on the sap flow rate.

4.3.8 Temporal variation of sap flow rate with air temperature on different days

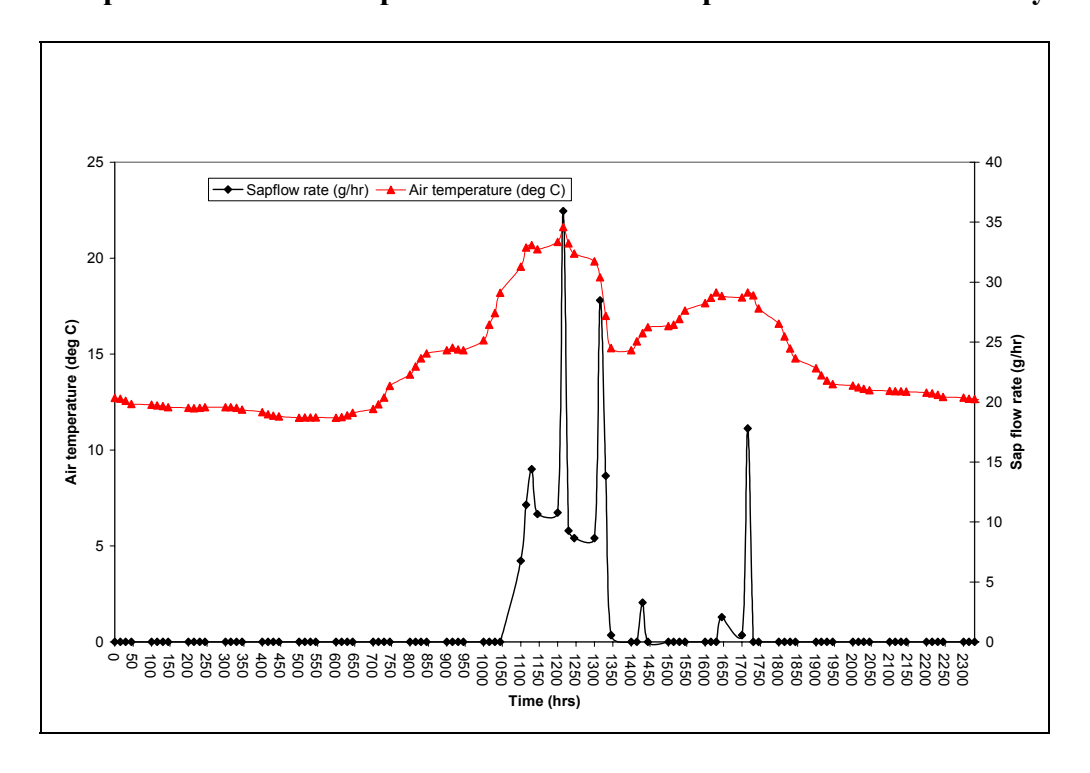


Figure 4.21: Temporal variation of sap flow rate and air temperature on day 32, 2010

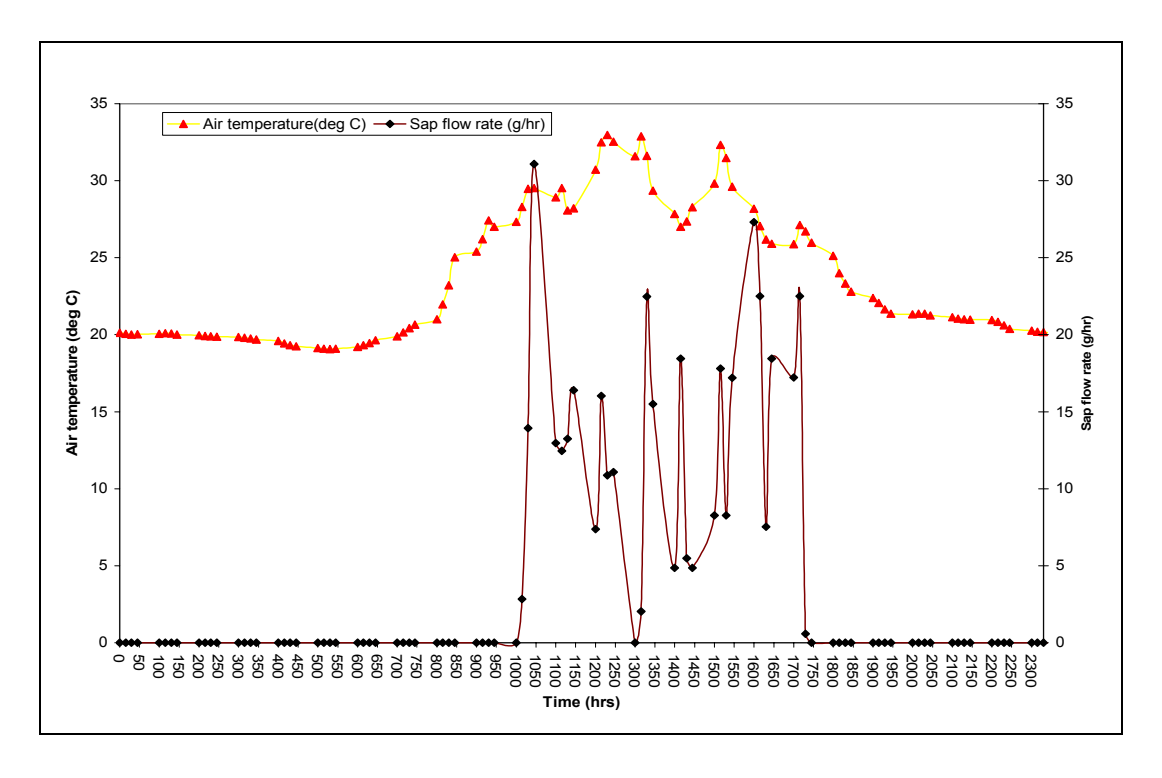


Figure 4.22: Temporal variation of sap flow rate and air temperature on day 33, 2010

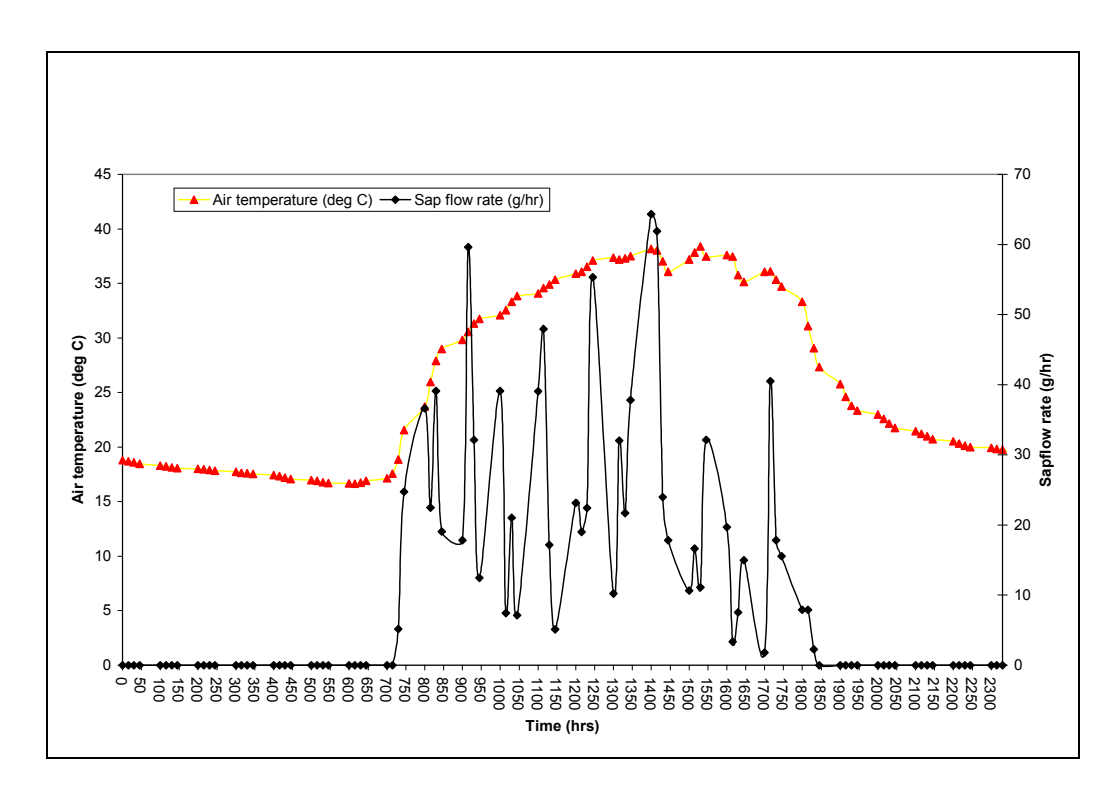


Figure 4.23: Temporal variation of sap flow rate and air temperature on day 38, 2010

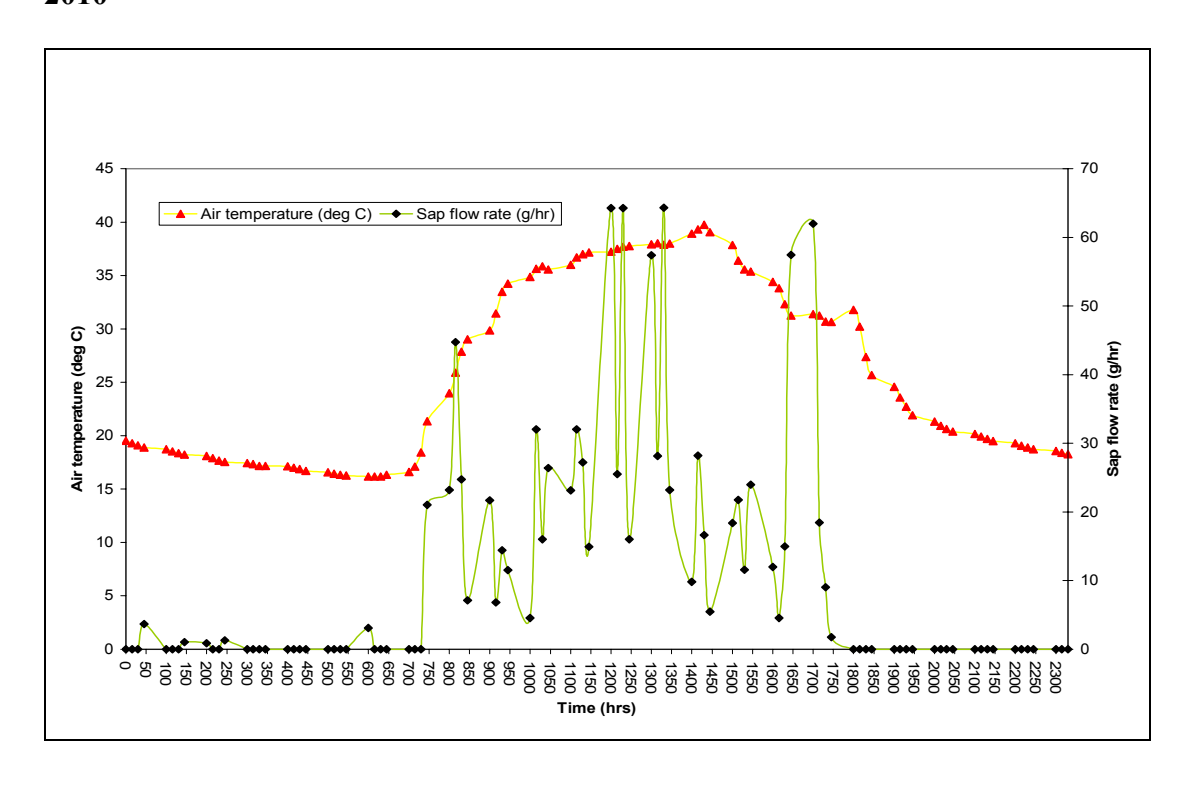


Figure 4.24: Temporal variation of sap flow rate and air temperature on day 39, 2010

Table 4.8: A summary of sap flow rates and air temperatures for four days

Day of year in 2010	Air temperature(°C)					
	Maximum (time)	Minimum (time)	Sap Flow g/hr			
32	34.6	18.68	10.10			
33	32.97	19.07	18.63			
38	38.39	16.65	38.96			
39	39.76	16.17	43.27			

Figure 4.21 to 4.24 are showing temporal variation of the sap flow rate and air temperature. Sap flow rate seems to follow in most cases the pattern of the air temperature with the two parameters attaining their peak values around the same time. The sap flow rate was sometimes not consistent with the air temperature like after 14:50 hrs, this can be attributed to mechanisms employed by the plant to reduce water losses and also the fact that not only air temperature influences loss of water but other factors like relative humidity, soil moisture, and to a lesser extend the wind.

4.3.9 Variation of sap flow readings over 10 days with weather variables

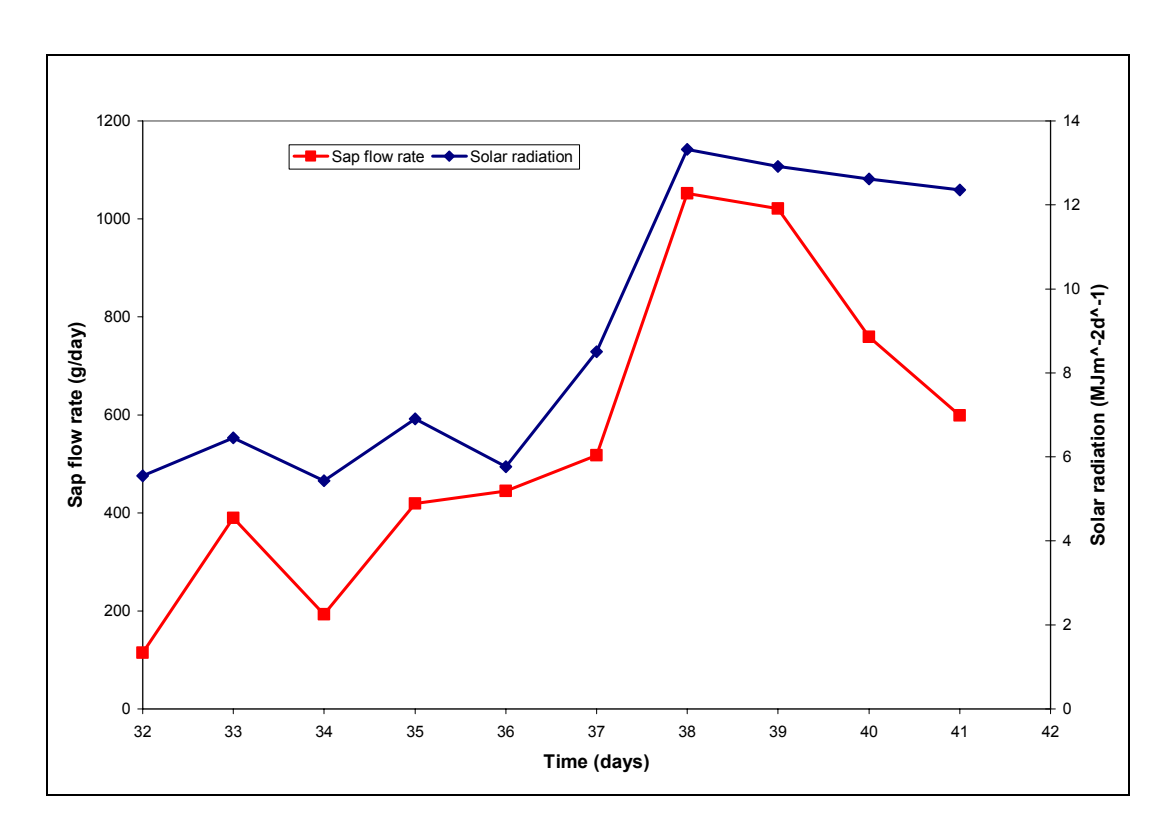


Figure 4.25: A summary of the variation of sap flow rate with solar radiation over 10 days

Figure 4.25 show that the sap flow rate had the same form of as solar radiation. The pattern was indicative of the fact that solar radiation drives the loss of water in crops which was in line with the theory. The maximum sap flow rate recorded over the ten days in question was 0.98 L day⁻¹m⁻² on day 38 where the solar radiation daily maximum value was 12.62 MJm⁻² day⁻¹and air temperature values was 37.96 °C. In addition the picture given was that the sap flow gauge was operating normally.

Table 4.9: Conversion of units (Allen et al., 1998)

Units	equivalence
m ³ per hectare per day (m ³ ha ⁻¹ day ⁻¹)	$1 \text{ m}^3 \text{ ha}^{-1} \text{ day}^{-1} = 0.1 \text{ mm day}^{-1}$
Litre per second per hectare (1 s ⁻¹ ha ⁻¹)	$1.1 \mathrm{s}^{-1} \mathrm{ha}^{-1} = 8.640 \mathrm{mm day}^{-1}$
Litre day ⁻¹ m ⁻²	$0.83 \text{lday}^{-1} \text{m}^{-2} = 1 \text{mmday}^{-1}$

Table 4.10: A summary of sap flow rate, crop evapotranspiration and the weather variables

Day of year (2010)	FAO Penman- Monteith ETc Total (Lm ⁻² day ⁻¹)	Sap flow rate (Lm ⁻² day ⁻¹)	Total daily solar radiation (inside) (MJm ⁻² day ⁻¹)	Maximum daily Air temperature (°C)
32	0.85	0.11	6.45	34.60
33	1.08	0.36	7.09	32.97
34	0.92	0.18	5.43	33.68
35	1.16	0.39	6.91	32.38
36	0.96	0.41	5.76	33.78
37	1.61	0.46	8.50	35.70
38	2.22	0.98	13.32	38.39
39	2.22	0.95	12.92	39.76
40	3.33	0.71	12.62	37.96
41	3.43	0.56	12.35	38.35
Averages	1.86	0.53		

Table 4.10 gives a summary of the variation of transpiration rate as measured by a sap flow gauge, a plant based method and as estimated using the FAO Penman-Monteith method which was a meteorological method with the weather variables i.e. solar radiation and air temperature. Maximum water losses were experienced on day 38 as indicated by the sap flow gauge method and was on day 41 using the FAO Penman-Monteith method. Minimum values of water loss were indicated on day 32 using both the

plant based method and using the meteorological method. Differences in days and total amounts arose because the FAO Penman-Monteith method also includes water lost from the soil through evaporation and since canopy cover of the crops was not 100% therefore water lost is a sum of transpired and evaporated water.

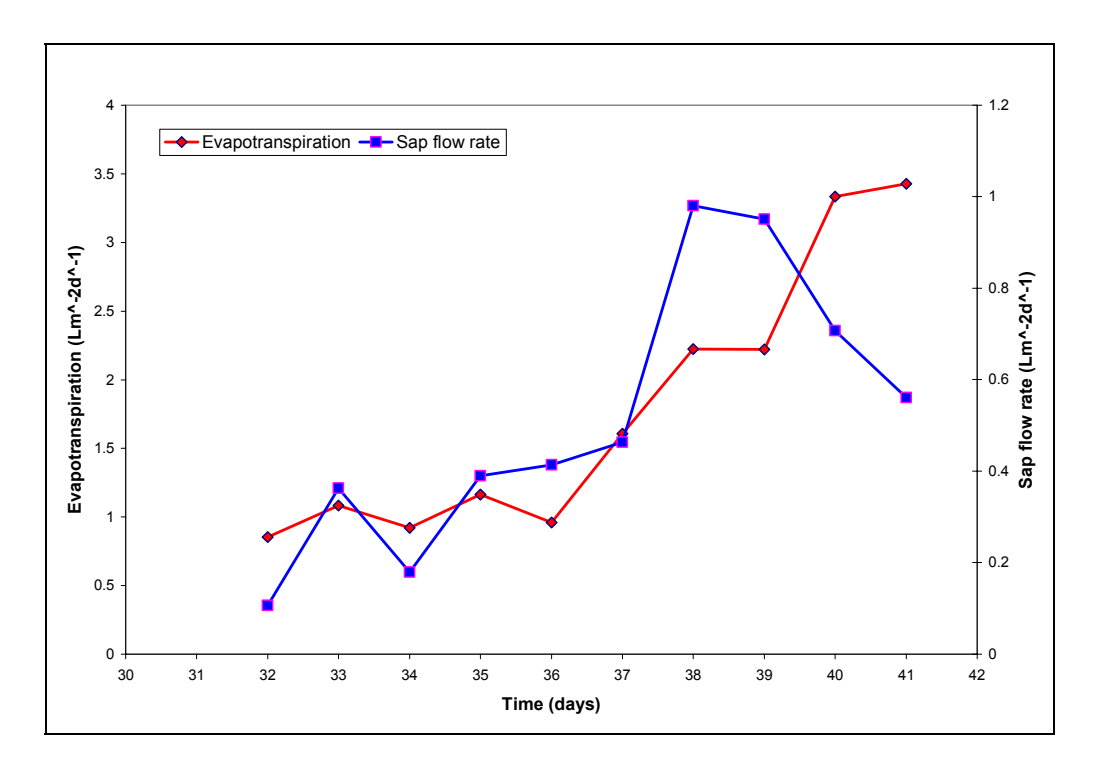


Figure 4.26 Variation of sap flow rates and crop evapotranspiration calculated using the Penman Monteith equation

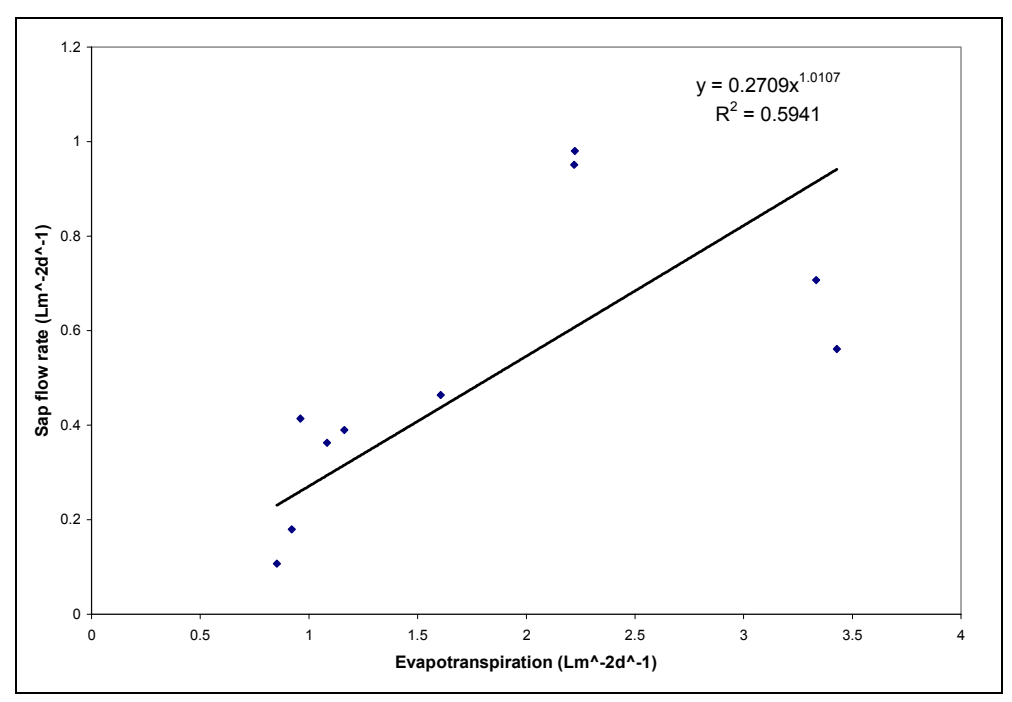


Figure 4.27: Correlation between sap flow rate and crop evapotranspiration

The correlation between the sap flow rate and crop evapotranspiration was 59.41 % and the two vary exponentially. There was a weak linear relationship and this indicates that transpiration rate was not always inline with factors that drive evapotranspiration in crops. Sometimes there is stomatal closure on the crop due to other physiological responses which stops transpiration but evapotranspiration will still be taking place.

4.4 The automatic irrigation control system

This section had results of the testing of components and implementation of the irrigation control system both in the agro-meteorology laboratory and the greenhouse.

Table 4.11: Climatic data outside the greenhouse

Day	Daily total	Air te	mperatui	re (°C)	Relati	ive humi	dity (%)	Maximum PAR
	solar	Max	Min	Mean	Max	Min	Mean	$(\mu molm^{-2}s^{-1})$
	radiation							
	MJm ⁻² d ⁻¹							
105/106	26.59	24.33	15.12	19.646	91.6	49.26	69.73	933
106/107	20.48	25.83	14.76	18.025	94.8	45.35	83.10	847
107/108	17.21	25.22	14.73	18.615	94	53.04	81.71	828
108/109	23.21	26.87	16.16	19.622	94.1	49.24	82.42	964
109/110	23.60	27.25	15.95	21.134	91.8	44.07	72.54	876
110/111	9.19	26.21	15.25	17.827	94.8	51.57	88.01	691

Table 4.12: Climatic data inside the greenhouse

Day	Daily total solar	Aiı	r tempe	rature	Re	lative hu %	ımidity	Daily maximum PAR
	radiation MJm ⁻² d ⁻¹	Max	Min	Mean	Max	Min	Mean	μmolm ⁻² s ⁻¹
105/106	4.84	34.02	15.7	23.33	89	29.57	60.14	933
106/107	2.97	34.95	15.48	20.41	91.4	28.86	74.87	847
107/108	2.41	31.87	15.38	20.28	92.5	36.04	75.67	828
108/109	4.39	37.38	16.34	22.19	92	27.74	73.41	964
109/110	4.14	36.35	16.46	23.59	88	27.31	65.44	876
110/111	1.58	33.13	15.49	19.06	91.8	34.78	82.25	691

Table 4.11 and table 4.12 show the climatic data of the environment outside the greenhouse and inside the greenhouse. Maximum daily total solar radiation was attained on day 105/106 period for both environments with the outside value being 8.771 MJm⁻²d⁻¹ and inside being 4.837 MJm⁻²d⁻¹. Relative humidity attained its highest value on day 110/111 period for both environments on the same day, with 88 % for outside and 82.2 % for inside the greenhouse. The highest daily maximum for PAR is attained on day 108/109 period with a value of 964 μmolm⁻²s⁻¹ as the inside value. It clearly shows the climate inside the greenhouse is influenced by the external environment. Air temperature

maximum values are attained on the same day(day 108/109) with values of 26.87 °C for outside the greenhouse and 37.38 °C, the difference being due to the wind speeds outside the greenhouse being higher than inside therefore more sensible heat energy is dissipated outside.

Table 4.13: Readings used to calculate the drip emitter rate from the Pedrollo water pump

Amount of water (litres)	Time taken (minutes)
2	17.40
2	16.30
2	16.58
Average time for four drip pipes	16.76
Average time for one drip pipe	67.00
Drip emitter rate for one pipe	1.79 l/hr

Table 4.14: Readings used to calculate the drip emitter rate from the Penman-Monteith based

Amount of water (litres)	Time taken (minutes)	
2	13.40	
2	13.30	
2	13.35	
Average time for four drip pipes	13.36	
Average time for one drip pipe	53.44	
Drip emitter rate for one pipe	2.2455 l/hr	

Tables 4.13 and 4.14 show experimental readings that were used to calculate the drip emitter rates using a pump to draw water and straight from the tap which is the grower's practice. The drip emitter rate of the pump is slightly higher than that of the tap with a value of 2.2455 litres per hour and a tap one with 1.79 litres per hour.

Table 4.15: Daily transpiration rate for the control system, the time allocated to the pump and the daily totals for the weather variables.

DOY	Transpiration rate (l/day/m²)_ Automated irrigation system	Time given to pump (minutes) (using drip emitter rate of 2.2455 L/hr)	Total daily solar radiation (inside) (MJm ⁻² d ⁻¹)	Maximum daily air temperature (°C)
105-106	0.35	9.44	4.84	34.02
106-107	0.26	6.89	2.97	34.95
107-108	0.22	6.24	2.41	21.07
108-109	0.23	12.51	2.41	31.87
	0.47		4.40	37.38
109-110		20.14		
	0.75		4.14	36.35
110-111	0.68	18.28	1.58	33.13
Total used	2.75	73.50		

Table 4.15 shows values of transpiration rate as computed by the control program based on sap flow rate equations according to Sakuratani, 1981; Baker and van Bavel 1981. The sap flow rate was computed in units of Lm⁻² day⁻¹. Only one sap flow gauge was used in the experiment and was made to run for six days. The total water used in six days was 2.75 litres. The average water used was 0.288 litres m⁻² day⁻¹. The corresponding weather variables show that the maximum solar radiation was 4.84 MJm⁻²d⁻¹on day 105/106. On the other hand sap flow rate was maximum on day 109/110 with a value of 0.75 litres. Again the maximum value of weather variables and sap flow rates are not attained on same days. There was agreement though with the minimum values for the two variables.

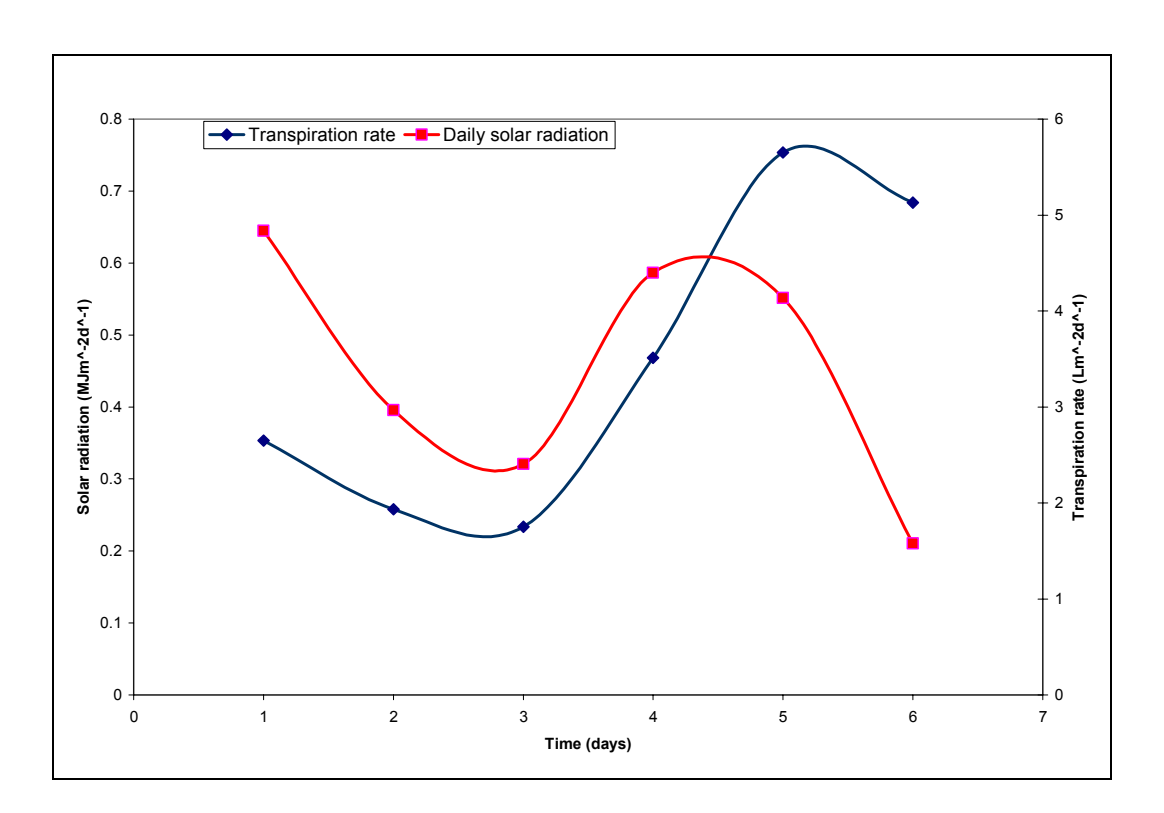


Figure 4.28: Variation of the irrigation control sap flow rate and weather variables over 6 days

Figure 4.28 show graphical variation of sap flow rate and the weather variables over 6 days. On the first day solar radiation was high and the following day solar radiation was low because it was cloudy. Since the greenhouse shelter traps in long wave thermal radiation, a drop in solar radiation on day 106/107 did not result in a drop of transpiration rate. The transpiration rate seemed to follow the form of solar radiation on the last three days of the experiment; hence solar radiation was effectively driving the transpiration rate in these days. Air temperature was following the form and trend of solar radiation.

4.4.1 Investigative crop treatments

The control system was compared with two other treatments in which the leaf temperature was monitored.

Table 4.16: Daily totals of water used by the two systems for 32 crops

Day of year	Total daily water used_Penman Monteith (Lday ⁻¹)	Automatic system_(Lday ⁻¹)	Differences (Lday ⁻¹)
(105-106)	28.64	11.31	17.33
(106-107)	28.64	8.25	20.39
(107-108)	28.64	7.48	21.17
(108-109)	28.64	14.99	13.65
(109-110)	28.64	24.11	4.53
(110-111)	28.64	21.89	6.75
,	171.84 L	88.03 L	83.81 L

Table 4.16 shows the total water used over six days. The automated irrigation control used 88.03 litres and the current practice which supplied a fixed amount of water of 171.84 liters. There is a difference of 48.77 % which is almost half the amount of water that could be saved by the grower's current practice. Total water used was 171.84 L for the existing method and 88.03 L for the automated system.

Table 4.17: Leaf temperatures on three treatments

	Maximum leaf temperatures (°C)				Minimum leaf temperatures (°C)		
Day	Stressed	Automated	Penman	Stressed	Automated	Penman	
	crop	irrigation	Monteith	crop	irrigation	Monteith	
		system	based		system	based	
(105-106)	34.31	29.79	29.79	16.92	12.86	13.43	
(106-107)	34.03	29.69	29.59	16.55	12.70	13.54	
(107-108)	30.82	26.84	26.56	16.40	12.55	13.22	
(108-109)	36.05	31.94	31.88	17.31	13.46	14.43	
(109-110)	35.31	30.81	30.81	17.66	13.63	13.97	
(110-111)	32.76	28.65	28.19	18.69	12.66	13.25	

Table 4.18: A summary of total solar radiation for inside and outside the greenhouse

(inside) MJm ⁻² day ⁻¹	(outside) MJm ⁻² day ⁻¹	Day
4.836724	26.5957	(105-106)
2.968579	20.47927	(106-107)
2.405672	17.2049	(107-108)
4.399786	23.2074	(108-109)
4.135614	23.60432	(109-110)
1.579635	9.189144	(110-111)

Table 4.17 shows the leaf temperature for the three investigative treatments i.e. a stressed treatment in which water supply was cut for six days and there are leaf temperatures from the current grower's practice an the automated irrigation system. Leaf temperatures for the stressed treatment will be higher than those of the current grower and the automated system both in daily maximum and minimum values. The variation in leaf temperatures is is following the solar radiation trend i.e. when the total daily solar radiation is maximum (on day 105/106) the leaf temperature will also be maximum. It is observed that the well watered crop transpires more than the stressed one hence cooling down the leaf surface

temperatures as opposed to the stressed one which closes the stomatal pores to minimize water loss hence higher leaf surface temperatures.

Table 4.19: Potential crop evapotranspiration (ET₀) over 6 days using the FAO Penman-Monteith method

DAY OF YEAR	DATE	Treatment 1 (Stressed) Total daily ETo (mm/hr)	Treatment 2 (FAO Penman-Monteith) Total daily ETo (mm/hr) Current grower practice	Treatment 3 (automatic irrigation control) Total daily ETo (mm/hr)	Total daily solar radiation (inside) radiation MJm ⁻² day ⁻¹
(105-106)	16/04/10		_		
(106-107)	17/04/10	3.48	2.74	2.78	4.84
		2.49	1.89	1.92	2.97
(107-108)	18/04/10	2.49	1.09	1.92	2.91
,		2.13	1.72	1.69	2.40
(108-109)	19/04/10				
(100 110)	20/04/40	2.98	2.32	2.29	4.39
(109-110)	20/04/10	2.00	2.06	2.04	4.1.4
(110-111)	21/04/10	3.90	3.06	3.04	4.14
(110 111)	21/01/10	1.59	1.26	1.26	1.58
Total over					
6 days		16.56	12.98	12.98	

Table 4.19 shows the evaporative demands of the three treatments. The stressed treatment has the highest ETo value which translates in high affinity for water for the atmosphere. The moisture demand by the atmosphere is followed by the current grower and the least demand is for the automated system. The demand for water is directly affected by the humidity level of the air around and when crops are well watered, evaporated and

transpired water makes the atmosphere humid and less demanding for moisture, the opposite happens for the stressed crops where water supply was cut.

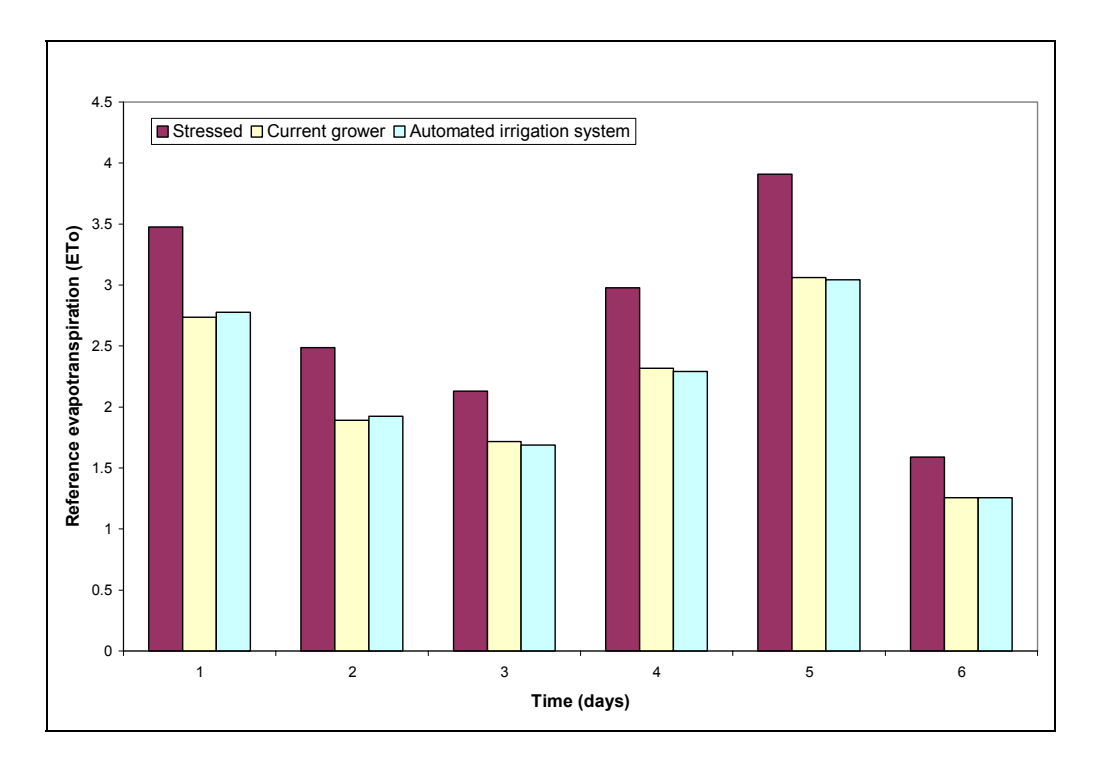


Figure 4.29: Showing a comparison of the ET₀ for the irrigation control system, stressed treatment and the current grower's practice.

Figure 4.29 shows a bar graph for the three treatments comparing the water demand of the atmosphere. The ET_o values for the Penman-Monteith based and that for the automated irrigation control are almost the same since there was good supply of water to the soil therefore resulting in good vapour enrichment of the atmosphere above the treatments. The opposite was shown by the stressed treatment which had high values for ET_o because of low moisture content of the soil and closure of the stomatal pores as an adaptive measure to reduce excessive water loss from the crops.

CHAPTER 5

Conclusions and Recommendations

Sap flow rates seem to be strongly driven by the solar radiation mostly and less by other factors as graphs of the solar radiation and sap flow rate have the same shape in most cases during daytime. Other factors that may influence sap flow rates are wind speed, air temperature and exposure to light of the crop. Typical water losses estimated by the sap flow gauge were from 0 to 0.980 litres m⁻² day⁻¹ with an average of 0.512 litres m⁻² day⁻¹. The daytime total solar radiation maximum value was 12.917 MJ m⁻² day⁻¹and the minimum was 5.429 M J m⁻² day⁻¹ for the ten day period. Relative humidity is minimum during the day because the solar radiation was present during the day and it induced air motions that spread water vapour molecules and made some to escape through the vents of the greenhouse. At night relative humidity was maximum because there was no solar radiation, the air was relatively still and all evaporated and transpired water made the atmosphere inside the greenhouse more humid as there was not enough energy to make the vapour rise and escape through the greenhouse openings. Relationship between sap flow rates and relative humidity is arrived at because of the form of the curves which seemed to be reflections of each other as the sap flow graphs had peaks when relative humidity had troughs and vice versa for diurnal variations. A comparison of the water loss from the plants using the Penman –Monteith method over the ten days showed that crop evapotranspiration rate had an average value of 1.861 mm/day as opposed to the sap flow rate average value of 0.528 mm/day. The former method calculates water loss from the evaporated water and the transpired one (meteorologically based) hence the higher the value and the latter only registers the transpired water. Correct estimation of water loss was given by the plant based method which gives the transpired water only and this helps the grower to supply the exact amount required to replace water lost, avoids over irrigation or under irrigation, saves water and money. Proper shielding of the gauges, choosing the right stem/branch size, and correct voltage supply to power the gauge are some recommendations as described in the manual (van Bavel 1987) as failure to meet any of these results in erroneous readings. Effective transpiration in plants started around 9:30 am for all the days that were investigated and ceased around 4pm as observed from the graphs.

The automated irrigation control system gave results for the transpiration computed from the stem heat balance method of sap flow gauges. The response time of the system was good and it worked efficiently to replace exactly the lost amount of water. The leaf temperatures as indicated from the three treatments showed that the crops were receiving the right amounts of water to cool down the leaf temperatures as the maximum leaf temperature was 31.94 °C and corresponded to the day when the solar radiation was at the peak daily total value inside the greenhouse with a value of 4.84 MJ m⁻² day⁻¹. The Penman-Monteith based treatment showed again leaf temperature values that were similar to those of the automated system with a maximum value of 31.88 °C with maximum air temperature being 36.35 °C which indicated that the crops were receiving the right amount of water to cool down the leaf temperatures. The stressed treatment showed very high leaf temperatures with a maximum of 36.05 °C which was not very different from the maximum air temperature on this day which was 36.35 °C. This clearly showed that leaves could not be cooled down since there was not much water coming

from the roots and also stomatal closure as an adaptation to reduce excessive water loss. The corresponding average ETo values obtained over 6 days were 2.77 mm/day, 2.163 mm/day and 2.1630 mm/day for the stressed treatment(a), the Penman-Monteith based (b), and the automated irrigation (c) respectively. A good supply of water resulted in less moisture demand by the atmosphere above the crop canopies for (b) and (c), and little or no supply of water to crops gave a less humid atmosphere, hence the high affinity for moisture by air above treatment (a).

The performance of the treatments could only be indicated by the water demand of the atmosphere (ETo values) above them because of time constraints. Ideally other indicators of the performance of the crops are physiological and morphological development (leaf sizes, fruit sizes, root developments, leaf colour e.t.c.) and these give a better comparison. The automated irrigation control saved time, labour, energy and water. The system improved water use efficiency and productivity as opposed to the Penman-Monteith based that over irrigated and water logging was imminent which inhibits proper root respiration and cause leaching that washes away the necessary nutrients.

On the irrigation control system instruments like the K8000 card, the K6714 relay card and the amplifying circuit needed proper packaging. Packaging avoids: short circuits which result in unwanted voltage drops; prevents electrocution to the user; avoids damage of equipment from water; reduces complexity of the equipment and makes the system easy to comprehend and user friendly.

Prior to assembling of the control system, testing for signal transfer from the datalogger to the computer can be done outside the greenhouse environment if resources and time permit. The greenhouse environment was difficult to operate under as there are high temperatures that sometimes soar to 39 °C. If a technical problem arises, troubleshooting can take time and this was better done outside the greenhouse where temperatures are bearable.

A different transpiration rate probe that give out electrical signals of a more significant current value was recommended to improve the quality of the results since this evades signal amplification which in most cases slightly distorts the original sensor signal.

A database system should be installed together with the computer program. The database stores all the information that it is instructed to when the system is running. Since all components of the system are electrically driven; loss of power will not result in loss of data.

Use of a microcontroller chip in place of the cards and the computer provides a good alternative. A microcontroller chip system just entails programming of the chip with the necessary instructions, installation of the necessary probes and a pump for water. The chip does all the decision making process and actuates the pump when necessary. Even when the power is cut, it resumes running when power is restored, there is no need for human intervention.

REFERENCES

Acock, B. & Grange, R.I (1981). Equilibrium models of leaf water relations. In Rose & Charles-Edwards.(1981), pp. 29-47.

Allen RG,Pereira LS,Raes D,Smith M. 1999. Crop evapotranspiration. FAO Irrigation and drainage Paper 56.Rome: FAO.

Andriolo, J.L.A.; Streck, N.A.; Buriol, G.A.; Ludke, L; Duarte, T.S. 1998 growth, development and dry matter distribution of a tomato crop as affected by environment. *Journal of Horticulture Science & Biotechnology*, v. 73, p. 125-130,

Baille A.(1994).Irrigation management strategy of greenhouse crops in Mediterranean, Countries. Acta Horticulture, 361:105-22.

Baker, J.M. and C.H.M. van Bavel. 1987. Measurement of mass flow of water in stems of herbaceous plants. Plant, Cell, and Environment 10: 777-782.

Balek, J., and O Pavlik. 1977. Sap stream velocity as an indicator of the transpirational process. J. Hydrol. 34:193-200.

Bates LM, Hall AE. 1981. Stomatal closure with soil water depletion not associated with changes in the bulk leaf water status. Oecologia 50, 62-65.

Bloodworth, J.E., J.B.Page, and W.R.Cowley. 1955. a thermoelectric method for determining the rate of water movement in plants. Soil Sci.Soc.Am.Proc. 19:411-414.

Boulard T.& Baille A.(1993).A simple greenhouse climate control model incorporating the effects of aeration and evaporative cooling.Agric.For.Meteorology,65:145-157.

Brough DW, Jones HG, Grace J, 1986. Diurnal changes in the water content of stems of apple trees as influenced by irrigation. Plant, cell and Environment 9, 1-7.

Burquez R.(1987).Leaf thickness and water deficits in plants: a tool for field studies. *Journal of Experimental Botany***38,109-114.**

Campbell Scientific Inc. (2007). Instruction manual for model HMP45C temperature and relative humidity probe, Revision 2/07. Campbell Scientific Limited, 815 West 1800 North Logan, Utah 84321 - 1784, USA (http://www.campbellsci.com)

Cermak J, Cienciala E E, Kucera J,Lindroth A, Bednarova E. 1995. Individual variation of sap flow rate in large pine and spruce trees and stand transpiration: a pilot study at the central NOPEX site. Journal of Hydrology 168, 17-27.

Cermak J, Deml M,Penka M. 1973. A new method of sap flow rate determination in trees. Biologia Plantarum (Praha) 15, 171-8.

Cermak J, Jenik J, Kucera J, Zidek V, 1984. Xylem water flow in a crack willow tree (Salix fragilis L.) in relation to diurnal changes of environment. Oecologia 64, 145-51.

Cermak J, Kucera J, Penka M. 1976. Improvement of the method of sap flow rate determination in full-grown trees based on heat balance and direct electric heating of xylem. Biologia Plantarum (Praha) 18. 105-10.

Cermak J,Kucera J 1981. The compensation of natural temperature gradient at the measuring point during **sap flow**-rate determination in trees. *Biologia Plantarum* 23,469-471

Challa, H.; Bakker, J. 1998 Potential production within the greenhouse environment. In: Enoch, Z.; Stanhill, G., (Eds.) *Ecosystems of the world. The greenhouse ecosystem*. Amsterdan: Elsevier, p. 333-348

Cohen Y,Fuchs M,Green GC. 1981. Improvement of the heat pulse method determining sap flow in trees. Plant, cell and Environment 4,391-397.

Colaizzi PD,Barnes EM,Clarke TR, Choicy, waller PM,Haberland J, Kostrzewski M.2003. water sress detection under high frequency sprinkler irrigation with water deficit index. Journal of Irrigation and Drainage Engineering 129, 36-42.

Cosgrove, D.J.(1986). Biophysical control of plant cell growth. Annual Review of Plant Physiology, 37, 377-405.

Dane JH, Topp GC (eds). 2002. methods of soil analysis. Part 4: Physical methods. Soil science Society of America Books Series: 5. Madison, WI: Soil Scienc Society of America.

De Graaf R.& Van Den Ende J.(1981). Transpiration and evapotranspiration of green house crops. Acta Horticulturae, 119:241-7.

Doorenbos, J., and W.O. Pruitt.1975. Guidelines for predicting crop water requirements. FAO Irrig. Drain. Pap., Rome, 24

Dugas W.A 1990. sap flow in stems. In: Instrumentation for studying Vegetation Canopies for remote sensing in optical and thermal Infrared Regions.N.S Goel and J.M.Normans, eds. Remote sensing Reviews, Volume 5:225-235. Harwood Academic Publishers, New York.

Eisenberg, D & Kauzmann, W.(1969). The structure and properties of water.Oxford:Oxford University Press.

Estefanel. V.; Buriol, G.A.; Andriolo, J.L. 1998. Disponibilidade de radiação solar nos meses de inverno para o cultivo do tomateiro (*Lycopersicon esculentum Mill.*) na região de Santa Maria. *Ciência Rural*, Santa Maria, v. 28, n. 4, p. 553-559,

Evans DE, Sadler EJ, Camp CR, Millen JA, 2001. Spatial canopy temperature measurements using centre pivot mountd IRTs. Proceedings of the 5th International Conference on Precision Agriculture, Bloomington, Minnesota, July, 2000, 1-11.

FAO Irrigation and drainage Paper 56,2004.Crop Evapotranspiration-Guidelines for computing crop water requirements.pp65-66

FAO. *Protected cultivation in the Mediterranean climate*. Rome: FAO, 1990. 313 p. (FAO Plant Production and Protection Paper, 90).

Fereres E, Goldhamer DA. 2003. Suitability of stem diameter variations and water potential as indicators for irrigation scheduling of almond trees. Journal of Horticultural Science and Biotechnology 78, 139-144.

Garcia-Orellana, Y., Ruiz –Sanchez, M.c., alarco'n, JJ., Conejero, W., Ortun o M.F., Nicola's, E. And Torrecillas, A. 2007. Preliminary assessment of the feasibility of using maximum daily trunk shrinkage for irrigation scheduling in lemon trees, Agricultural water management 89: 167-171

Granier A.(1987). Evaluation of transpiration in a Douglas fir stand by means of a **sap-flow**, measurements. *Tree*, *physiology* **3**, 309-319.

HMP45C temperature and relative humidity probe User guide 2000. Campbell scientific Ltd.UK

Horticultural Promotion Council of Zimbabwe, 2000. UNCTAD Conference

http://winplc.bvsystems.be

http:/bvsystems.be/k8000

Huguet.J,Lorendeau.JY,Pellous(1992). Specific,micromorphormetric reactions of fruit trees to **water stress** and irrigation scheduling automation. *Journal of horticultural science* **67,**631-40.

Jones (1973). Estimation of plant water status with the beta gauge. *Agricultural Meteorology* 11,345-355.

Jones HG.1985.Physiological mechanisms involved in the control of leaf water status:implications for the estimation of tree water status.Acta Horticultuae **171**,291-

Jones,H.G 2004 irrigation scheduling: advantages and pitfalls of plant based methods. Journal of Experimental Botany 55 pp2-15.

Kacira M, Ling PP, Short TH.2002. establishing crop water stresss index (CWSI) threshold values for early, non-contact detection of plant water stress. Transactions of the American Society of Agricultural Engineers 45, 775-780.

Kacira M, Ling PP.2001 Design and development of an automated non-contact sensing system for continuous monitoring of planthealth and growth. Transactions of the American Society of Agricultural Engineers 44, 989-996.

Katsoulas N; Baille A;Kittas C (2001). Effect of mwasting on transpiration and conductances of a greenhouse rose canopy. Agricultural and Forest Meteorology, 106 (3), 233-247

Kipp and Zonen instructional manual, Rontgenweg 1 2624 BD Delft Holland, P.O Box 507 2600 AM Delft Holland

Kline,..,J.R. Martin,C.F.Jordan, and J.J Kovanda.1970. Measurement of transpiration in tropical trees with tritiated water. Ecology 51:1068-1073.

Kucera J, Cermak J, Penka M. 1977. Improved thermal method of continual recording the transpiration flow rate dynamics. Biologia Plantarum (Praha) 19, 413-20.

Laberche J., Musard M.&DE Villele O (1977). Les irrigations sous abri. bulletin Technique et d'Information du Ministere de l'Agriculture, 317:185-93.

Lake J.V., Postlethwaithe J.D., Slack G. and Edwards R.J (1966). Seasonal variation in the transpiration of glasshouse plants. Agric. Meteorology, 3: 167-196

Lapuerta, J.C. 1995 Anatomy and physiology of the plant. In: NUEZ, F., (Coord.) *El cultivo del tomate*. Madrid: Mundi-Prensa, p. 43-91.

Li SH, Huguet JG. 1990. Controlling water status of plants and scheduling irrigation by the micromorphometric method for fruit trees. ActHorticulturae 278, 33-341.

LI-COR Terrestrial Radiation sensors, Type SZ instruction manual, LI-COR, inc. 4421 Superior Street, P.O. Box 4425 Lincoln, NE 68505 USA

Lockhart, J.A. (1965). Analysis of irreversible plant cell elongation. Journal of Theoretical Biology, 8, 264-75.

Monteith J.L. (1973). Principle of Environmental Physics. Arnold Ed., London, 241 pp.

Morries L.G, Neale F.E, Postlethwaithe J.D.(1957). The transpiration of glasshouse crops and its relationship to the incoming radiation. J. Agric. Eng. Reseach, 2:111-22.

Nobel, P.S. (1991). Physicochemical and environmental plant physiology. New York: Academic Press

Owston, P.W., J.L. Smith, and H.G. Halverson. 1972. Seasonal water movement in tree stems. Forest Sci. 18:266-272.

Penman H.L (1948). Natural evaporation from water, soil and grass.R. Soc. London Proc.Ser.A, 193: 120-45.

Pruitt, W.O. 1966. Empirical method of estimating evapotranspiration using primarily evaporation pans. In Proc. Conf.Evapotran., St. Joseph, MI: ASAE. Chicago, IL, 57-61.

Q-7.1 Net Radiometer instruction manual, 1996 .Campbell scientific, inc 815W Logan, UT 84321-1784 USA.

Q-7.1 Net Radiometer instruction manual, 1996 .Campbell scientific, inc 815W Logan, UT 84321-1784 USA.

R.E White 2006. Principles and practice of soil science 4th ed ,Blackwell Publishing, 350 Main st. Malden, MA 0214-5020, USA pp74.

Rosenberg N.J, Blad B.L, Verma S.B 1983. Microclimate, The Biological Environment 2nd edition, pp255-256

RS components Midrand S.A 1999 email: technical @rs.co.za

Sakuratani, T.1981. A heat balance method for measuring water flux in the stem of intact plants. J. agric. Met.(Japan) 37:9-17.

Slayter, R.O (1967). Plant water relationships. London: Academic Press

Stangellini C., Bosma A. H., Gabriels P.C.J. and Werkhoven C. (1990). The water consumption of agricultural crops: how coefficients are affected by crop geometry and microclimate. Acta Horticulturae, 278: 509-15

Swanson RH, Whitfield DWA. 1981. A numerical analysis of heat pulse velocity theory and practice. Journal of Experimental Botany 32, 221-39.

Swanson RH. 1994. significant historical developments in thermal methods for measuring sap flow in trees. Agricultural and Forest Meteorology 72, 113-32.

Swanson, R.H.1972. Water transpired by trees is indicated by heat pulse velocity. Agric. Meteorol. 10:277-281.

Tube solarimeter User manual 1993.Delta- T Devices Ltd.,128 Low road, Burwell, Cambridge CB5 OEJ, UK.

Annexes

Annex A Control program for the automated irrigation sytem

```
Public Class Form1
  Dim winple As Object
 Dim IO1 As Long
 Dim IO2 As Long
  Dim sumOfTR As Double
 Dim TR, TR3 As Double
 Dim Time As Double
 Dim addedvalue As Integer = 1
 Dim count 1 As Integer = 1
 Dim Time1 As Integer
 Dim Vin, AH, BH, CH As Double
  Private Sub Form1 Load(ByVal sender As System.Object, ByVal e As
System. EventArgs) Handles MyBase. Load
    Timer3. Enabled = False
  End Sub
  Private Function ppp()
    Dim AD2 As Double
    Dim AD3 As Double
    Dim AD4 As Double
    winplc = CreateObject("PWinPLC.PowerWinPLC")
    AD1 = winplc.getADState(1)
    AD2 = winplc.getADState(2)
    AD3 = winplc.getADState(3)
    AD4 = winplc.getADState(4)
    Dim Pin, R, dT, Qv, Kst, A, dX, Qr, Ksh, Qf, F, Cw, Lav, La, LAI, TR1 As Double
    Dim F1 As Double
    Vin = (AD1 * 0.0025)
    AH = (AD2 * 0.0025)
    BH = (AD3 * 0.007)
    CH = (AD4 * 0.0055)
    Ksh = 0.67
    Cw = 4.186
    dX = 0.004
    Kst = 0.54
    R = 162.2
    A = 0.000116
    Lav = 0.26846733
    La = 0.26846733
```

```
LAI = 0.5
    Pin = (Vin * Vin) / R
    dT = (BH - AH) / (0.04)
    Qv = Kst * A * (dT / dX)
    Or = Ksh * CH
    Qf = Pin - Qr - Qv
    F = Qf / (Cw * dT)
    F1 = F * 3600
    TR = F1 / (La * 1000)
    TR1 = TR * 0.268467333
    If dT = 0 Then
      TR = 0
    End If
    txt3.Text = Vin
    txt4.Text = AH
    txt5.Text = BH
    txt6.Text = CH
    txt1.Text = TR
    Return TR
  End Function
  Private Sub Timer1 Tick(ByVal sender As System.Object, ByVal e As
System. EventArgs) Handles Timer1. Tick
    Timer1.Start()
    Call ppp()
    If TR < 0 Then
      TR3 = 0
    Else
      TR3 = TR
    End If
    sumOfTR = sumOfTR + TR3
    txt2.Text = sumOfTR
    Time = sumOfTR * (495000 / 4)
    Time1 = Time
    txt10.Text = Time1
    LwastBox3.Items.Add(TR3)
  End Sub
  Private Sub Timer2 Tick(ByVal sender As System.Object, ByVal e As
System. EventArgs) Handles Timer 2. Tick
    Timer2.Start()
    Timer3.Enabled = True
    Timer3.Start()
    LwastBox1.Items.Add(sumOfTR)
    LwastBox2.Items.Add(Time1)
    LwastBox3.Items.Add(LwastBox3.Items.Count + 1)
```

```
End Sub
  Private Sub Timer3 Tick(ByVal sender As System.Object, ByVal e As
System. EventArgs) Handles Timer3. Tick
    count1 += 1
    If count1 < Time1 Or count1 = Time1 Then
      Call forIo()
    Else: Timer3.Stop()
      sumOfTR = 0
      count1 = 0
      winplc.clearIOch(1)
      winplc.clearIOch(2)
    End If
  End Sub
  Private Function forIo() As Boolean
    winplc.setIOch(1)
    winplc.setIOch(2)
    forIo = True
  End Function
  Private Sub Button3 Click(ByVal sender As System.Object, ByVal e As
System. EventArgs) Handles Button3. Click
    MsgBox("Are You Sure You Want To Quit The Program",
MsgBoxStyle.OkCancel)
    System.Environment.Exit(0)
  End Sub
  Private Sub SaveFileDialog1 FileOk(ByVal sender As System.Object, ByVal e As
System.ComponentModel.CancelEventArgs) Handles SaveFileDialog1.FileOk
  End Sub
  Private Sub SaveToolStripMenuItem Click(ByVal sender As System.Object, ByVal e
As System. EventArgs) Handles SaveToolStripMenuItem. Click
  End Sub
  Private Sub Timer4 Tick(ByVal sender As System.Object, ByVal e As
System. EventArgs) Handles Timer4. Tick
    Timer4.Start()
    1b17.Left = 1b17.Left - 20
```

Annex B

Program for outside station (1)

};CR10X

MODE 1

SCAN RATE 5

1:P17

1:1

2:P10

1:2

3:P22

1:1

2:0

3:100

4:0

4:P1

1:1

2:35

3:1

4:3

5:.1

6:-40

5:P1

1:1

2:35

3:2

4:4

5:.1

6:0

6:P1

1:1

2:35

3:3

4:5

5:34.341

6:0

7:P1

1:1

2:35

3:4

4:6

5:-258.27

6:0

8:P92

1:0

2:30

3:10

9:P77

1:1110

10:P71

1:6

2:1

11:P0

MODE 2

SCAN RATE 5

1:P96

1:71

2:P0

MODE 3

1:P0

MODE 10

1:28

2:64

3:0

4:586568

5:2048

MODE 12

1:0

1:0

1:0

MODE 11

1:46010

2:63084

3:1280

4:20

5:0

6:1

7:8

8:2.8795

9:99

10:0

11:1.25

Annex C

Program for inside station (2)

```
; {CR23X}
*Table 1 Program
 01: 5.0000 Execution Interval (seconds)
1: Panel Temperature (P17)
1: 1
         Loc [ IntTemp
2: Batt Voltage (P10)
      Loc [ BatVolt
1: 2
3: Do (P86)
1: 49
        Turn On Switched 12V
4: Delay w/Opt Excitation (P22)
1: 1
           Ex Channel
2: 0
           Delay W/Ex (units = 0.01 sec)
3: 100
          Delay After Ex (units = 0.01 sec)
           mV Excitation
4: 0
5: Volt (SE) (P1)
1: 1
           Reps
2: 35
           5000 mV, 50 Hz Reject, Fast Range
3: 1
           SE Channel
4: 3
           Loc [ Tair
                        1
5: .1
           Mult
6: -40
           Offset
6: Volt (SE) (P1)
1: 1 Reps
2: 35
           5000 mV, 50 Hz Reject, Fast Range
3: 2
           SE Channel
4: 4
           Loc [ RH
                          ]
5: .1
           Mult
6: 0
           Offset
7: Do (P86)
1: 59
          Turn Off Switched 12V
8: Volt (SE) (P1)
1: 1
           Reps
           5000 mV, 50 Hz Reject, Fast Range
2: 35
3: 3
           SE Channel
4: 5
          Loc [ SolarRa 1 ]
5: 72.31 Mult
6: 0
           Offset
9: Volt (SE) (P1)
          Reps
2: 35
           5000 mV, 50 Hz Reject, Fast Range
3: 4
           SE Channel
4: 28
          Loc [ nrad ]
5: 9.6
           Mult
```

```
6: 0 Offset
10: Volt (SE) (P1)
1: 1
            Reps
2: 35
            5000 mV, 50 Hz Reject, Fast Range
3: 5
            SE Channel
4: 7
            Loc [ PAR
                           1
5: -249.72 Mult
6: 0
            Offset
11: Thermocouple Temp (DIFF) (P14)
1: 2
            Reps
2: 35
            5000 mV, 50 Hz Reject, Fast Range
3: 4
            DIFF Channel
4: 1
           Type T (Copper-Constantan)
5: 1
            Ref Temp (Deg. C) Loc [ IntTemp ]
6: 8
            Loc [ Tleaf 1 ]
7: 1
            Mult
8: 0
            Offset
12: Volt (SE) (P1)
1: 1
            Reps
2: 35
            5000 mV, 50 Hz Reject, Fast Range
3: 12
            SE Channel
4: 10
            Loc [ Tleaf 3
                           ]
5: .004
            Mult
6: 0
            Offset
13: Volt (SE) (P1)
1: 3
            Reps
2: 35
            5000 mV, 50 Hz Reject, Fast Range
3: 13
            SE Channel
4: 11
            Loc [ Tleaf 4 ]
5: 1
           Mult
            Offset
6: 0
14: Thermocouple Temp (DIFF) (P14)
1: 2
            Reps
2: 35
            5000 mV, 50 Hz Reject, Fast Range
3: 11
            DIFF Channel
4: 1
            Type T (Copper-Constantan)
            Ref Temp (Deg. C) Loc [ IntTemp ]
5: 1
6: 14
            Loc [ Vin 1
                           ]
7: 1
            Mult
8: 0
            Offset
15: If time is (P92)
1: 0
           Minutes (Seconds --) into a
2: 15
            Interval (same units as above)
3: 10
            Set Output Flag High (Flag 0)
16: Real Time (P77)
1: 1110
           Year, Day, Hour/Minute (midnight = 0000)
17: Average (P71)
1: 18
            Reps
            Loc [ IntTemp
2: 1
```

```
18: Sample (P70)
1: 18    Reps
2: 1    Loc [ IntTemp ]

*Table 2 Program
   01: 0.0000    Execution Interval (seconds)

*Table 3 Subroutines
End Program
```

Annex D

Day of year (Julian) calendar

	Jan	Feb	Mar	Apr	May	Jun	Jul	Aug	Sep	Oct	Nov	Dec
1	1	32	60	91	121	152	182	213	244	274	305	335
2	2	33	61	92	122	153	183	214	245	275	306	336
3	3	34	62	93	123	154	184	215	246	276	307	337
4	4	35	63	94	124	155	185	216	247	277	308	338
5	5	36	64	95	125	156	186	217	248	278	309	339
6	6	37	65	96	126	157	187	218	249	279	310	340
7	7	38	66	97	127	158	188	219	250	280	311	341
8	8	39	67	98	128	159	189	220	251	281	312	342
9	9	40	68	99	129	160	190	221	252	282	313	343
10	10	41	69	100	130	161	191	222	253	283	314	344
11	11	42	70	101	131	162	192	223	254	284	315	345
12	12	43	71	102	132	163	193	224	255	285	316	346
13	13	44	72	103	133	164	194	225	256	286	317	347
14	14	45	73	104	134	165	195	226	257	287	318	348
15	15	46	74	105	135	166	196	227	258	288	319	349
16	16	47	75	106	136	167	197	228	259	289	320	350
17	17	48	76	107	137	168	198	229	260	290	321	351
18	18	49	77	108	138	169	199	230	261	291	322	352
19	19	<i>50</i>	78	109	139	170	200	231	262	292	323	353
20	20	51	79	110	140	171	201	232	263	293	324	354
21	21	52	80	111	141	172	202	233	264	294	325	355
22	22	53	81	112	142	173	203	234	265	295	326	356
23	23	54	82	113	143	174	204	235	266	296	327	357
24	24	55	83	114	144	175	205	236	267	297	328	358
25	25	56	84	115	145	176	206	237	268	298	329	359
26	26	57	85	116	146	177	207	238	269	299	330	360
27	27	58	86	117	147	178	208	239	270	300	331	361
28	28	59	87	118	148	179	209	240	271	301	332	362
29	29	60	88	119	149	180	210	241	272	302	333	363
30	30		89	120	150	181	211	242	273	303	334	364
31	31		90		151		212	243		304		365

Add 1 to values (not bold, nor in italics) during leap years.

Annex E

Table 4.21: Showing 15 minute interval results of comparing sap flow signals for the data logger and after amplification with gain set at 1000

AH (mV)	AH(V)	BH(mV)	BH(V)	CH(mV)	CH(V)
datalogger	amplified	datalogger	amplified	datalogger	amplified
0.124	0.034	0.088	0.014	0.124	0.035
0.124	0.034	0.105	0.031	0.124	0.035
0.133	0.043	0.115	0.041	0.133	0.044
0.14	0.05	0.117	0.043	0.144	0.055
0.145	0.055	0.144	0.07	0.163	0.074
0.12	0.03	0.152	0.078	0.182	0.087
0.092	0.005	0.171	0.077	0.209	0.114
0.068	-0.019	0.16	0.066	0.206	0.111
0.104	0.017	0.177	0.083	0.231	0.136
0.094	0.007	0.107	0.013	0.185	0.090
0.123	0.036	0.078	-0.016	0.185	0.090

